ABSTRACT

Pranita Katwa. MAST CELLS AND THE IL-33/ST2 AXIS ARE ESSENTIAL DETERMINANTS OF CARBON NANOTUBE TOXICITY (under the direction of Jared M. Brown, Ph.D.) Department of Pharmacology and Toxicology, June 28, 2012.

The rise of nanomaterial use in a variety of applications, including biomedical imaging and drug delivery, has led to concern about the potentially hazardous impacts on human health. Mast cells are critical for innate and adaptive immune responses, often modulating allergic and pathogenic conditions, including pulmonary and cardiovascular diseases. Mast cells are well known to act in response to danger signals through a variety of receptors and pathways including IL-33 and the IL-1 like receptor ST2. The aim of this study was to investigate involvement of mast cells and the IL-33/ST2 axis in the pulmonary and cardiovascular toxicities induced by engineered multi-walled carbon nanotubes (MWCNTs) following oropharyngeal aspiration. We assessed inflammatory, fibrotic, and functional responses in the lung, as well as cardiac ischemia-reperfusion (IR) injury responses in C57BL/6, $Kit^{W\text{-}sh}$ (mast cell deficient), $Kit^{W\text{-}sh}$ reconstituted with either wild-type or $ST2^{-/-}$ mast cells, and $ST2^{-/-}$ deficient mice. Mice with a sufficient population of mast cells (C57BL/6 and reconstituted $Kit^{W\text{-}sh}$ mice) exhibited significant pulmonary inflammation, exhibited by increased neutrophils and associated with elevated IL-33, impaired pulmonary function, increased granuloma formation, and collagen deposition 30 days following exposure to MWCNT. Additionally, exacerbation of myocardial infarction was observed in the same groups of mice 1 day following MWCNT exposure. These toxicological effects of MWCNTs were observed only in mice with a sufficient population of mast cells and were not observed when mast cells were absent or incapable of responding to IL-33 ($Kit^{W\text{-}sh}$, $Kit^{W\text{-}sh}$

reconstituted with $ST2^{-/-}$ mast cells or $ST2^{-/-}$ mice). These findings establish for the first time, an unrecognized, but critical role for mast cells and the IL-33/ST2 axis in orchestrating adverse pulmonary and cardiovascular responses to an engineered nanomaterial, giving insight into a previously unknown mechanism of toxicity. In identifying the importance of the IL-33/ST2 axis and mast cells in this novel mechanism of toxicity, our study provides a means of addressing current concerns regarding nanoparticle exposures and the safety of engineered nanomaterials for use in biomedical applications in identifying a realistic therapeutic target for potential nanoparticle induced toxicities.

MAST CELLS AND THE IL-33/ST2 AXIS ARE ESSENTIAL DETERMINANTS OF CARBON NANOTUBE TOXICITY

A Dissertation

Presented to

the Faculty of the Department of Pharmacology and Toxicology

Brody School of Medicine at East Carolina University

In Partial Fulfillment

of the Requirements for the Degree

Doctor of Philosophy in Pharmacology and Toxicology

by

Pranita Katwa

June 28, 2012

MAST CELLS AND THE IL-33/ST2 AXIS ARE ESSENTIAL DETERMINANTS OF CARBON NANOTUBE TOXICITY

by

Pranita Katwa

APPROVED BY:

DIRECTOR OF DISSERTATION _____
Jared M. Brown, Ph.D.

COMMITTEE MEMBER _____
James C. Bonner, Ph.D.

COMMITTEE MEMBER _____
Jamie C. DeWitt, Ph.D.

COMMITTEE MEMBER _____
David A. Taylor, Ph.D.

COMMITTEE MEMBER _____
Christopher J. Wingard, Ph.D.

CHAIR OF THE DEPARTMENT OF PHARMACOLOGY AND TOXICOLOGY _____
David A. Taylor, Ph.D.

DEAN OF THE GRADUATE SCHOOL _____
Paul J. Gemperline, Ph.D.

To my family,

whose strength has been a blessing every day.

ACKNOWLEDGEMENTS

From the conceptual stages to the last written page of this thesis, I owe the deepest gratitude to my advisor, Dr. Jared Brown. I have been amazingly fortunate to have an advisor who has truly led by example and provided me with inspiration and encouragement. His patience, support and unfaltering guidance are what have enabled successes and accomplishments throughout my dissertation work.

I would also like to thank my committee members: Drs. David Taylor, Jamie DeWitt, Chris Wingard and Jamie Bonner, all of whom, in different ways, have helped mentor me. Whether by providing practical advice, guidance, or encouragement, each of my committee members has been an invaluable asset in my professional growth as a scientist, and for that I am immensely thankful.

Though my advisor and committee members have ensured the success of my thesis project, there are a great many others who have helped in its production and contributed to a memorable graduate school experience. I want to thank all the faculty and staff of the Dept. of Pharmacology and Toxicology. In particular, I want to thank my lab members Susana Hilderbrand, Dr. Xiaojia Wang, Abdullah Aldossari, Josh Pitzer, and Dr. Jonathan Shanahan, for all their help. I am especially grateful to Dr. Xiaojia Wang for our countless hours of work together and for all her support on this project. In addition, I want to acknowledge my fellow graduate students, who have shared with me the highs and lows of this journey. A special thanks to Stefanie Burleson who has spent many a late night with me in the name of research, and whose friendship I will always deeply value.

Lastly, I want to thank my family. My parents, Laxman and Geeta have always provided me with unconditional love and support, an unwavering beacon of light that has helped me through the toughest of times. And I could not imagine any success without my brother, Prashant, who has always been the voice of reason in my life. Finally, I express my heart-felt gratitude to my loving fiancé, Shaum, who has provided emotional support and encouragement, and who has been with me every step of the way.

TABLE OF CONTENTS

LIST OF FIGURES

4.1 BALF from MWCNT exposed mice results in mast cell activation via the IL-33/ST2 axis

5.1 Neutrophil cell counts, histopathology and collagen content in lungs of mice instilled with MWCNT

6.1 Raman spectroscopy of lung histology

7.1 Altered pulmonary function following MWCNT instillation

8.1 MWCNT induced exacerbation of myocardial ischemia reperfusion injury

9.1 Mechanism of MWCNT induced pulmonary and cardiovascular toxicity

4.1 Changes in pulmonary function as determined by Snapshot perturbation after carbon black instillation

4.2 Changes in pulmonary function as determined by Quicktime-3 and PVr-P perturbation following carbon black instillation

4.3 Differential cell counts in C57BL/6 mice 30 days following carbon black exposure

4.4 Expression of IL-33 mRNA in MLE-12 murine lung epithelial cells at 2, 4, and 24 hours following MWCNT exposure

4.5 Expression of IL-33 mRNA in C10 lung epithelial cells at 2, 4, and 8 hours post-exposure to MWCNTs

4.6 IL-33 mRNA expression at 4 hours following MWCNT treatment in C10 cells primed with LPS

4.7 IL-33 protein levels in C10 lung epithelial cells 24 hours following MWCNT exposure

4.8 IL-33 mRNA expression in murine lung fibroblasts following MWCNT exposure

LIST OF TABLES

LIST OF ABBREVIATIONS

Ang II	Angiotensin II
ASM	Airway smooth muscle
ASMC	Airway smooth muscle cell
BAL	Bronchoalveolar lavage
BALF	Bronchoalveolar lavage fluid
BET	Brunauer-Emmett-Teller equation
BJH	Barrett–Joyner–Halenda method
bFGF	Basic fibroblast growth factor
BMMCs	Bone marrow derived mast cells
C	Compliance
Cst	Static compliance
c-Kit_+	$CD34^{+/}CD117^{+}$ cells
CNTs	Carbon nanotubes
COPD	Chronic obstructive pulmonary disease
Cre-Master	Cre-mediated mast cell eradication
cys-LT	Cys-leutkotrienes
DEP	Diesel exhaust particles
E	Elastance
Est	Static elastance
eta	Hysteresivity
FcεRI	High affinity IgE Receptor
FcγRI	High affinity IgG Receptor

FKN	Fractalkine
FOT	Forced oscillation technique
G	Tissue damping
G-CSF	Granulocyte colony-stimulating factor
GM-CSF	Granulocyte-macrophage colony-stimulating factor
GPCR	G-protein coupled receptor
HMGB1	High mobility group box 1
IFN-γ	Interferon-γ
I	Inertance
IEP	Isoelectric point
IL	Interleukin
IL-1RAcP	IL-1 receptor accessory protein
IR	Ischemia reperfusion
IRAK	IL-1R associated kinase
ITAM	Immunoreceptor tyrosine-based activation motif
LDH	Lactate Dehydrogenase
LPS	Lipopolysaccaride
MACE	Major adverse cardiovascular events
MAPKs	Mitogen-activated protein kinases
MCP-1	Monocyte chemotactic protein 1
MHC	Major histocompatibility complex
MIP-1β	Macrophage inflammatory protein-1β
MMP	Matrix metalloprotease

MWCNTs	Multi-walled carbon nanotubes
MyD88	Myeloid differentiation primary response gene 88
NF-HEV	Nuclear factor preferentially expressed in high endothelial venules
NF-κB	Nuclear factor κB
NIOSH	National Institute of Occupational Safety and Health
NO	Nitric oxide
NOEL	No observable effect level
OPN	Osteopontin
OVA	Ovalbumin
OX40L	OX40 ligand
PAMP	Pathogen associated molecular pattern
PAR-2	Protease-activated receptor 2
PDGF-AA	Platelet derived growth factor AA
PGD_2	Prostaglandin D_2
PGE_2	Prostaglandin E_2
PI3K	Phosphoinositide 3 kinase
PLC	Phospholipase C
PM	Particulate matter
PR3	Proteinase 3
PV	Pressure-volume
ROS	Reactive oxygen species
R	Resistance
Rn	Newtonian resistance

Rrs	Respiratory resistance
SEM	Scanning electron microscopy
SCF	Stem cell factor
sST2	Soluble ST2 receptor
TGF-β	Transforming growth factor-β
Th	T helper
TLC	Total lung capacity
TLRs	Toll-like receptors
TNF-α	Tumor-necrosis factor-α
TRAF	TNF receptor associated factor
VCAM-1	Vascular cell adhesion molecule-1
Xrs	Respiratory reactance
Z	Respiratory impedance

CHAPTER 1: INTRODUCTION

Nanomaterials

In recent years, nanomaterials have become more prominent in a variety industries and applications. The Project of Emerging Nanotechnologies identifies a 521% increase in inventory of nanotechnology-based products from 2006 to 2011 (The Project, 2012). Currently, the United States, ahead of Europe and East Asia, demonstrates an inventory of over 500 nanoparticle containing consumer products, an increase from less than 150 products in 2006 (The Project, 2012). Consumer products containing nanomaterials fall into a variety of categories including health and fitness, automotive, food and beverage, electronics, and applicances, all of which have exhibited a rise in the number of products from 2006 to 2011 (The Project, 2012). Increased interest in nanoparticles, such as carbon nanotubes (CNTs), is due to their unique physical and chemical properties including high mechanical strength, high electrical conductivity and lightweight structure (Ajayan et al., 1999; Endo et al., 2008b; Lin et al., 2004). These characteristics have made CNTs ideal for use in conductive and high-strength composites, sensors, energy conversion devices, drug delivery systems, as well as other biomedical applications (Baughman et al., 2002; Martin and Kohli, 2003).

In the innovative arena of drug delivery, CNTs are being utilized as carriers of a variety of therapeutics. As many drugs are associated with limited bioavailability, solubility and selectivity, resulting in an abundance of adverse effects, CNTs provide a new approach to improve the pharmacokinetic aspects of a drug. By functionalizing CNTs with specific peptides, for example, can increase affinity for receptors, by

enabling greater intracellular localization for a peptide that normally has low cellular uptake (Bianco et al., 2005). CNTs can be functionalized in numerous ways not only to enhance drug delivery but also to target antigen presentation and gene delivery. The addition of antigens to a CNT carrier can be used to elicit a specific immune response through numerous immune cell types to generate antigen-specific antibodies (Bianco et al., 2005). CNTs are advantageous in this regard as no antibodies are produced in response to the carrier, demonstrating a unique and promising method of vaccine delivery (Lin et al., 2004; Bianco et al., 2005). Gene therapies also show great promise in the treatment of cancers, genetic disorders and other diseases, but are administered through a viral vector, which often results in undesired immune responses (Bianco et al., 2005). The use of CNTs as non-viral vectors in gene therapy allows for an alternate means of delivery that is specific to DNA bio-interactions (Bianco et al., 2005). The means by which CNTs may enhance and contribute to any given application demonstrates the potential for CNTs in several fields, and is evident in the novel applications of drug delivery.

While the use of CNTs may be advantageous in many disciplines, there is cause for concern as the potential health hazards are not fully understood. The means of exposure to CNTs can be intentional (e.g. drug delivery) or unintentional (environmental or occupational) and is currently unregulated in most industries and countries. Therefore, it is of great interest to further examine CNT toxicity and the implications on human health and safety.

Carbon Nanotubes

Multi-walled carbon nanotubes (MWCNTs), a particular type of CNT, are widely used and as a result, have been the subject of multiple investigations regarding their potential toxicity. Several studies have identified that MWCNT exposure induces adverse cardiovascular and pulmonary effects including: inflammation, fibrosis and altered lung function.

CNT Induced Pulmonary Toxicity

Exposure to MWCNTs has been shown to elicit cytotoxic responses in several cell types found in the lung (Cavallo et al., 2012; Di Giorgio et al., 2011). In cultured human lung epithelial cells, one of the first cell types likely to encounter inhaled particulates, exposure to MWCNT resulted in decreased cell viability as demonstrated by an increased lactate dehydrogenase (LDH) release, a marker of cell cytotoxicity and cell membrane integrity (Cavallo et al., 2012). The damage to cell membranes induced by MWCNTs was evident in scanning electron microscopy (SEM) images, which displayed internalization of MWCNT by lung epithelial cells and compromised membrane integrity leading to cell death (Cavallo et al., 2012). Similarly, macrophages exposed to MWCNT *in vitro* exhibited cytotoxicity, particularly though necrosis (Di Giorgio et al., 2011). MWCNTs not only induce cytotoxicity that results in the release of mediators, they initially stimulate both pulmonary epithelial cells and macrophages to produce pro-inflammatory mediators such as TNF-α (Di Giorgio et al., 2011).

Moreover, the size-associated aspects of nanomaterials also accentuate the biopersistance of nanoparticles and evasion of clearance mechanisms. The shape and

length of CNTs predispose them to increased retention time within tissues prior to clearance. Retention of CNT fiber in the murine pleural space, for example, was shown to be length dependent (Murphy et al., 2011). Furthermore, due to their length and fiber-like dimensions, CNTs have been shown to negatively impact macrophages which internalize MWCNTs through unsuccessful phagocytosis of the particles in their entirety, displaying numerous penetrations sustained out to 56 days and likely responsible for the production of reactive oxygen species (ROS) associated with MWCNT exposure (Di Giorgio et al., 2011; Mercer et al., 2010; Murphy et al., 2012; Ryman-Rasmussen et al., 2009a). The development of pulmonary inflammation following MWCNT exposure has been shown to manifest through the infiltration of immune cells, like macrophages and neutrophils, as well as the production of pro-inflammatory cytokines and chemokines (Aiso et al., 2010; Han et al., 2010). Specifically, exposure to MWCNT has been reported to result in the activation of numerous pulmonary cell types and the subsequent production of pro-inflammatory cytokines including interleukin (IL)-1β, IL-6, IL-33 and osteopontin (OPN) (Inoue et al., 2009; Katwa, in submission 2012; Wang et al., 2011a).

In addition, mice sensitized to ovalbumin (OVA) and subsequently exposed to MWCNT demonstrated significant pulmonary neutrophil infiltration and increased cytokine expression including IL-5 and IL-13, affirming the ability of MWCNTs to potentiate allergic responses in mouse models of asthma (Ryman-Rasmussen et al., 2009b). In asthma, the presence of certain T helper (Th) 2 cytokines such as IL-13 can further enable the release of other cytokines, which directly modulate aspects of the disease. In animal models of asthma, the release of IL-13 by mast cells and other cell

types has been shown to induce airway hyperreactivity by activating receptors on airway smooth muscle cells (ASMC) (Brightling et al., 2003b). MWCNTs can also augment pre-existing pulmonary inflammation induced by initial lipopolysaccaride (LPS) activation of the immune response (Inoue et al., 2008). These MWCNT induced inflammatory responses are further supported by increased numbers of neutrophils within bronchoalveolar lavage fluid (BALF) and lung tissue, observed as early as 24 hours and persisting for up to 30 days post-exposure (Kim et al., 2010; Porter et al., 2010).

Doses of MWCNTs comparable to those observed in human exposure levels have been shown to elicit pulmonary fibrotic responses as early as 7 days post-exposure as exhibited by increased collagen deposition, development of granulomas and fibrosis in murine lungs (Porter et al., 2010). As MWCNTs elicit pulmonary inflammatory cell recruitment, macrophages and other cell infiltrates are known to contribute to the composition of pulmonary granulomas observed as early as 30 days following exposure (Wang et al., 2011a). The development of fibrotic tissue resulting from MWCNT exposure has also been associated with increased production of platelet derived growth factor AA (PDGF-AA) by macrophages and epithelial cells (Cesta et al., 2010). Data from several other studies also demonstrate granulomatous and fibrotic tissue formations at 30, 60 and 90 days following MWCNT exposure (Huizar et al., 2011; Ma-Hock et al., 2009; Wang et al., 2011a). Several other pro-fibrotic mediators are known to be involved in MWCNT mediated fibrosis. Despite its role in asthmatic responses, IL-13, along with PDGF-AA and transforming growth factor (TGF-β) is considered a fibrogenic mediator (Ryman-Rasmussen et al., 2009b). IL-13 has been

reported to upregulate TGF-β and stimulate its production in pulmonary macrophages and epithelial cells (Lee et al., 2001). Furthermore, it can also upregulate PDGF-AA to induce the growth and proliferation of lung fibroblasts, the primary cell type responsible for collagen deposition within lung tissue and the morphological changes observed in the pathogenesis of fibrotic diseases (Ingram et al., 2004). As with pulmonary inflammation, pre-existing allergic conditions may prime the immune system to also augment pulmonary fibrotic responses including increased deposition of collagen and exacerbation of airway fibrosis, as seen in mice sensitized with OVA following MWCNT inhalation (Ryman-Rasmussen et al., 2009b).

CNT Induced Cardiovascular Toxicity

The toxicity of MWCNT on the cardiovascular system is largely unknown; however, some recent *in vitro* studies have suggested adverse effects on cell viability, permeability, migration and ROS generation in endothelial cells (Pacurari et al., 2012; Walker et al., 2009). Specifically, endothelial cells exposed to MWCNTs demonstrated increased LDH and IL-8 release, mediators indicating cytotoxic responses (Pacurari et al., 2012). In addition, the functionality of endothelial cells was reported to have been compromised due to altered vascular endothelial-cadherin localization, formation of stress fibers and disrupted actin cytoskeleton structures coupled with decreased tubule formation, in the presence of MWCNTs (Walker et al., 2009). It has also been reported that the observed changes in cytoskeleton structures are a result of ROS generation, well known to result in endothelial dysfunction (Pacurari et al., 2012). These factors are especially important in maintaining the integrity of endothelial cells, which act as barrier

cells in the cardiovascular system. *In vivo*, MWCNTs have been shown to exacerbate Ischemia Reperfusion (IR) injury response as early as 1 day post-exposure, demonstrating a potential for MWCNTs to modulate pre-existing cardiovascular conditions(Urankar, in submission 2012a).

IL-33

IL-33 is a novel cytokine belonging to the IL-1 superfamily and has recently been termed an “alarmin” for its ability to alert the immune system during injury (Moussion et al., 2008; Schmitz et al., 2005). Known to play a role in both innate and adaptive immune responses, IL-33 has been described as a mediator in several disease pathologies including fibrosis, asthma, allergic responses, anaphylaxis and cardiovascular disease (Haraldsen et al., 2009; Liew et al., 2010). Like other alarmins, also known as endogenous danger signals, IL-33 activates immune cells and subsequent inflammatory processes in response to cellular trauma or necrosis through a receptor mediated signaling pathway (Kono and Rock, 2008). As shown in Figure 1.1, IL-33 is able to impart its numerous cellular effects through binding to its receptor ST2, which is known to heterodimerize with the IL-1 receptor accessory protein (IL-1RAcP) (Chackerian et al., 2007). Upon activation of the ST2 receptor, propagation of signal transduction is induced by recruitment of Myeloid differentiation primary response gene 88 (MyD88), IL-1R-associated kinase (IRAK) 1, IRAK4 and TRAF6 to the ST2/IL-1RAcP receptor complex (Figure 1.1) (Schmitz et al., 2005; Suzuki et al., 2002). Many of these recruited adaptor proteins are central to the signaling of the IL-1 superfamily of cytokines (Janssens and Beyaert, 2002). Downstream signaling of the ST2 receptor

leads to the activation of the mitogen-activated protein kinases (MAPKs) and nuclear factor κB (NF-κB), proteins known to modulate transcription of numerous Th2 cytokines and subsequent immune responses (Figure 1.1) (Gadina and Jefferies, 2007). Furthermore, several studies have indicated that the soluble ST2 receptor (sST2) acts as a decoy receptor by sequestering IL-33 and inhibiting additional stimulation of the IL-33/ST2 signaling pathway shown in Figure 1.1, to reduce the resulting inflammatory responses in a negative feedback loop (Hayakawa et al., 2007; Palmer et al., 2008).

IL-33 is acknowledged in not only initiating, but also in modulating immune responses. The potential of IL-33 to carry out these functions is dependent upon its activity and has been a subject of great debate. As a member of the IL-1 family of cytokines, it was initially believed to be processed by caspase-1 from a full length, pro-IL-33 form to a mature, cleaved form, similar to IL-18 (Schmitz et al., 2005). However, more recent studies have indicated that IL-33 may be regulated by other proteases such as neutrophil elastase, cathepsin G and neutrophil proteinase 3 (PR3) to yield an active mature IL-33 (Bae et al., 2012; Lefrancais et al., 2012; Zhiguang et al., 2010). While full length IL-33 is biologically active, cleavage of IL-33 by these proteases results in a more active form, often secreted during an inflammatory response (Zhiguang et al., 2010).

IL-33 has also been proposed to have dual functional roles, acting as a traditional, intracellular cytokine as well as a regulatory intra-nuclear cytokine (Haraldsen et al., 2009). Intracellularly, IL-33 can be found constitutively co-localized to the nucleus in several cell types including endothelial and epithelial cells. In endothelial cells, IL-33 has been found to act as a heterochromatin-associated nuclear factor, displaying transcriptional repressor properties, similar to high mobility group box 1

(HMGB1) and nuclear factor preferentially expressed in high endothelial venules (NF-HEV) (Carriere et al., 2007). Like HMGB1, IL-33 can also be released extracellularly during cellular necrosis or trauma (Luthi et al., 2009; Scaffidi et al., 2002). This is in contrast to cells undergoing apoptosis, which retain IL-33 intracellularly (Luthi et al., 2009). It has been proposed that the function of IL-33 as an alarmin is centered on its release during cell injury, potentially facilitating disease pathologies (Oboki et al., 2011).

IL-33/ST2 Pathway in Pulmonary Pathophysiology

IL-33 has been implicated in a variety of pulmonary conditions. In lung tissue the ST2 receptor was preferentially expressed in microvascular endothelial cells as well as airway epithelial cells, and was found to drive inflammation with the production or release of Th2 cytokines upon activation by IL-33 (Yagami et al., 2010). It has also been reported that over-expression of IL-33 in a murine allergic asthma model displayed spontaneous pulmonary inflammation as evidenced by eosinophilic infiltration, goblet cell hyperplasia and an increase in inflammatory factors including IL-5, IL-8 and IL-13 (Zhiguang et al., 2010). Furthermore, linical studies report acute exacerbations in patients with asthma associated with increased levels of serum sST2 resulting from the activation of the IL-33/ST2 pathway (Oshikawa et al., 2001). However, the role of IL-33 in pulmonary pathophysiology is not strictly limited to allergic or inflammatory disease. Patients with systemic sclerosis, an autoimmune disease, demonstrate an association of increased serum IL-33 levels with the extent of pulmonary fibrosis (Yanaba et al., 2011).

IL-33/ST2 Pathway in Cardiovascular Disease

While some studies have examined the relationship between the IL-33/ST2 pathway and adverse cardiovascular events, it remains largely unexplored. However, IL-33 has been shown to activate endothelial cells to promote angiogenesis and vascular permeability through the IL-33/ST2 pathway signaling molecule TNF receptor associated factor (TRAF) and subsequent activation of the PI3K/Akt/eNOS pathway to mediate downstream nitric oxide (NO) dependent signaling (Choi et al., 2009). Moreover, IL-33 activation of the PI3K/Akt/eNOS pathway resulting in NO production is necessary for the facilitation of both vascular permeability, crucial for infiltration of mast cells, and angiogenesis, a physiological event that is pivotal in development, wound healing and inflammatory diseases (Folkman, 1995). Clinically, elevated levels of sST2 have been observed in patients who had experienced hospitalization, reinfarction, and heart failure, all of which were combined for a primary endpoint termed major adverse cardiac events (MACE) (Dhillon et al., 2011). Further analysis exhibited a potential for sST2 to be a predictor of left ventricle functional recovery, reinfarction and mortality following myocardial infarction (Dhillon et al., 2011; Weir et al., 2010). Further study is required to delineate IL-33 involvement in the cardiovascular system and potentially adverse cardiac events.

IL-33 Targets

It is well established that IL-33 targets a variety of cell types including macrophages, eosinophils, basophils and epithelial, endothelial, dendritic, T, and mast cells (Oboki et al., 2011). As a key player in several immune pathways, the activation of

the ST2 receptor by IL-33 on several immune cells including mast cells has been shown to induce the release of a variety of Th2 pro-inflammatory cytokines such as IL-6 and IL-13 (Enoksson et al., 2011). In particular, mast cells, one of the few cell types to highly express the ST2 receptor, release a host of cytokines including IL-1β, IL-6, IL-13, MCP-1 and TNF-α following activation via the ST2 receptor (Iikura et al., 2007; Moulin et al., 2007). Therefore, mast cells may be key players in many IL-33/ST2 pathway mediated immune responses or disease pathologies.

Mast Cells

Mast Cell Growth and Differentiation

Mast cells develop from $CD34^{+/}CD117^{+}$ (c-Kit^{+}) hematopoietic stem cells that originate in the bone marrow (Kirshenbaum et al., 1991). While these pluripotent hematopoetic stem cells may also give rise to basophils, hematopoietic stem cells, unlike many involved in myeloid and lymphoid differentiation, do not down-regulate c-Kit receptor expression. Therefore, in the presence of stem cell factor (SCF), a ligand for the c-Kit receptor, progenitor cells differentiate and mature within various tissues as mast cells (Brown et al., 2008). Another cytokine known to promote growth of mast cells is IL-9. IL-9, along with SCF, has been shown not only to increase mast cell growth and promote the release of mast cell progenitors from bone marrow, but also to facilitate the production of mast cell proteases and other cytokines (Matsuzawa et al., 2003; Wiener et al., 2004). Mast cell maturation and migration from the peripheral vasculature into tissues requires the influence of several mediators including IL-3, α4 integrins and vascular cell adhesion molecule-1 (VCAM-1). Mast cell recruitment to the

lung, for example, is dependent upon expression of α4β1 and α4β7 integrins, which are able to interact with pulmonary endothelial VCAM-1 to enable migration into lung tissue (Abonia et al., 2006). In addition, the chemokine receptor CXCR2 is known to modulate the expression of VCAM-1 and is required for proper migration of mast cell progenitors to host tissues (Hallgren et al., 2007).

Mast Cell in Host Tissues

Mast cells are found in a variety of tissue types and easily distinguished by the metachromatic staining of their granules, as first discovered by the scientist Paul Erlich (Beaven, 2009). In humans, they are most commonly known to reside around mucosal membranes and connective tissues and thus found in higher density in tissues of the gastrointestinal tract and skin (Yong, 1997). However, mast cells do exist in most tissue types including the stomach, colon, lymph nodes, brain, heart and lungs (Ghanem et al., 1988; Weidner and Austen, 1991). They are found in the thalamus, hypothalamus, and various nuclei of the brain, as mast cell mediators have been known to impact neuronal responses as well as vascular function, altering permeability of the blood-brain barrier (Wilhelm et al., 2005; Zhuang et al., 1996; Zhuang et al., 1997). Mast cells have long been identified in cardiac and arterial tissues, but the potential role of mast cells in the cardiovascular system has been elusive until recent years wherein cardiac mast cells have been implicated in several pathophysiological conditions (Bot et al., 2007; Dvorak, 1986; Ghanem et al., 1988; Gilles et al., 2003). Similarly, mast cells have been known to be involved in several pulmonary pathophysiological conditions and are able to modulate immune responses due to their anatomical locations. In the lung, mast cells

reside throughout the lung parenchyma, in the surrounding connective tissue, as well as in the mucosal regions of the respiratory tract (Patterson and Suszko, 1971). The close proximity of mast cells to the smooth muscle layer within the respiratory tract ideally positions them to be able to influence airway hyperreactivity in the pathology of asthma as will be discussed later in greater detail (Brightling et al., 2003b). As is evident with asthma, mast cells are able to contribute to several disease pathologies due to their unique locations in certain tissues.

Mast Cells Phenotypes

There are two commonly recognized phenotypes of mast cells, which are delineated by their protease contents. Mast cells that only contain tryptase are referred to as the MC_T phenotype, while mast cells that contain tryptase, chymase, carboxypeptidase and cathepsin G are denoted as the MC_{TC} phenotype (Pejler et al., 2009). A third phenotype, MC_C, defined by mast cells that only contain chymase, has also been reported, though not often identified in tissues (Bradding et al., 1995). In the human lung, MC_{TC}, the phenotype generally associated with connective tissue mast cells, have been predominantly seen in pulmonary vessels and the pleura (Andersson et al., 2009). In contrast, the MC_T mucosal phenotype mast cells were discovered in higher proportion near the epithelium of the conducting airways, as well as throughout the lung parenchyma (Andersson et al., 2009; Schwartz et al., 1987). The heterogeneity of mast cells throughout the human body, currently characterized by protease content into the MC_T and MC_{TC} phenotypes, can be further categorized in numerous ways due to varying attributes within phenotypes. While the identification of

specific proteases within mast cells is a widely accepted means of phenotype classification, it is also understood that mast cell phenotype is driven by the microenvironment.

Mast cells are able to respond to mediators in their microenvironments that contribute to a specific phenotype. Cord blood derived mast cells cultured with IL-4 and Th2 cytokines in addition to the required mast cell growth factor, SCF, demonstrated a MC_{TC} connective tissue phenotype *in vitro* (Hsieh et al., 2005). However, when co-cultured with human airway epithelial cells, the mast cells, originating with a MC_{TC} phenotype, eventually developed a MC_T phenotype (Hsieh et al., 2005). Classically, mast cells with a MC_T phenotype have been known to develop an eicosanoid phenotype resulting in increased cys-leukotrienes or (cys-LT) production, classically enhanced following IgE-dependent activation. However, in culture, mast cells were only able to display an eicosanoid phenotype following IgE-dependent high affinity IgE receptor (FcεRI) stimulation and priming with IL-4 and other Th2 cytokines (Hsieh et al., 2005). In addition to epithelial cell derived Th2 cytokines, SCF expression by epithelial cells has been shown to directly impact mast cell survival in co-cultures *in vitro*. Thus epithelial cells may play a significant role in directing mast cell mediated responses, potentially through the expression of SCF (Hsieh et al., 2005). Similarly, it has been proposed that endothelial cells may regulate mast cell function as both cell types in close proximity to connective tissues of blood vessels. In the presence of pro-inflammatory factors such as TNF-α, endothelial cells also upregulate SCF factor, promoting mast cell survival and proliferation (Konig et al., 1997). Furthermore, increases in mast cell number were observed in co-culture systems with endothelial

cells, as wells as increases in VCAM-1 and E-selectin, enabling mast cell adhesion (Mierke et al., 2000). Mast cells display great phenotypic plasticity and the microenvironments driving these mast cell phenotypes contribute greatly to mast cell function in specific biological compartments.

Mast Cells in Lung Immunology

Mast Cells in Innate Immunity

Mast cells play an important role as key effector cells in innate immunity. Once activated, mast cells serve to regulate functions of other effector cells including dendritic cells and neutrophils, which act to propagate an innate immune response or to bridge the gap between innate and adaptive immunity, as is the case with dendritic cells. The release of TNF-α and IL-1 by mast cells has been shown to induce chemotaxis and differentiation of dendritic cells and neutrophils to a targeted location of infection or inflammation (Cumberbatch et al., 2001; Zhang et al., 1992). Other mediators released from mast cells, such as histamine, stimulate antigen presentation by dendritic cells through increasing expression of the major histocompatibility complex (MHC) class II molecules and facilitate further release of cytokines like MCP-1 to recruit additional immune cells and potentially activate the adaptive immune system (Caron et al., 2001).

During an innate immune response, the activation of mast cells and the release of their mediators can occur through several pathways. It has long been established that mast cells have the ability to directly bind and phagocytose or opsonize pathogens. In doing so, mast cells have been shown to process pathogenic proteins and act as antigen presenting cells to T lymphocytes to further facilitate the immune response

(Frandji et al., 1996; Malaviya et al., 1996). Another important facet of mast cell function in innate immunity and host defense is the ability of mast cells to recognize numerous pathogens as well as endogenous danger signals through the direct activation of pathogen associated molecular pattern (PAMP) receptors such as toll-like receptors (TLRs), scavenger receptors and several others. The TLRs belong to the IL-1 superfamily of receptors, many of which are expressed on mast cells (McCurdy et al., 2003; Varadaradjalou et al., 2003). Activation of the various TLRs enables the release of specific cytokine or chemokine profiles, formulating differential immune responses to the particular pathogenic or to the endogenous insults at hand. Additionally, mast cells can also be activated through the complement system, traditionally initiated when C1 complement factors bind to IgG-antigen or IgM-antigen complexes to propagate opsonization, chemotaxis and other means of fighting infection. Mast cells not only play a role in bacterial infections, but similarly in parasitic and viral infections, acting as sentinels of the innate immune system (Marshall, 2004).

Mast Cells in Adaptive Immunity

Though historically viewed as cells of the innate immune system, mast cells are often associated with Th2 responses and adaptive immunity due to their classical activation and degranulation through antigen-dependent crosslinking of the high affinity IgE receptor, FcεRI. This allergic response results from the release of preformed mediators, such as proteases, cytokines, and chemokines, from the granular stores within mast cell (Metcalfe et al., 2009). This early response is then followed by a late response four to six hours later wherein mast cells synthesize additional mediators for

further release (Tkaczyk et al., 2006). The mast cell can also be activated through other immunoglobulin receptors, such as the high affinity IgG receptor (FcγRI) known to bind monomeric IgG_1 and IgG_3 isoforms with high affinity, in the presence of interferon-γ (IFN-γ). With IFN-γ stimulation, it has been demonstrated that human mast cells express higher levels of FcγRI and that aggregates of FcγRI are capable of inducing mast cell degranulation and enhancing cytokine release indcluding TNF-α, IL-3, IL-4, IL-13 and GM-CSF (Okayama et al., 2000). Interestingly, it has also been shown that aggregation of IgG_1, unlike IgG_3 aggregates, can still activate FcγRI on mast cells to elicit degranulation, and that subsequent IgG complexes can initiate C3a formation to synergistically facilitate mast cell activation through the C3a G-protein coupled receptor (GPCR) expressed on mast cells (Ali et al., 2000; Woolhiser et al., 2004).

Along with immunoglobulin receptor activation, mast cells are able to modulate another key function of adaptive immunity through antigen presentation. Like most cell types, mast cells express MHC class I, and are able to process bacterial antigens and present to T cells for further clonal expansion (Malaviya et al., 1996). While not constitutively expressed, MHC class II expression can be induced in mast cells via TNF-α or γ-IFN stimulation, enabling antigen presentation to T cells (Frandji et al., 1996). These mast cell and T cell interactions are supported by the mast cell expression of the co-stimulatory molecule OX40 ligand (OX40L), known to be involved with T cell proliferation and polarization (Kashiwakura et al., 2004; Ohshima et al., 1998). The ability of mast cells to express OX40L also enables interactions with B cells and has been shown to induce B cell production of IgE in the presence of IL-4, thus driving many allergic and Th2 responses (Gauchat et al., 1993; Yoshikawa et al., 2001). The

production of IgG_1 by IL-4 stimulated B cells can also be facilitated by mast cell protease I (Yoshikawa et al., 2001). With the release of cytokines such as IL-4 and IL-13, mast cells can influence the polarization of naïve T helper cells.

Another cell type crucial to an adaptive immune response is the dendritic cell. The dendritic cell is foremost an antigen presenting cell, expressing high levels of MHC class II at full maturity following exposure to an antigen. Investigation of mast cell and dendritic cell interactions has provided evidence suggesting mast cell components such as TNF, IL-1, prostaglandin E_2 (PGE_2) propagate dendritic cell migration and maturation (Cumberbatch et al., 2001; Kabashima et al., 2003). While inducing the maturation of dendritic cells, PGE_2 has also been shown to promote the transformation of these cells into the DC2 phenotype, which can facilitate a Th2 shift in T cell phenotype (Kalinski et al., 1997). Thus mast cells can either directly or indirectly influence the polarization of naïve T cells to favor an adaptive immune response.

Activation Pathways

Mast cells, known to have diverse functions in both innate and adaptive immunity, can be activated through a variety of means. One of the most common and best-studied mechanisms of mast cell activation is the crosslinking of the high affinity IgE receptor, FcεRI, by IgE and antigen, leading to an adaptive immune driven Th2 response. The binding of antigen-IgE complexes to FcεRI initiates a signal transduction pathway beginning with the phosphorylation of the FcεRI cytosolic domains, immunoreceptor tyrosine-based activation motifs (ITAMs), and eventually leading to downstream activation of phospholipase C (PLC) isoforms, resulting in calcium release

through store operated calcium channels in the endoplasmic reticulum, and eventually degranulation of the mast cell (Metcalfe et al., 2009). This activation pathway is a feature of type I hypersensitivity or allergic responses, largely driven by mast cell activation and the release of preformed mediators such as proteases and cytokines from cytoplasmic granules during degranulation (Metcalfe et al., 2009).

Mast cells are also involved in innate immune responses, several of which are initiated by alternative activation pathways including the TLRs, scavenger receptors and other PAMP receptors. The TLRs are a family of receptors that are specific to the binding of different pathogen components. In the case of TLR-4, binding of specific pathogen components, such as LPS from gram-negative bacteria, activates the mast cell and promotes release of cytokine profile specific for the receptor (Varadaradjalou et al., 2003).

An additional mast cell induced innate immune response to pathogen is the activation of mast cells through the complement system. Though the complement system itself plays an important role in host defense of bacterial infections through opsonization and chemotaxis of other effector cells, it is also known for its ability to activate mast cells. Complement factors, particularly C3 and C4 proteins of the classical pathway, have been shown to be crucial in mast cell activation, as mice deficient in C3 and C4 proteins displayed significantly reduced degranulation. When reconstituted with human C3 proteins, C3-/- mice in a model of bacterial infection exhibited levels of mast cell degranulation and cytokine release comparable to wild type animals (Prodeus et al., 1997). Activation of mast cells by C3a and C5a complement proteins occurs through the corresponding GPCR expressed by the mast cell, initiating

the phospholipase C or phosphoinositide 3 kinase (PI3K) signaling cascades to mobilize calcium for degranulation and stimulate cytokine or chemokine production (Ali et al., 2000). Activation of the complement pathway can also be simultaneously stimulated by the binding of IgG to a mast cell IgG receptor FcγRIII, resulting in direct opsonization of pathogens by bacteria and triggering of the classical complement pathway with mast cell activation and subsequent initiation of the inflammatory cascade, both facilitated through the C3 complement protein (Baumann et al., 2001).

Mast cells are recognized as quintessential elements of the innate and adaptive immune systems. Thus, the activation pathways of mast cells may also be indispensable to both types of immune response. The activation of mast cells by IL-33 and the ST2 receptor may occur as an innate or adaptive immune response, as the cytokine itself has been shown to mediate pathogenic conditions involving both (Haraldsen et al., 2009; Liew et al., 2010). As previously described, IL-33 initiates activation of the mast cell through its receptor, ST2. Upon binding of its ligand, the ST2 receptor dimerizes with IL-1RAcP to begin recruitment of adaptor proteins and propagate signal transduction downstream to promote synthesis of pro-inflammatory cytokines and other mediators imperative to mast cell activation during an immune response (Chackerian et al., 2007; Schmitz et al., 2005; Suzuki et al., 2002).

Activation of the mast cell can facilitate the aforementioned effector cell functions, such as opsonization or clearance of pathogens or release of mediators to induce vascular permeability, smooth muscle cell contraction or even collagen deposition by fibroblasts. However, it is prudent to recognize that activation of mast cells can also facilitate immunomodulatory functions of the mast cell described

previously. Through the release of certain mediators, mast cells can influence other immune cells to increase chemotaxis, maturation and differentiation. They can also present antigen to T-cells and promote immunoglobulin production by B-cells, particularly IgE (Gauchat et al., 1993). These functions are positive modulators of immune function, however, mast cells also possess negative immunomodulatory functions, most commonly by means of IL-10 production leading to immunosuppression; thus establishing mast cells as important regulators of the immune system (Frossi et al., 2010).

Mast Cells and Pulmonary Disease

Mast Cells in Asthma

Mast cells have been known to play a role in several pulmonary diseases including asthma and fibrosis. Asthma is defined by thickening of the basement membrane, airway hyperresponsiveness, and eosinophilic airway inflammation resulting in the release of Th2 cytokines; all responses which can be notably impacted by mast cells (Alkhouri et al., 2011). The symptoms and pathology of asthma, with the exception of airflow obstruction and airway hyperresponsiveness, are almost identical to those of eosinophilic bronchitis (Brightling et al., 2002). Additionally, significant infiltration of mast cells in the ASMC layers is found in asthmatic patients and markedly absent in patients with eosinophilic bronchitis or normal healthy individuals (Brightling et al., 2003a). Mast cell implication in the pathophysiology of asthma is mainly centered on the presence and location of mast cells in the lung tissue as well as the mediators they release. Mast cells are known to release Th2 cytokines such as IL-4 and IL-13, which

have been shown to contribute to airway inflammation during asthma through activation of receptors on ASMCs specific for these cytokines (Brightling et al., 2003b). The ability of mast cells to modulate airway smooth muscle (ASM) is further enhanced by co-localization in the ASM during asthma (Brightling et al., 2003b). The ASM can also secrete mediators to stimulate migration of immune cells, particularly mast cells, with the release of chemotactic factors such as CXCL10 and CX3CL1 (also known as Fractalkine or FKN) (Brightling et al., 2005; El-Shazly et al., 2006). Both these mediators have been known to induce chemotaxis through the CXCR3, a chemokine receptor on mast cells, which demonstrates a significantly increased expression in asthmatics compared to non-asthmatics (Brightling et al., 2005; El-Shazly et al., 2006).

Several studies have investigated different mast cell phenotypes and the potential phenotype-specific release of mediators in contributing to the pathogenesis of asthma. Increased numbers of mast cells found within ASMCs, previously identified as the MC_T phenotype, have been associated with increased levels of tryptase mRNA and protein in BALF of asthmatic patients (Brightling et al., 2005; Brightling et al., 2002). Mast cell tryptase is known to potentiate ASM hyperresponsiveness, an important and distinguishing feature in asthma pathophysiology (Sekizawa et al., 1989). It is important to note that the MC_T mast cell phenotype is typically expressed within the lungs, particularly the submucosa and epithelium of normal, non-asthmatic subjects (Balzar et al., 2011). In delineating mild and severe asthma, it was found that while mild asthmatics displayed this high infiltration of the normal MC_T mast cell phenotype, severe asthmatics displayed lower levels of total mast cells with a switch to the MC_{TC} phenotype, supported by a characteristic increase in carboxypeptidase CP3A and

prostaglandin D_2 (PGD_2) levels (Balzar et al., 2011; Lewis et al., 1982). Despite this decrease in total mast cells in patients suffering from severe asthma, levels of tryptase remained high in these asthmatics as mast cells of the MC_{TC} phenotype are known to produce 2-3 times more tryptase compared to MC_T phenotypes (Balzar et al., 2011; Schwartz et al., 1987). Unlike many tissue types, which exhibited a reduction in the number of mast cells in severe asthmatics, the pulmonary epithelium continued to display increased mast cell numbers, suggesting that the epithelium may contribute to the differentiation and survival of the MC_{TC} phenotype.

It has been suggested that epithelial cells may release mediators known to promote the development of the MC_{TC} phenotype, such as TGF-β and other Th2 cytokines (Balzar et al., 2011; Veldhoen et al., 2008). Thus, the location of mast cells, their phenotypes, as well as mediators they release, are all aspects that contribute to the pathogenesis of asthma.

Mast Cells in Pulmonary Fibrosis

Pulmonary fibrosis is often a characteristic of interstitial diseases and can manifest in several forms. One of the most common forms of pulmonary fibrosis is idiopathic pulmonary fibrosis and is attributed to an unknown cause. In pulmonary fibrotic conditions, an increase in mast cells has been identified and correlated with the degree of severity in fibrosis (Inoue et al., 1996; Pesci et al., 1993). Furthermore, tissue taken from pulmonary fibrosis patients displayed mast cells in young interstitial and alveolar connective tissues containing fibroblasts, and were determined to have fewer granules present (Pesci et al., 1993). The absence of normal numbers of granules

within mast cells suggests a correlation with increased levels of histamine, tryptase and other mast cell mediators found in BALF of patients with pulmonary fibrosis, often released during the process of chronic degranulation (Pesci et al., 1993). Several mast cell mediators, including tryptase, basic fibroblast growth factor (bFGF) and chymase, have been implicated in advancing pro-fibrotic pulmonary pathologies. The release of tryptase by mast cells has been shown to stimulate fibroblast proliferation and collagen synthesis through protease-activated receptor 2 (PAR-2) (Akers et al., 2000). Like tryptase, bFGF is a mediator released by pulmonary mast cells and largely associated with lung fibrosis (Inoue et al., 1996). Interestingly, bFGF release from the HMC-1 human mast cell line was determined to be an IgE-independent mechanism as HMC-1 cells lack complete and functional IgE receptors (Inoue et al., 1996). Another important factor in mast cell mediated fibrosis is chymase. Chymase is involved in modulating the pathogenesis of fibrosis partially through the activation of transforming growth factor beta (TGF-β), a pro-fibrotic mediator involved in the induction of fibrosis (Tomimori et al., 2003). Bleomycin-induced fibrosis in rats was significantly increased as indicated by elevated collagen accumulation, but significantly diminished in the presence of a chymase inhibitor and in a mast cell deficient (i.e. Ws/Ws) rat strain (Tomimori et al., 2003). In addition, it has also been suggested that the pulmonary fibrotic toxicities induced by paraquat dichloride, a widely used herbicide, is also mediated through mast cell chymase activation of TGF-β and Angiotensin II (Ang II) (Lang et al., 2010; Orito et al., 2004). The role of mast cell chymase has been established in the conversion of Ang I to Ang II in several tissue types including pulmonary tissue (Lindberg et al., 1997). Furthermore, Ang II induces a mitogenic response in human lung fibroblasts modulated

by TGF-β, facilitating pro-fibrotic conditions (Marshall et al., 2000). These studies provide potential roles for mast cells and their mediators in modulating the pathogenesis of pulmonary fibrosis.

Mast Cells and Environmental Exposures

The location of mast cells within various tissues has been proven to be pivotal in not only immune responses to pathogens, but also xenobiotic insults. As discussed previously, mast cells play a distinct role in innate immunity, often acting as the first line of defense in pathogen recognition and subsequent initiation of host defense mechanisms. Given the importance of mast cells in innate immunity, mast cells may also be critical immune cells in response to environmental exposures. Respiratory exposures to ambient particles, diesel exhaust particles, asbestos, silica and C60 have all implicated the involvement of mast cells in the resulting immune responses.

Ambient Particles

The adverse effects of ambient particulate matter (PM) are well known and have been reported to impact several physiological aspects including the respiratory system. Studies have shown a positive correlation between PM exposures and hospital visits for respiratory diseases including asthma and chronic obstructive pulmonary disease (COPD) (Atkinson et al., 2001; Peel et al., 2005). Several pulmonary and immune cell types, such as alveolar macrophages and bronchial epithelial cells, have been implicated in the production of IL-6, granulocyte-macrophage colony-stimulating factor (GM-CSF), macrophage inflammatory protein-1β (MIP-1β), monocyte chemotactic

protein-1 (MCP-1) and other pro-inflammatory mediators in response to PM exposure (Ishii et al., 2005). In addition to these cell types, mast cells have been shown to play an important role in amplifying the PM induced inflammatory response (Alfaro-Moreno et al., 2008). *In vitro*, co-cultures of macrophages, alveolar epithelial cells and endothelial cells demonstrate an increased granulocyte colony-stimulating factor (G-CSF), MIP-1β, IL-8, and IL-6 production in the presence of mast cells (Alfaro-Moreno et al., 2008). Of the mediators that are notably released, GM-CSF, G-CSF, MIP-1β and MCP-1 are well known to induce recruitment or proliferation of monocytes, macrophages and other granulocytes. Therefore, mast cells may be an important component in the initiation and sustained recruitment of inflammatory cells to PM exposure. As many of the adverse respiratory effects of PM exposure include asthma and other allergic responses, several studies have investigated mast cells in PM induced allergic responses. Ambient PM in conjunction with airborne allergen exposure has been reported to exacerbate allergic asthmatic responses in mice potentiated by sustained mast cell activation (Jin et al., 2011). Furthermore, organic dust exposed horses with equine heaves, similar to human occupationally or environmentally induced asthma, characterized with neutrophilic airway inflammation and obstruction, have demonstrated increased mast cell numbers in bronchial epithelium and tryptase production in BALF following an allergen challenge (Dacre et al., 2007).

Diesel Exhaust

Urbanization in many countries throughout the world has resulted in the rise of motor vehicle generated air pollutants. Diesel exhaust particles (DEP) contribute

significantly to the particulate matter emissions in urban areas, with particles that range from 20nm to 200nm in size, composed of hydrocarbons, metals, gases and other materials (Riedl and Diaz-Sanchez, 2005). Several studies have examined the health effects of DEP exposures. In healthy human volunteers from low particulate environments, BALF and bronchial tissue samples display neutrophil and mast cell infiltration, associated with increased pro-inflammatory mediators following short term DEP exposures (Behndig et al., 2006; Salvi et al., 1999). Moreover, an increase in mast cell activation was observed with DEP exposure as determined by a rise in BALF methyl histamine, a mast cell specific mediator known to mediate endothelial cell permeability and most likely contributing to the observed inflammatory cell infiltrates in peripheral blood (Salvi et al., 1999). In sensitized humans, DEP exposure augments allergic responses resulting in mast cell production of IL-4 and subsequently driving a Th2 response (Wang et al., 1999). The exacerbated Th2 response with DEP and antigenic challenge has also been observed in mice, particularly resulting in allergic eosinophilic airway inflammation. However, this response was notably absent in mast cell deficient mice, indicating the involvement of mast cells in mediating DEP inflammation and exacerbation of allergic responses (Ichinose et al., 2002).

Asbestos

The inhalation of asbestos fiber has been well characterized to induce pulmonary inflammation, fibrosis, and mesothelioma (Mossman et al., 2011; Padilla-Carlin et al., 2011). In rats, intratracheal exposure to chrysotile asbestos fibers resulted in peribronchial pulmonary fibrosis and an increase in mast cells within or surrounding the

fibrotic tissue projections, associated with a subsequent increase of serotonin and histamine release, a response that is ablated in rats not exposed to chrysotile (Keith et al., 1987). Similar data have been reported with crocidolite, amosite and anthophyllite asbestos fibers (Wagner et al., 1984). While the exact role of mast cells in asbestos-induced pulmonary toxicity is undefined, mast cells have been implicated in several pulmonary fibrotic diseases and thus may be involved in mediating the fibrotic toxicities observed following exposure to asbestos fibers.

Silica

The inhalation of crystalline silica, most commonly through occupational exposures, results in the development of silicosis, an interstitial lung disease characterized by fibrotic nodules, inflammatory cell infiltrates, thickening of the alveolar interstitium and the production of pro-inflammatory mediators such as TNF-α, TGF-β and IL-1 (Vanhee et al., 1995). Though the production of these cytokines has often been attributed to alveolar macrophages, mast cells have been shown to produce a similar array of mediators in the presence of silica including MCP-1, IL-13 and TNF-α (Brown et al., 2007). Furthermore, it has been established that mast cells are able to modulate the pulmonary effects of silica through the activation of scavenger receptors (Brown et al., 2007). In a clinical study, lung tissue of subjects occupationally exposed to silica not only demonstrated a significant increase in total pulmonary mast cells found to be near fibrotic nodules, but also found these mast cells to be positive for bFGF, correlating with the severity of fibrosis (Hamada et al., 2000). Additional studies have reported similar results with increased mast cell numbers in acute and intermediary

lesions representative of various fibrotic remodeling stages (Delgado et al., 2006). Mast cells may mediate the development of fibrosis and the remodeling of lung tissue through increased release and activity of mast cell proteases such as chymase, known to be involved in tissue remodeling and shown to decrease the severity of silica induced pulmonary toxicity when inhibited (Brown et al., 2007; Takato et al., 2011). The role of mast cells in mediating the pulmonary toxicities of silica exposure include the induction of inflammation through the production of pro-inflammatory cytokines as well as the modulation of fibrotic tissue through the increase in protease activity.

C60

C60 or fullerenes, like CNT and other engineered nanoparticles, can be functionalized and subsequently utilized in a plethora of applications such as drug delivery. The potential for the use of C60 in the medical field is due primarily to the capability of adding modified side chain functional groups to permit greater biocompatibility and thus allow for use in the treatment of a variety of disease pathologies (Satoh and Takayanagi, 2006). Interestingly, C60 has displayed uniquely favorable outcomes in modulating allergic responses for potential therapeutic purposes (Norton et al., 2010; Ryan et al., 2007). Water-soluble derivatives of C60, like those with tetraglycolic acid or N-ethyl moieties, were able to inhibit mast cell cytokine production and degranulation, due to the trafficking of fullerenes in mast cell endoplasmic reticulum and subsequent inhibition of calcium release, required for FcεRI receptor-mediated degranulation (Dellinger et al., 2010; Norton et al., 2010; Ryan et al., 2007). In vivo, these fullerene derivatives were able to attenuate mast cell-driven

anaphylaxis reactions and possibly provide a means for targeting the activation of mast cells and subsequent release of mediators during allergic responses (Norton et al., 2010; Ryan et al., 2007).

Goal of Research and Statement of Hypothesis

MWCNT have been shown to elicit pulmonary and cardiovascular toxicity including pulmonary inflammation, fibrosis, altered lung function, as well as exacerbated myocardial ischemia reperfusion injury. While several studies have investigated the pulmonary and cardiovascular toxicities, few have examined the means by which MWCNT elicit such adverse responses and the underlying mechanisms have remained elusive.

The goal of this research project was to identify and evaluate the mechanism(s) of MWCNT induced pulmonary and cardiovascular toxicities. Mast cells have previously been shown to mediate the toxicity of particles such as silica. In addition, the role of mast cells in several pulmonary and cardiovascular pathophysiologies including inflammation, fibrosis, remodeling, and allergic disease, has been clearly established. Thus, it was essential to examine the potential involvement of mast cells in modulating the MWCNT induced adverse effects resulting in pathological conditions. Furthermore, in elucidating the underlying mechanisms of toxicity, we identify a means of addressing the concerns of nanoparticle exposure, whether by alleviating adverse side effects of drug delivery systems that utilize MWCNT or by identifying targets of future therapeutics to treat MWCNT exposure. The impact of this research could provide crucial insight into many of the issues that currently impact the fields of nanotoxicology and nanotechnology.

Specific Aims

Aim 1: *Evaluate the development of pulmonary inflammation and fibrosis following instillation of MWCNTs in C57BL/6 and mast cell deficient B6.Cg-Kit$^{W\text{-}sh}$ mice.*

This specific aim will compare expression of pro-inflammatory and pro-fibrotic cytokines, histological changes and pulmonary function as indicators of fibrosis between C57BL/6 and B6.Cg-Kit$^{W\text{-}sh}$ mast cell deficient mice exposed to MWCNTs. B6.Cg-Kit$^{W\text{-}sh}$ mice reconstituted with bone marrow derived mast cells (BMMCs) will also be evaluated for the endpoints listed above to further confirm the differences between C57BL/6 and B6.Cg-Kit$^{W\text{-}sh}$ mast cell deficient mice.

Aim 2: *Establish the role of IL-33 and ST2 facilitated activation of mast cells in MWCNT mediated pulmonary fibrosis.*

This aim will test the hypothesis that MWCNT exposure results in an increase in lung epithelial production of IL-33, subsequent activation of mast cells through the ST2 receptors, resulting in increases in pulmonary inflammatory and fibrotic responses. Knockout mice for IL-33 and ST2 will be used to investigate cytokine expression, and histological changes to determine the role of IL-33 in MWCNT induce fibrosis.

Aim 3: *Identify specific mechanism(s) of MWCNT induced activation of mast cells in vitro via IL-33.*

This aim will test the hypothesis that IL-33 activates mast cells via the ST2 receptor to produce MWCNT induced adverse pulmonary fibrotic effects. BMMCs will be co-cultured with IL-33 producing lung epithelial cells to further examine mast cell activation and subsequent release of pro-fibrotic mediators with exposure to MWCNT.

Figure 1.1 IL-33 and ST2 Receptor Signaling Pathway

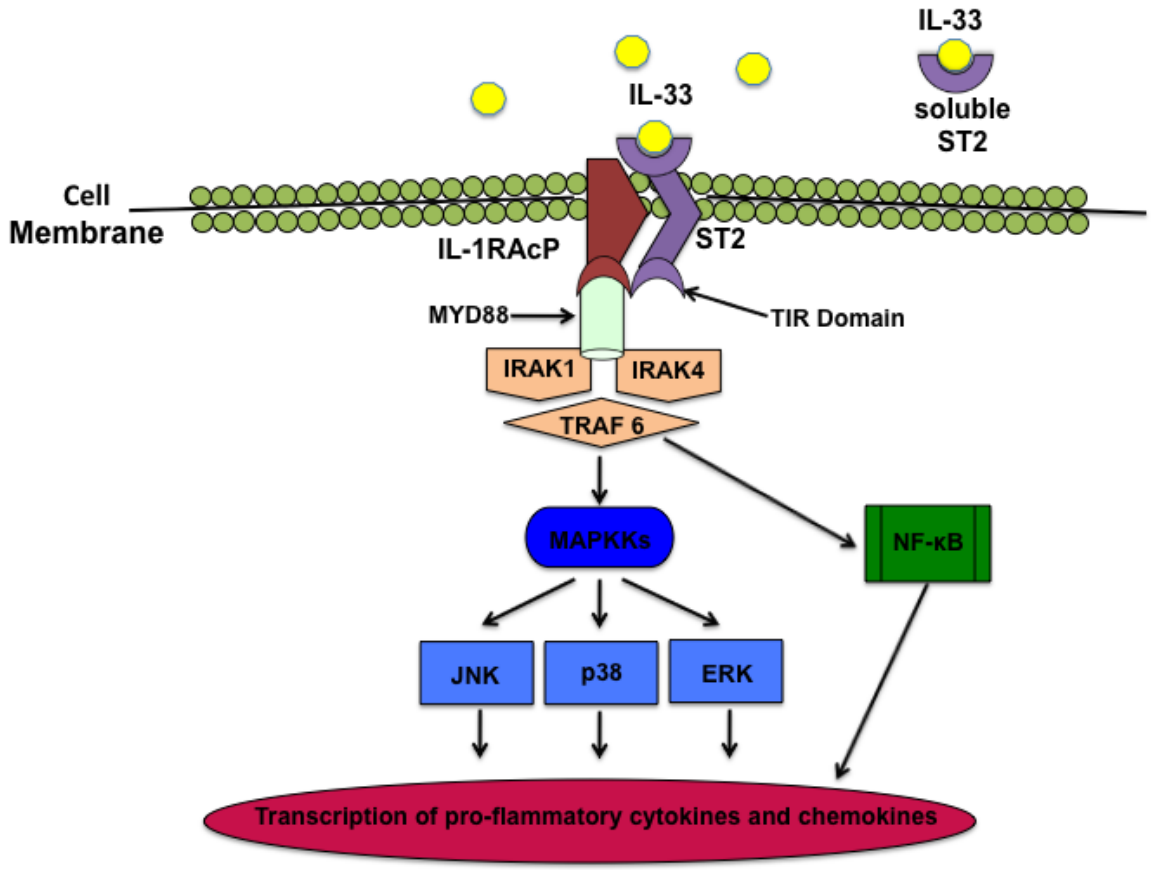
IL-33
IL-33
soluble
ST2
Cell
Membrane
IL-1RAcP
ST2
MYD88
TIR Domain
IRAK1
IRAK4
TRAF 6
MAPKKs
NF-κB
JNK
p38
ERK
Transcription of pro-flammatory cytokines and chemokines

CHAPTER 2: MULTI-WALLED CARBON NANOTUBE INSTILLATION IMPAIRS PULMONARY FUNCTION IN C57BL/6 MICE

PUBLISHED: Wang X, Katwa P, et al. Particle and Fibre Toxicology 2011, 8:24

SUMMARY

Background: Multi-walled carbon nanotubes (MWCNTs) are widely used in many disciplines due to their unique physical and chemical properties. Therefore, some concerns about the possible human health and environmental impacts of manufactured MWCNTs are rising. We hypothesized that instillation of MWCNTs impairs pulmonary function in C57BL/6 mice due to development of lung inflammation and fibrosis.

Methods: MWCNTs were administered to C57BL/6 mice by oropharyngeal aspiration (1, 2, and 4 mg/kg) and we assessed lung inflammation and fibrosis by inflammatory cell infiltration, collagen content, and histological assessment. Pulmonary function was assessed using a FlexiVent system and levels of Ccl3, Ccl11, Mmp13 and IL-33 were measured by RT-PCR and ELISA.

Results: Mice administered MWCNTs exhibited increased inflammatory cell infiltration, collagen deposition and granuloma formation in lung tissue, which correlated with impaired pulmonary function as assessed by increased resistance, tissue damping, and decreased lung compliance. Pulmonary exposure to MWCNTs induced an inflammatory signature marked by cytokine (IL-33), chemokine (Ccl3 and Ccl11), and protease production (Mmp13) that promoted the inflammatory and fibrotic changes observed within the lung.

Conclusions: These results further highlight the potential adverse health effects that may occur following MWCNT exposure and therefore we suggest these materials may pose a significant risk leading to impaired lung function following environmental and occupational exposures.

INTRODUCTION

The use of nanomaterials has been prominent in recent years due to their diverse properties and applications. Carbon nanotubes, in particular, possess the potential for numerous modifications and display unique physical and chemical properties, making them the ideal choice for product development in technological and biomedical industries (Martin and Kohli, 2003). Despite increasing use of carbon nanotubes, there is limited research on the potentially detrimental effects to human health and safety. In existing studies of carbon nanotube exposure in animal models, multi-walled carbon nanotubes (MWCNT) have been shown to potentiate allergic, inflammatory and fibrotic pulmonary responses. These effects have been associated with significant increases in pro-inflammatory cytokines such as IL-5, IL-6, IL-33 and others (Inoue et al., 2009). Inoue *et al.* determined that MWCNT exposure augments pulmonary inflammation induced by initial LPS activation of cytokines (Inoue et al., 2008). Post-exposure periods as early as 7 days have demonstrated increased collagen accumulation, development of granulomas and fibrosis in murine lungs exposed to MWCNT levels comparable to human exposure levels (Porter et al., 2010). Ma-Hock *et al.* showed similar data with MWCNT inhalation in rats 90 days post-exposure (Ma-Hock et al., 2009). Development of fibrotic tissue in lungs of mice exposed to MWCNT has been shown to correlate with increased macrophage and epithelial cell mediated production of platelet derived growth factor AA (PGDF-AA), a major mediator of pulmonary fibrosis (Cesta et al., 2010). In addition to inducing adverse pulmonary effects, exposure to MWCNTs has also been shown to augment pre-existing allergic responses. Ryman-Rassmusen *et al*. demonstrated that mice

exposed to MWCNT following ovalbumin sensitization developed significantly increased airway fibrosis and lung inflammation compared to mice that were not treated with MWCNTs but challenged with ovalbumin (Ryman-Rasmussen et al., 2009b). This suggests that pre-existing allergic conditions may predispose individuals to adverse effects of MWCNTs (Ryman-Rasmussen et al., 2009b). While these data validate the potential adverse effects, few studies have been conducted to confer these findings in the context of pulmonary physiology. A recent study by North *et al.* demonstrates altered pulmonary function with exposure to particulate matter (North et al., 2011). It was shown that in animals challenged with ovalbumin, exposure to ambient air particles augments airway resistance and hyperresponsiveness (North et al., 2011). While MWCNTs are known to augment pre-existing allergic conditions, they are also able to independently produce adverse pulmonary responses. However, the effects of MWCNTs on pulmonary function have yet to be determined.

Pulmonary function testing is a valuable tool to evaluate phenotypic characteristics of mouse respiratory disease that might be caused by nanoparticle exposure. Hamilton *et al.* have demonstrated that BALB/c mice exposed to carbon nanoparticles had increased airway hyperresponsiveness as measured by changes in PenH using barometric whole body plethysmography (Hamilton et al., 2008). This study suggests potential for nanoparticles to influence pulmonary function; however, alterations in specific lung function parameters have not been reported. The FlexiVent provides a method to directly measure pulmonary function via the use of preprogrammed ventilator and system-specific maneuvers such as forced oscillation technique (FOT) (Vanoirbeek et al., 2010). FOT measures the respiratory impedance

(Z) which is considered a detailed measurement of pulmonary mechanics (Glaab et al., 2007). FOT is an administration of small pressure oscillations at the airway opening using an external generator while simultaneously recording the oscillatory pressure and flow signals (Navajas and Farre, 2001; Shalaby et al., 2010). Respiratory impedance (Z) is a complex quantification represented by two components: respiratory resistance (Rrs) and reactance (Xrs). Rrs is derived from airways and lung tissue resistance, whereas Xrs is determined by the inertial (I) and elastic (E) properties of the respiratory system (Sellares et al., 2009). This technique provides a means of distinguishing central airways from peripheral airways and lung parenchyma.

In the current study, we tested the hypothesis that instillation of MWCNTs impairs pulmonary function in C57BL/6 mice due to development of lung inflammation and fibrosis. As will be shown, mice instilled with MWCNTs exhibited increased inflammatory cell infiltration, collagen deposition, and granuloma formation that led to deteriorating pulmonary function 30 days following instillation. Pulmonary exposure of MWCNTs induces an inflammatory signature marked by cytokine (IL-33), chemokine (Ccl3 and Ccl11), and protease (Mmp13) production which collectively promote inflammatory and fibrotic changes within the lung.

METHODS

Animals

Male C57BL/6 mice were obtained from Jackson Laboratories (Bar Harbor, ME, USA) at 9 to 10 weeks of age. The average weight of the C57BL/6 mice was 27.4 ± 0.58 g. Mice were randomly assigned to five groups (6-8 mice/group) which included naïve, vehicle (10% surfactant in saline), 1 mg/kg, 2 mg/kg, or 4 mg/kg MWCNTs. Mice received a single dose of MWCNTs by oropharyngeal aspiration of 1, 2, or 4 mg/kg body weight of MWCNTs or 10% surfactant in saline as vehicle control, following administration of isoflurane anesthesia (Wingard et al., 2011). Clinical grade surfactant (Infasurf) was kindly provided by ONY company (Amherst, NY, USA). Pulmonary function testing was performed on mice 30 days post-instillation. Following pulmonary function measurements mice were euthanized for bronchoalveolar lavage and collection of lung tissue. All animal procedures were conducted in accordance with the National Institutes of Health guidelines and approved by the East Carolina University Institutional Animal Care and Use Committee. All animals were treated humanely and with regard for alleviation of suffering.

MWCNT Characterization

Commercial grade multi-walled carbon nanotubes were generously provided by NanoTechLabs, Inc (Yadkinville, NC). We performed transmission and scanning electron microscopy studies using Hitachi H-9500, S-4800 microscopes to obtain length, diameter distribution and elemental composition. Raman spectra were obtained using Ar+ ion excitation at 514.5 nm coupled with a Dilor XY triple grating monochromator

equipped with thermoelectric cooled CCD. The surface area, pore volume and pore size distribution of the MWCNTs were obtained using a physisorption analyzer (Micromeritics ASAP 2010) and derived based on the Brunauer-Emmett-Teller (BET) equation (Brunauer, 1938) and the Barrett–Joyner–Halenda (BJH) method (Barrett, 1951). The MWCNTs were dispersed in a saline solution containing 10% surfactant at 2 µg/µl and the mixture was bath-sonicated (1510R-MTH, Branson Ultrasonics Corp.) for 45 minutes to obtain a suspension. The hydrodynamic size distribution, a parameter describing the effective diameter of a diffusing particle, was characterized using dynamic light scattering (Nanosizer S90, Malvern Instruments). The zeta potential and isoelectric point (IEP) are primary indicators for describing the surface charge and stability of MWCNT suspension, and were determined using a zeta potential device (Zeta ZS, Malvern Instruments) with the pH value of the suspension adjusted from 2 to 7 using HCl.

Thermogravimetric analysis

The thermogravimetric analysis of our MWCNT was carried out in a Perkin Elmer Thermogravimetric Analyzer Pyris 1 TGA. About 40-50 % of the volume of the platinum pan was filled with MWCNTs. The sample was then heated from 30°C up to 800°C at a heating rate of 20°C/min in an air atmosphere using an air flow rate of 20 ml/min. The final goal of this analysis was to determine the ash content of each sample. The following thermograms (Figure 2.2) confirm that ~4.8 wt% of catalyst was present in the sample.

Elemental Analysis

In order to confirm the catalyst composition, we obtained energy dispersive X-ray spectra of our samples on Hitachi S-4800 scanning electron microscope. The results reveal a Fe Ka line ~ 6.40 eV confirming the presence of Fe catalyst particles in our sample (See Figure 2.3).

Pulmonary Function Testing

Thirty days following instillation of MWCNTs, all mice were anesthetized, tracheostomized, and placed on the FlexiVent system (SCIREQ, Montreal, QC, Canada) for forced oscillatory measurements. Mice were anesthetized with tribromoethanol (TBE) (400 mg/kg) and paralyzed with pancuronium bromide (1 mg/kg) to prevent spontaneous breathing. Mice were ventilated with a tidal volume of 10 mL/kg at a frequency of 150 breaths/min and a positive end expiratory pressure of 3 cm H_2O to prevent alveolar collapse. Total lung capacity (TLC), Snapshot, Quickprime-3, and pressure-volume (PV) loops with constant increasing pressure (PVr-P) were consecutively performed using the Flexivent system. A TLC perturbation maximally inflates the lungs to a standard pressure of 30 cm H_2O followed by a breath hold of typically a few seconds to establish a consistent volume history. A snapshot perturbation maneuver uses a three-cycle sinusoidal wave of inspiration and expiration to measure total respiratory system resistance (R), dynamic compliance (C), and elastance (E). A Quickprime-3 perturbation, which produced a broadband frequency (0.5 to 19.75 Hz) over 3 seconds, measures Newtonian resistance which is a measure of central airway resistance (Rn), inertance (I), tissue damping (G), tissue elastance (H)

and hysteresivity (eta). PV loops were generated between 30 cm H_2O to -30 cm H_2O pressure to obtain vital capacity (A), the upper portion of the deflation PV curve (K), quasi-static compliance (Cst) and elastance (Est), and the area of PV loop (Area). All perturbations were performed until three acceptable measurements with coefficient of determination (COD) ≥ 0.9 were recorded in each individual subject.

BAL and Cell Differential Counts

After measuring pulmonary function parameters, the right lung of each mouse was lavaged *in situ* four times with a specific volume (26.25 mL/kg body weight) of ice-cold Hanks balanced salt solution (HBSS). The first aliquot of bronchoalveolar lavage fluid (BALF) was collected separately for cytokine analysis, while aliquots 2-4 were pooled. All BALF was centrifuged at 1000 g for 10 min at 4^{o}C. Total cells from all lavages were pooled and counted and 20,000 cells were centrifuged using a Cytospin IV (Shandon Scientific Ltd., Cheshire, UK) and stained with a three-step hematology stain (Richard Allan Scientific, Kalamazoo, MI, USA). Cell differential counts were determined by morphology with evaluation of 300 cells per slide.

Lung Histopathology

Unlavaged left lungs from C57BL/6 mice in each treatment group were inflated with 10% neutral buffered formalin fixative for 24-72 hrs. Lung tissue was then cut, processed, and embedded in paraffin, and 5 μM sections were mounted on slides. Sections were stained with hematoxylin and eosin (H&E) or Masson's trichrome stain to detect inflammatory, morphological changes and collagen deposition.

Sircol Collagen Assay

Soluble collagen content within total lung was determined using the Sircol Collagen Assay (Biocolor, Belfast, UK). Lavaged right lung was collected and homogenized in 2 mL of RIPA buffer including protease inhibitors. Supernatants were collected from each sample after centrifugation at 10,000 g for 10 minutes at 4°C. Sircol dye reagent (1 mL) was added to 50 µL of each sample or varying concentrations of collagen standard to generate a calibration curve. Following a 30 min incubation period, samples were centrifuged at 10,000 g for 10 minutes. The collagen-dye precipitate was reconstituted in 1 mL of alkali reagent and absorbance was read at 540 nm and total collagen content was calculated from the standard curve.

Mouse Fibrosis PCR-Array

Total RNA from left lung tissue of additional mice was isolated using a Qiagen RNeasy Mini Kit (Qiagen, Valencia, CA, USA) according to the manufacturer's recommendations. Total RNA (2.5 μg) was reverse-transcribed to cDNA using SABiosciences's RT^2 First Strand Kit (Qiagen, Frederick, MD, USA) and applied to Mouse Fibrosis PCR Arrays (Cat.# PAMM-120; 96-well format) following SABiosciences recommendations. Real-time PCR were performed in an Applied Biosystems StepOnePlus Real-Time PCR System (ABI, Foster City, CA, USA). Data were interpreted using SABiosciences' web-based PCR array analysis tool.

qPCR

Total lung RNA was reverse transcribed using a QuantiTect reverse transcription kit (Qiagen). Quantitative real-time PCR was performed using QuantiTect primer assays and SYBR green master mix to verify expression of Ccl3, Ccl11, Mmp13, and IL-33 found in the mouse fibrosis PCR-array. An Applied Biosystems StepOnePlus Real-Time PCR System (ABI) was used to obtain cycle threshold (Ct) values for target and internal reference cDNA levels. Target cDNA levels were normalized to GAPDH, an internal reference, using the equation $2^{-[\Delta Ct]}$, where ΔCt is defined as Ct_{target}- $Ct_{internal\ reference}$. Values shown are the average of six independent experiments.

ELISA and MMP13 Activity Assays

Chemokine (CCL3 and CCL11) and cytokine (IL-33) levels were quantified in BALF using DuoSet ELISA kits (R&D Systems, Minneapolis, MN) in accordance with the manufacturer's instructions. MMP13 activity assays were performed using SensoLyte® MMP-13 Assay Kit (AnaSpec, San Jose, CA). BALF (50 µL) containing MMP13 was activated with 1 mM 4-aminophenylmercuric acetate (APMA) and the assay was performed according to the manufacturer's recommendations. Fluorescence, resulting from enzyme-mediated conversion of the fluorogenic substrates, was immediately measured by a Synergy™ HT Multi-Detection Microplate Reader (BioTek, Winooski, VT) using black, round-bottom 96-well plates (Corning, Corning, NY) and continuously recording data every 5 min for 60 min. The relative fluorescence unit (RFU) was calculated by subtracting fluorescence in the substrate control well from all experimental wells. The MMP13 activity of test samples was calculated as the initial reaction velocity (V_o) in RFU/min.

Statistical Analyses

All data are presented as means ± SEM and were analyzed by one-way ANOVA, with differences between groups assessed using Bonferroni *post hoc* tests. Graphs and analysis were performed using GraphPad Prism 5 software (GraphPad, San Diego, CA). Differences were considered statistically significant at $p < 0.05$.

RESULTS

MWCNT Characterization

Our electron microscopy studies revealed that the MWCNTs used in this study were several microns long with a bi-modal diameter distribution exhibiting peaks at ~12.5 and 25 nm (Figures 2.1A, 2.1B & 2.1C). In MWCNT Raman spectra, the presence of strong disorder band ~1350 cm^{-1} indicates the defective nature of the nanotubes. Specifically, the ratio ($R=I_D/I_G$) between the intensity of disorder band (D-band) and graphite-like band (G-band) was found to be 0.65 (Figure 2.1D). The elemental analysis indicated presence of Fe catalyst in MWCNT samples (Figure 2.2 & 2.3). Further, the TGA studies showed that the MWCNT samples possess ~ 5 wt% of Fe catalyst (Figure 2.2 & 2.3). The surface area of the MWCNTs was determined to be 113.103 m^2/g, based on the BET equation. The pore volume of the MWCNTs, defined as the ratio of the MWCNTs' air volume to their total volume, was determined to be 0.688 cm^3/g utilizing the BJH method. The hydrodynamic sizes of the MWCNT suspension displayed two peaks, a major one at 200 ± 50 nm and another at 1,000 ± 150 nm (Figure 2.4A). The larger sized peak was caused by the bundling of the nanotubes through hydrophobic interaction and pi-stacking. The MWCNT suspension displayed a zeta potential of -44.6 mV, suggesting a very stable colloidal state of the nanomaterial.

MWCNTs Induce Pulmonary Inflammation and Granuloma Formation in C57BL/6 Mice

To investigate the inflammatory effects of MWCNT exposure that may be associated with function changes, C57BL/6 mice treated with 10% saline/surfactant or increasing doses of MWCNTs underwent bronchoalveolar lavage (BAL) 30 days post-exposure. Differential cell counts obtained from BAL demonstrated persistent inflammation with pulmonary infiltration of multiple cell types (Table 2.1). Statistically significant elevations in macrophage, epithelial cell, and neutrophil numbers were observed in animals exposed to the highest dose MWCNT (4 mg/kg), along with an overall increase in total cell recruitment ($p<0.001$). Exposure to both the 1 and 2 mg/kg MWCNT treatments displayed significant increases in epithelial and neutrophil cell counts ($p<0.05$) compared to mice treated with vehicle. Increases in eosinophil numbers were observed with MWCNT exposure, but did not reach significance compared to control mice. Histological evaluation of lung sections confirmed the altered inflammatory cell profile and additionally revealed increased collagen deposition as well as changes in lung morphology following MWCNT aspiration. Quantification of collagen content within lung tissue demonstrated a significant increase in MWCNT (4 mg/kg) exposed mice compared to naïve mice (Figure 2.5). However, no statistically significant difference was found between vehicle and MWCNT treated mice, nor was there a statistical difference between naïve and vehicle treated mice. Oro-pharyngeal aspiration of MWCNTs resulted in wide distribution of granulomatous foci containing MWCNT agglomerates and MWCNT laden macrophages throughout the lung parenchyma (Figure 2.6B) as well as peribronchiolar and perivascular regions (Figure 2.6B, 2.6D & 2.6F). In contrast, mice exposed to vehicle control did not display any inflammation or granulomas (Figure 2.6A, 2.6C, & 2.6E).

Instillation of MWCNTs in C57BL/6 Mice Elicits Dose-Dependent Changes in Pulmonary Function

To determine if MWCNT exposure elicits any physiologically relevant toxicity, we examined pulmonary function in C57BL/6 mice following instillation of vehicle, 1, 2, or 4 mg/kg of MWCNTs. As shown in Figure 2.7, the snapshot perturbation (Figure 2.7A, 2.7B & 2.7C) in C57BL/6 mice revealed a dose-dependent pulmonary response to MWCNT instillation with a statistically significant increase in R compared to vehicle treated and naïve mice (Figure 2.7A). Further, MWCNT instillation led to a statistically significant decrease in C as compared to the naïve mice, but this did not reach significance as compared to vehicle treated mice (Figure 2.7C). The quick-prime 3 perturbation (Figure 2.7D, 2.7E & 2.7F) further demonstrated a moderate dose dependent pulmonary response to MWCNTs with increases in Rn, G, and eta following pulmonary instillation of 1, 2, or 4 mg/kg MWCNTs. Mice treated with 4 mg/kg MWCNTs displayed significant increases in tissue damping (G) (Figure 2.7E) and hysteresivity (eta) (Figure 2.7F) compared to both the naïve and vehicle groups. Meanwhile, both G and eta displayed a significant dose dependent response to MWCNTs.

The PVr-P loop perturbations showed dose-dependent decreases in the deflating PV loop (K) (Figure 2.8B) and static compliance (Cst) (Figure 2.8C). Both reductions of K and Cst were statistically significant in the 4 mg/kg treated group compared to naïve mice; however, the change in Cst was not statistically different from vehicle control. As expected, Est showed the opposite trend as Cst, but differences between treatment

groups were not statistically significant. In contrast, the area between the limbs of the PV loop displayed a statistically significant increase in the 4 mg/kg treated mice compared to the vehicle group (Figure 2.8E), but was not statistically different from naïve or other MWCNT treated mice. No statistically significant differences were found between naïve and vehicle treated mice in Figure 2.7 and Figure 2.8.

Ccl3, Ccl11, Mmp13 and IL-33 are Increased in the Lungs and BALF of C57BL/6 Mice instilled with MWCNTs

To assess potential mechanisms involved in MWCNT directed pulmonary inflammation, fibrosis and alteration of lung function, we employed a mouse fibrosis PCR array to investigate the expression of 84 keys genes associated with fibrosis. Gene expression was analyzed using unlavaged lung tissue homogenates from mice exposed to vehicle or 4 mg/kg MWCNT. Messenger RNA levels of multiple fibrotic mediators that were up- or down-regulated > 2 fold in MWCNT instilled mice are shown in Table 2.2. To verify PCR array data on dose dependent changes in gene expression induced by MWCNT exposure, mRNA levels of *Ccl3*, *Ccl11*, and *Mmp13* were analyzed in vehicle, 1, 2, and 4 mg/kg MWCNT instilled mice. As shown in Figure 2.9, mRNA levels of *Ccl3*, *Ccl11*, and *Mmp13* were increased in all MWCNT-treated groups with a statistically significant increase observed in the 2 mg/kg MWCNT group compared to vehicle control.

In addition to mRNA levels of *Ccl3*, *Ccl11*, and *Mmp13*; we assessed protein levels of chemokines, Ccl3 (Mip1α) and Ccl11 (eotaxin), and activity levels of Mmp13 in BALF of vehicle and MWCNT instilled mice. Similar to mRNA levels, both Ccl3 and

Ccl11 levels were elevated in MWCNT instilled mice but did not reach significant levels when compared to vehicle treated mice (Figures 2.10A & 2.10B). Thirty days post-MWCNT instillation, we observed dose-dependent increases in Mmp13 levels as well as collagenase activity in BALF from MWCNT instilled mice with statistically significant increases in the 4 mg/kg MWCNT instilled mice compared to vehicle control (Figures 2.10C & 2.10D).

In addition to mRNA levels of *Ccl3*, *Ccl11*, and *Mmp13*; we assessed protein levels of chemokines, Ccl3 (Mip1α) and Ccl11 (eotaxin), and activity levels of Mmp13 in BALF of vehicle and MWCNT instilled mice. Similar to mRNA levels, both Ccl3 and Ccl11 levels were elevated in MWCNT instilled mice but did not reach significant levels when compared to vehicle treated mice (Figures 2.10A & 2.10B). Thirty days post-MWCNT instillation, we observed dose-dependent increases in Mmp13 levels as well as collagenase activity in BALF from MWCNT instilled mice with statistically significant increases in the 4 mg/kg MWCNT instilled mice compared to vehicle control (Figures 2.10C & 2.10D).

To further investigate mechanisms involved in the inflammatory response, we identified IL-33, a novel alarmin and Th2 cytokine, as a potential mediator in MWCNT induced pulmonary inflammation. While no dose dependent change was evident, gene expression analysis of lung tissue from mice 30 days post-exposure to 1, 2, or 4 mg/kg MWCNTs demonstrated a statistically significant >2-fold induction in *Il-33* (Figure 2.11A). Similarly, assessment of IL-33 protein expression in BALF exhibited a statistically significant increase for all dose groups compared to the vehicle control

(Figure 2.11B). There were no significant differences in *Il-33* gene expression or protein levels between MWCNT dose groups.

Table 2.1 Effect of MWCNT instillation on pulmonary cell populations in C57BL/6 mice

Treatment	Macrophages ($x10^3$)	Epithelial Cells ($x10^3$)	Neutrophils ($x10^3$)	Eosinophils ($x10^3$)	Lymphocytes ($x10^3$)	Total Cells ($x10^3$)
Vehicle	113.71 ± 11.51	22.60 ± 3.80	0.18 ± 0.09	0.25 ± 0.14	0.05 ± 0.05	136.77 ± 11.68
1mg/kg MWCNT	247.4± 20.77	22.0 ± 5.39^{Ŧ}	0.50 ± 0.25^{Ŧ}	0.66 ± 0.35	2.55 ± 1.90	273.17 ± 21.58
2mg/kg MWCNT	230.75 ± 52.41	18.85 ± 1.78^{Ŧ}	2.35 ± 1.24^{Ŧ}	1.55 ± 1.03	0.10 ± 0.10	253.60 ± 54.36.
4mg/kg MWCNT	331.62 ± 61.92**	59. 54 ± 6.34**	16.17 ± 3.90**	2.87 ± 1.67	1.24 ± 0.67	441.28± 68.13**

Values are mean ± SEM. N=6/group; *$p < 0.01$ vs vehicle; **$p < 0.001$ vs vehicle, $^{Ŧ}p < 0.05$ vs 4mg/kg MWCNT*

Figure 2.1 Characterization of MWCNT in Dry Powder Form

Characterization of multi-walled carbon nanotubes was determined using electron microscopy and Raman spectroscopy. (A & C) The diameter of the MWNCTs was determined by measuring individual nanotubes visualized by TEM. (B) This SEM image shows a bundle of MWCNTs, with individual nanotubes indicated by arrows. The length of individual nanotubes was determined to be several μm long using SEM. (D) The Raman spectrum of MWCNT obtained using 514.5 nm laser excitation. The presence of strong disorder band (I_D/I_G peak ratio) suggests the existence of structural defects as determined by Raman spectroscopy.

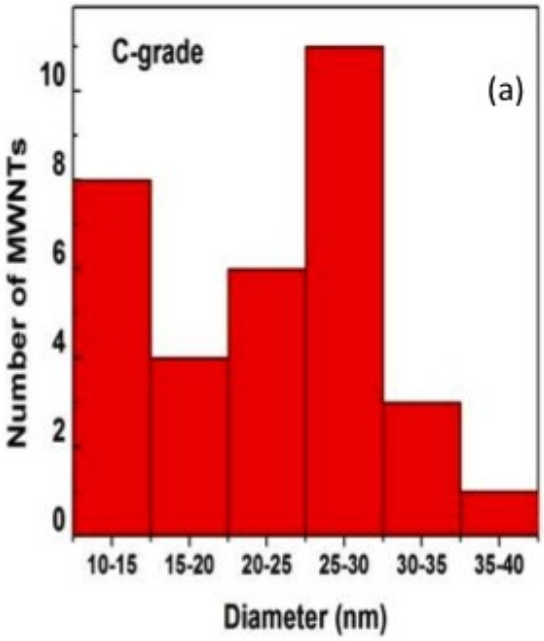
C-grade
(a)
Number of MWNTs
0
2
4
6
8
10
10-15
15-20
20-25
25-30
30-35
35-40
Diameter (nm)

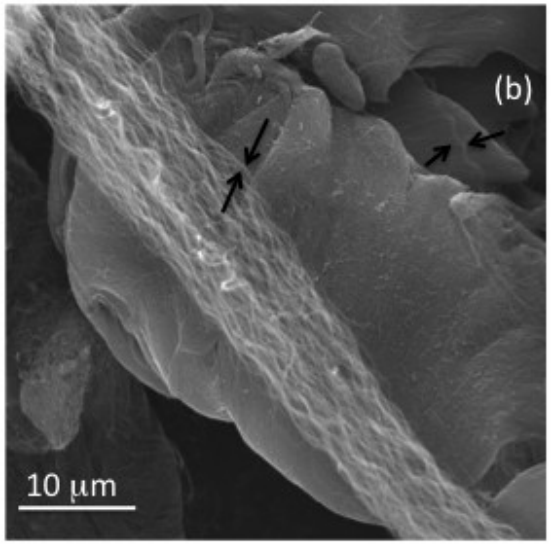
(b)
10 μm

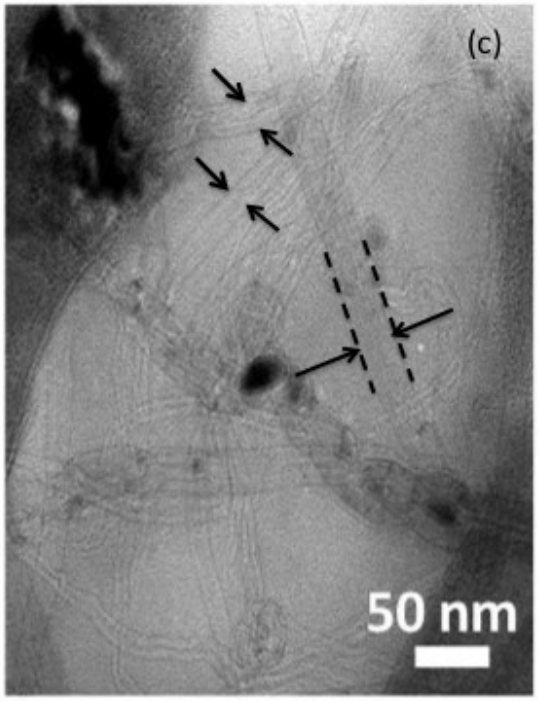
(c)
50 nm

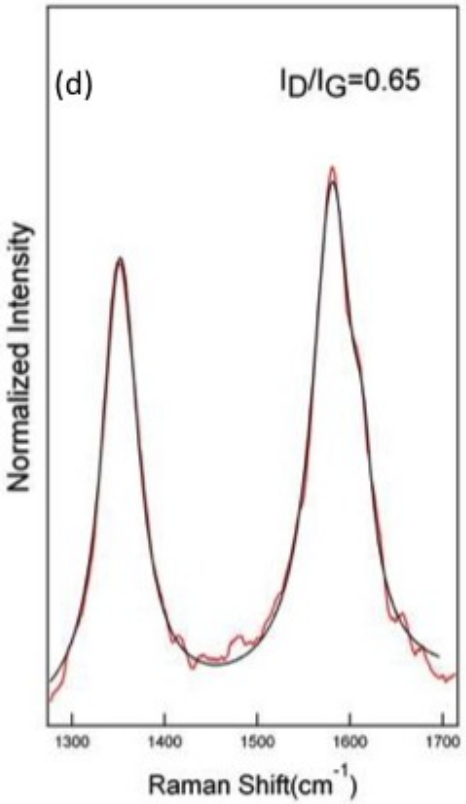
(d)
I_D/I_G=0.65
Normalized Intensity
1300
1400
1500
1600
1700
Raman Shift(cm^{-1})

Figure 2.2 Thermogravimetric analysis

The thermogram for MWCNT used in this study reveals that the catalyst amounts to ~4.8 wt% of the sample

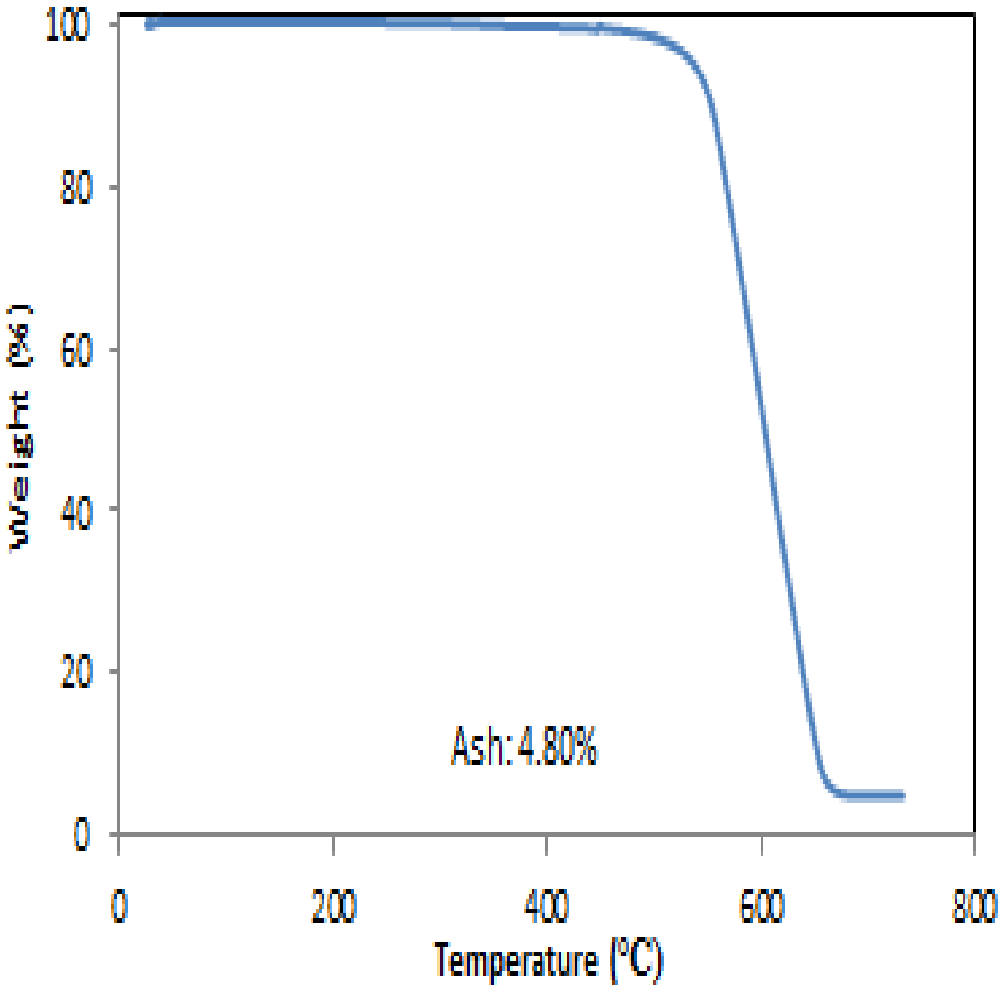
100
80
60
40
20
0
Weight (%)
Ash: 4.80%
0
200
400
600
800
Temperature (°C)

Figure 2.3 Elemental Analysis of MWCNT

The top panel shows the region of the sample used for obtaining the energy dispersive X-ray spectra. The bottom panel shows the presence of C or carbon (from MWCNTs and the SEM tape) along with the presence of Fe catalyst.

Figure 2.4 Characterization of MWCNT in Suspension

The size and charge characteristics of the MWCNTs were determined in a suspension of 10% surfactant saline. (A) The size of MWCNT bundles in suspension was determined by dynamic light scattering. (B) The zeta potential and isoelectric point (indicated by the arrow) were determined for the MWCNTs suspended in 10% surfactant saline solution.

A

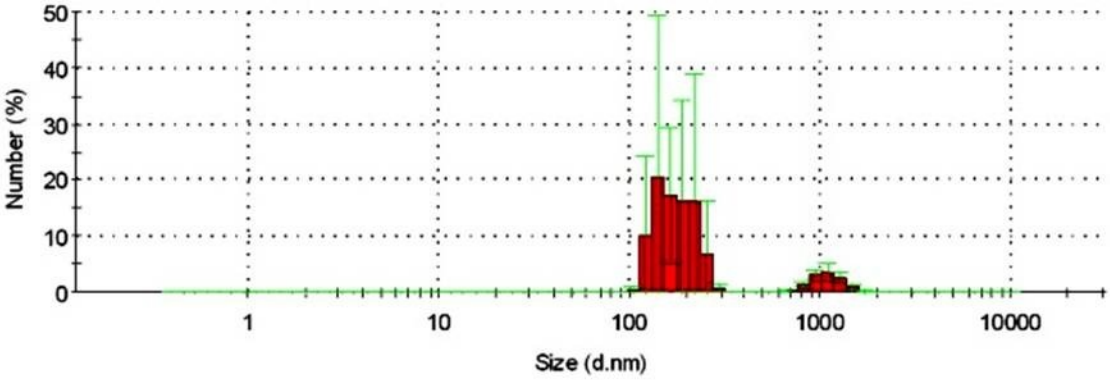
Number (%)
50
40
30
20
10
0
1
10
100
1000
10000
Size (d.nm)

B

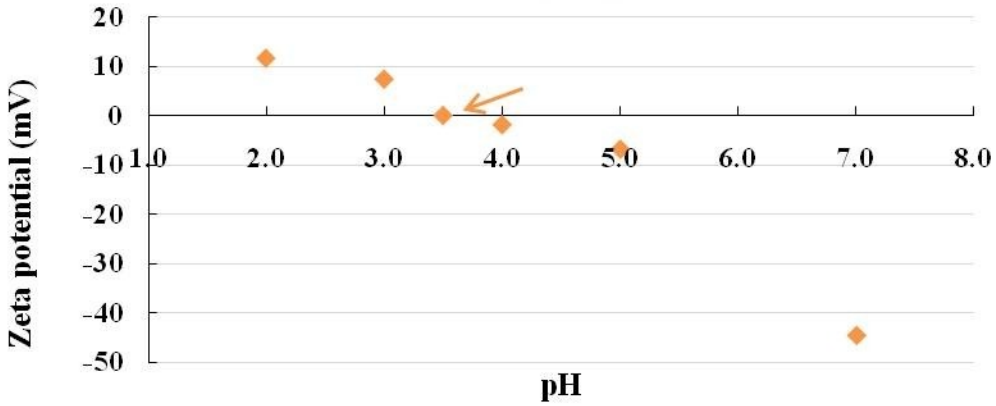
Zeta potential (mV)
20
10
0
-10
-20
-30
-40
-50
1.0
2.0
3.0
4.0
5.0
6.0
7.0
8.0
pH

Figure 2.5 Increased collagen content in lung tissue of MWCNT exposed C57BL/6 mice

Collagen content was determined by lung tissue harvested from mice 30 days post-exposure to vehicle control (10% surfactant in saline) or MWCNTs (1, 2, or 4 mg/kg). Mice exposed to the high dose MWCNT (4 mg/kg) displayed significant increase in collagen levels compared to naïve mice. All values are expressed as mean ± SEM (n=6-11). $^{*}p < 0.05$ compared to naïve mice and $^{+}p < 0.05$ compared between two groups. No significant differences were found between naïve and vehicle treated groups. In addition, differences between vehicle and treatment groups were not significant.

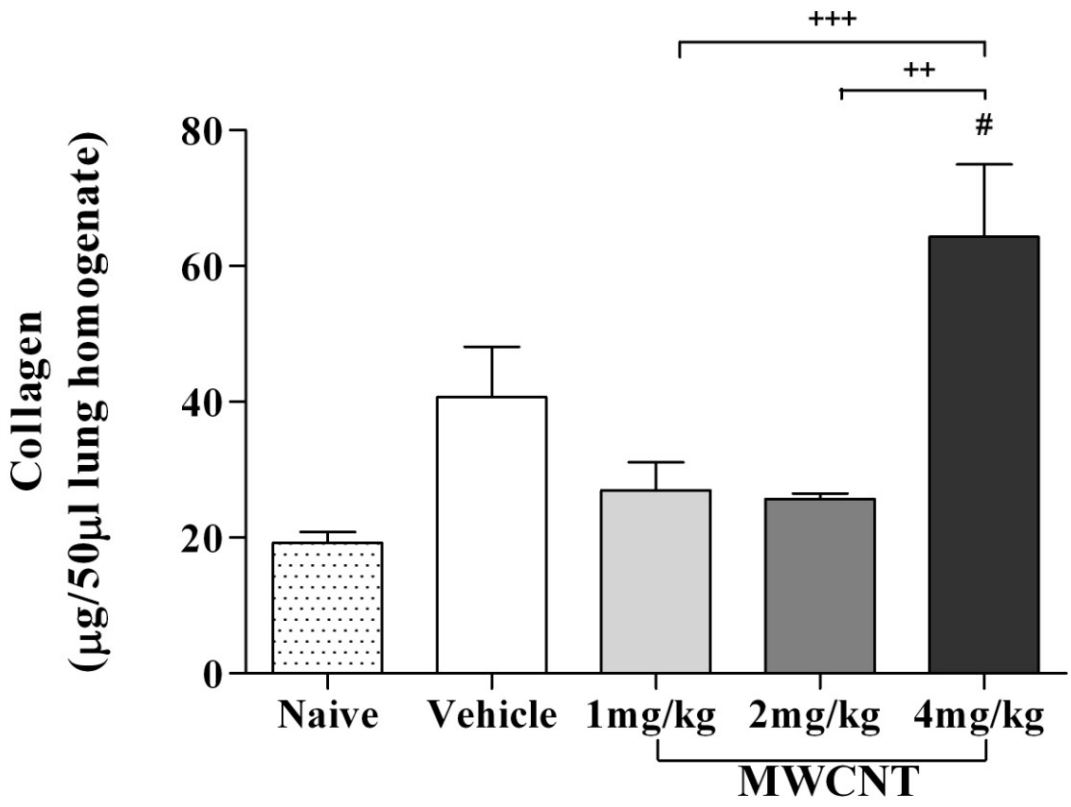
+++
++
#
80
60
40
20
0
Collagen
(μg/50μl lung homogenate)
Naive
Vehicle
1mg/kg
2mg/kg
4mg/kg
MWCNT

Figure 2.6 Histopathology of lungs exposed to MWCNT displays granulomatous and fibrotic tissue at 30 days post-exposure

Mice instilled with (A) 10% saline in surfactant vehicle control display normal lung morphology while mice instilled with (B) 4mg/kg MWCNTs exhibit widely dispersed deposition of MWCNT aggregates within lung tissue. Masson's trichrome staining shows collagen rich granulomas and surrounding fibrotic tissue (blue) in lungs of mice exposed to (D) MWCNTs, but not (C) vehicle control. H&E staining demonstrates granulomatous peribronchiolar foci in lungs of mice exposed to MWCNT (F) but not vehicle (E). Agglomerates of MWCNT within granulomas are indicated by arrows. Images are representative of 4 mice per group with original magnifications of 25x (A-B), 200x (C-D) and 400x (E-F).

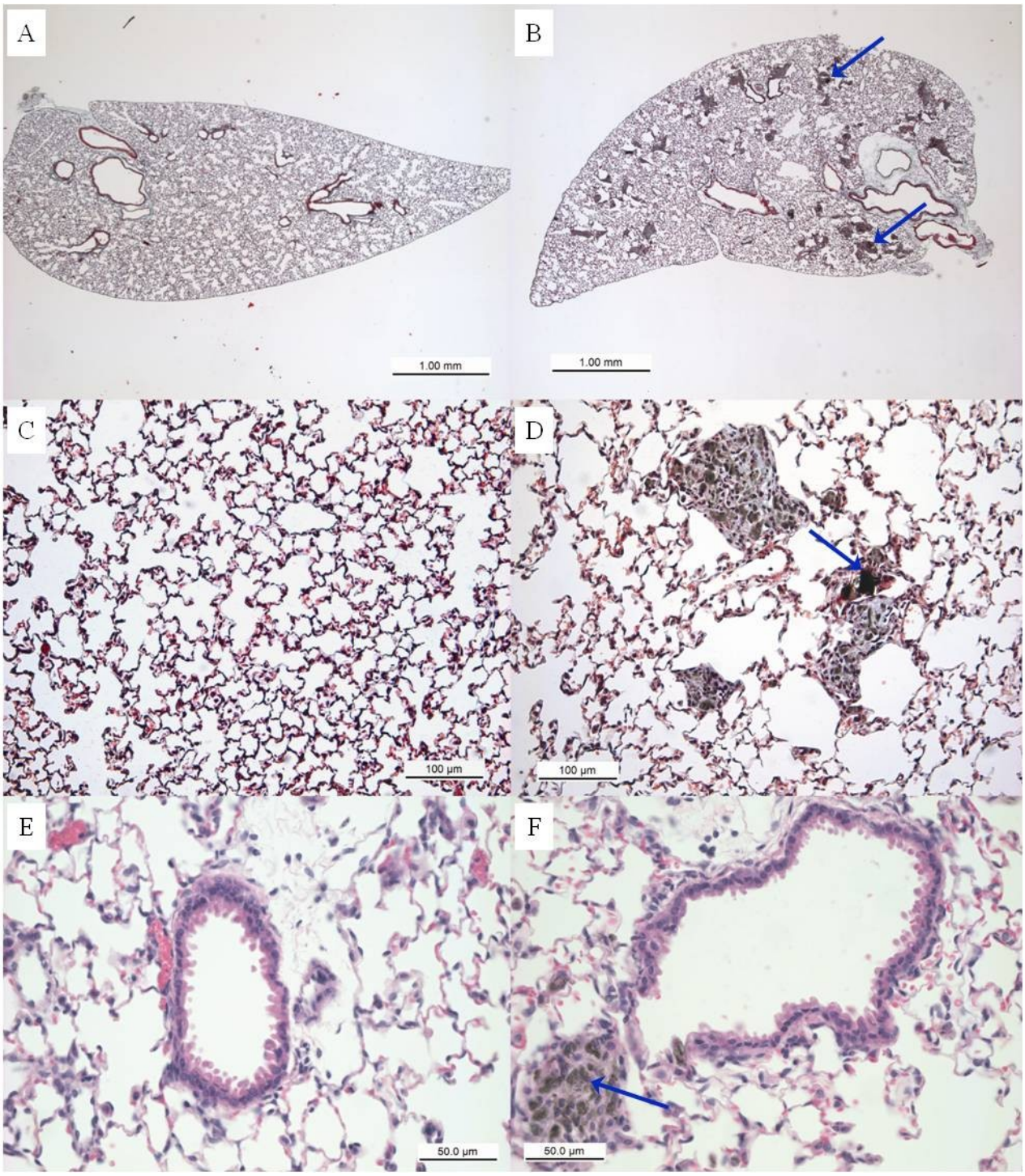
A
B
1.00 mm
1.00 mm
C
D
100 µm
100 µm
E
F
50.0 µm
50.0 µm

Figure 2.7 Impaired pulmonary function as determined by Snapshot and Quick-prime 3 perturbation after MWCNT instillation

The Snapshot and Quick-prime3 perturbations were performed in tracheotomized C57BL/6 mice instilled with increasing doses of MWCNTs. Since Snapshot perturbation measures the lung as a single compartment, the parameters, R (A), E (B), and C (C), are indicative of the whole respiratory system including lung and chest wall. On the other hand, Quick-prime 3 perturbation measures the lung as multiple compartments. The parameters can differentiate between central airway (Rn (D)) and peripheral lung tissue (G (E) and eta (F)). The mean ± SEM of six mice per group are shown, $*p < 0.05$ and $** p < 0.01$ compared with the naïve mice, $^{\#} p < 0.05$ and $^{\#\#} p < 0.01$ compared with the vehicle control (10% surfactant in saline) mice; $^{+} p < 0.05$, $^{++} p < 0.01$, and $^{+++} p < 0.001$ compared between two groups. No statistically significant differences were found between naïve and vehicle treated mice.

Snapshot perturbation

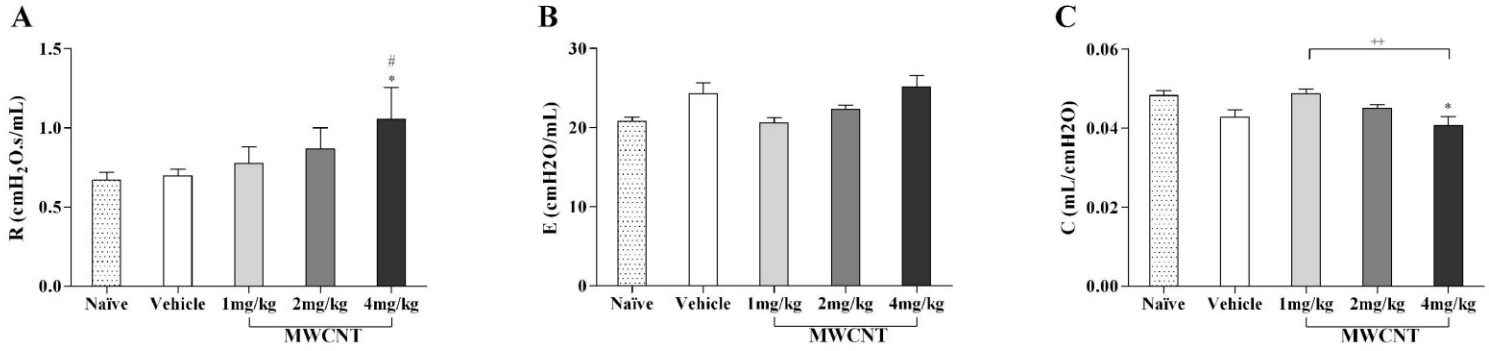

Quick-prime 3 perturbation

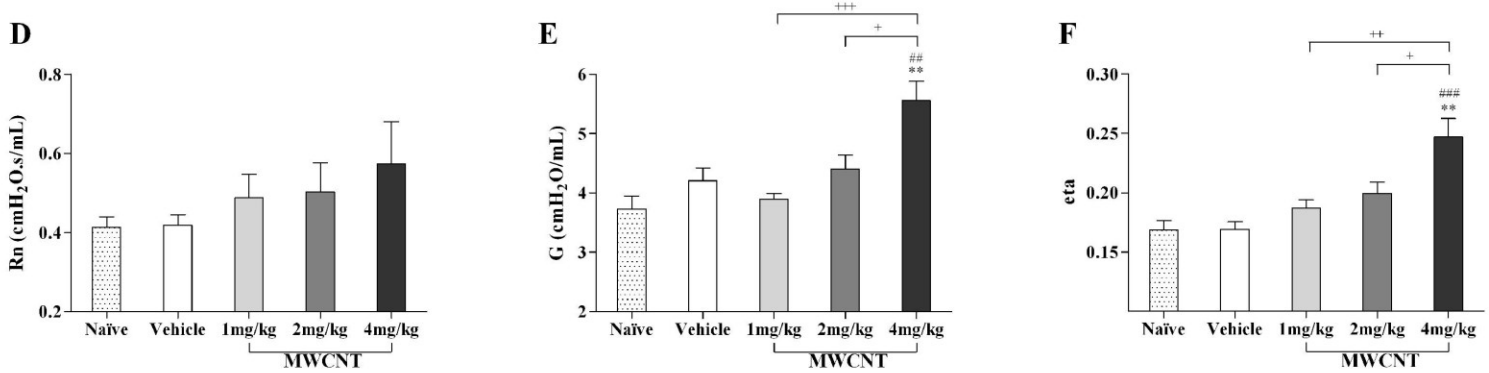

Figure 2.8 Impaired pulmonary function as determined by PVr-P perturbation after MWCNT instillation

The PVr-P perturbation was performed in tracheotomized C57BL/6 mice instilled with vehicle (10% surfactant in saline) or increasing doses of MWCNTs. From PV loops, perturbation parameters, (A) A, (B) K, (C) Cst, (D) Est, and (E) Area were determined. The mean ± SEM of six mice per group are shown, $^{*}p < 0.05$ and $^{**}p < 0.01$ compared with the naïve mice; $^{\#}p < 0.05$, $^{\#\#}p < 0.01$, and $^{\#\#\#}p < 0.001$ compared with the vehicle control mice; $^{++}p < 0.01$ compared between two groups. No statistically significant differences were found between naïve and vehicle treated mice.

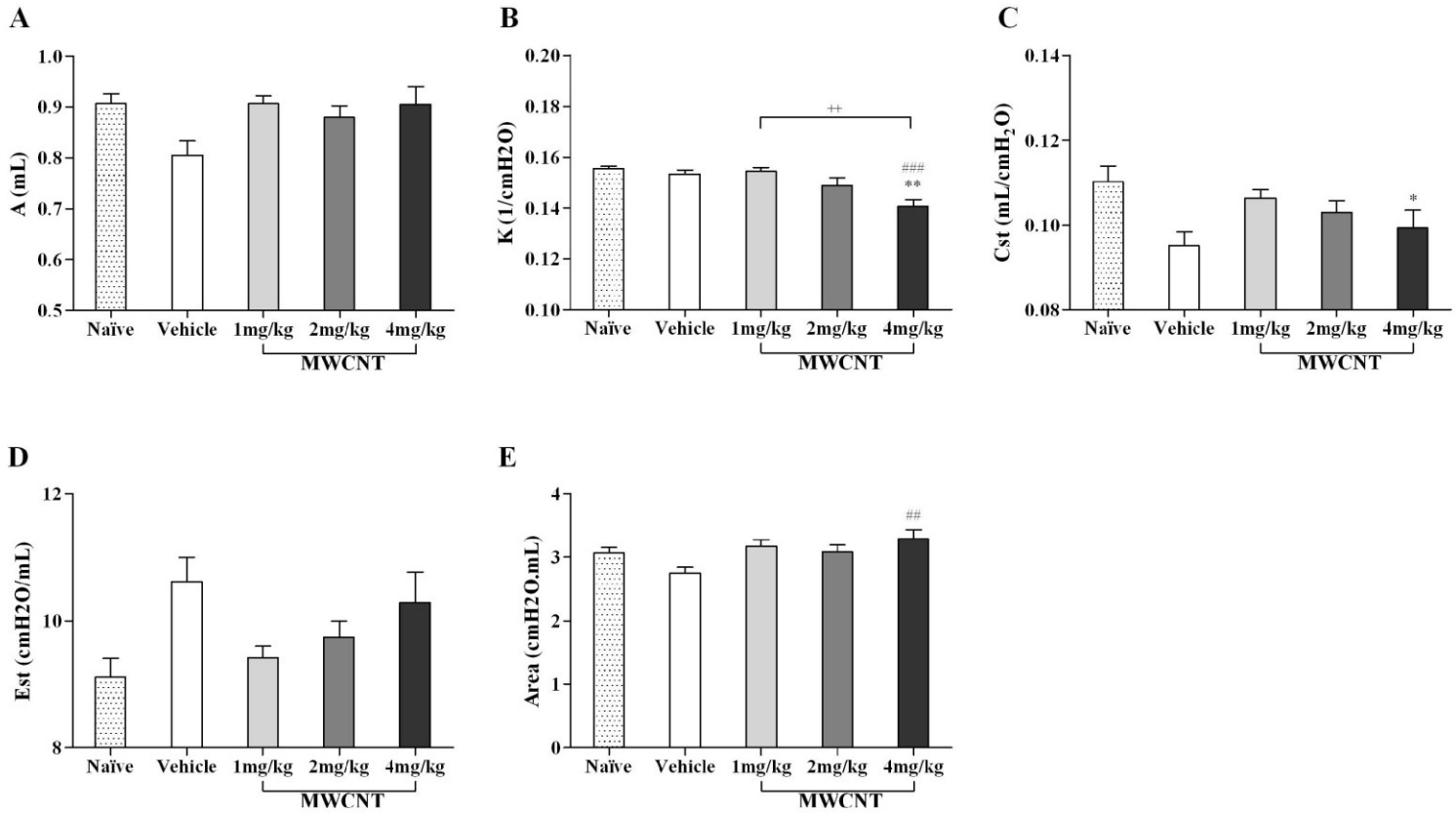
A
A (mL)
1.0
0.9
0.8
0.7
0.6
0.5
Naïve
Vehicle
1mg/kg
2mg/kg
4mg/kg
MWCNT
B
K (1/cmH2O)
0.20
0.18
0.16
0.14
0.12
0.10
++
###
**
C
Cst (mL/cmH2O)
0.14
0.12
0.10
0.08
*
D
Est (cmH2O/mL)
12
10
8
E
Area (cmH2O.mL)
4
3
2
1
0
##

Table 2.2 Lung pro-fibrotic gene expression in MWCNT instilled C57BL/6 mice compared to vehicle control

Gene	Description	p-Value	Fold Change
Mmp13	Matrix metallopeptidase 13	0.0253	7.92
Ccl3	Chemokine (C-C motif) ligand 3	0.0078	3.10
Ccl11	Chemokine (C-C motif) ligand 11	0.0038	2.76
Plau	Plasminogen activator, urokinase	0.0461	2.11
Cebpb	CCAAT/enhancer binding protein (C/EBP), beta	0.0243	-2.05
Jun	Jun oncogene	0.0366	-2.09
Eng	Endoglin	0.0007	-2.19
Fasl	Fas ligand (TNF superfamily, member 6)	0.0044	-2.20
Smad6	MAD homolog 6 (Drosophila)	0.0004	-2.40
Plg	Plasminogen	0.0290	-2.44
Serpina1a	Serine (or cysteine) peptidase inhibitor, clade A, member 1a	0.0312	-2.46

Figure 2.9 Induction of *Ccl3*, *Ccl11*, and *Mmp13* in lungs of C57BL/6 mice exposed to MWCNTs

Real-Time PCR analysis was performed in the left lung of vehicle (10% surfactant in saline), 1 mg/kg, 2 mg/kg, and 4 mg/kg MWCNTs instilled C57BL/6 mice for genes (A) *Ccl3*, (B) *Ccl11*, and (C) *Mmp13*. The mean ± SEM of six mice per group are shown, $^{\#}$ $p < 0.05$, $^{\#\#}$ $p < 0.01$, and $^{\#\#\#}$ $p < 0.001$ compared with the vehicle control mice; $^{+}$ $p < 0.05$ compared between two groups.

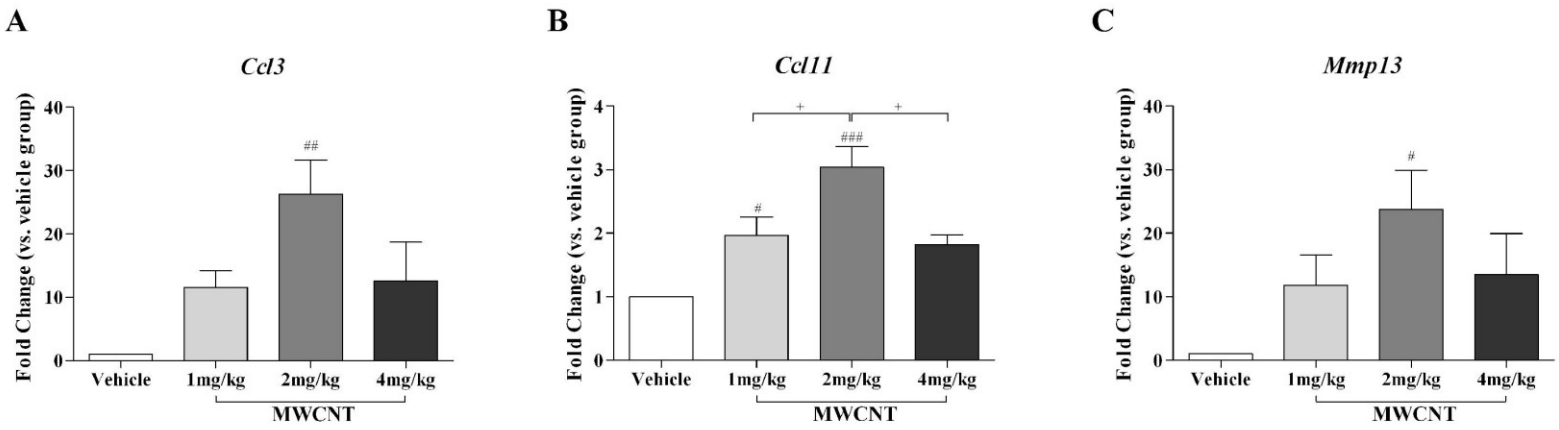
A
Ccl3
Fold Change (vs. vehicle group)
40
30
20
10
0
##
Vehicle
1mg/kg
2mg/kg
4mg/kg
MWCNT
B
Ccl11
Fold Change (vs. vehicle group)
4
3
2
1
0
+
+
#
###
Vehicle
1mg/kg
2mg/kg
4mg/kg
MWCNT
C
Mmp13
Fold Change (vs. vehicle group)
40
30
20
10
0
#
Vehicle
1mg/kg
2mg/kg
4mg/kg
MWCNT

Figure 2.10 Increased Ccl3, Ccl11, and activity of Mmp13 in BAL fluid after instillation with MWCNTs

ELISA analysis was performed in the BAL fluid of vehicle, 1 mg/kg, 2 mg/kg, and 4 mg/kg MWCNT instilled C57BL/6 mice for chemokines (A) Ccl3 and (B) Ccl11. Collagenase activity in the BAL fluid of vehicle control (10% surfactant in saline) and MWCNT instilled mice was measured using SensoLyte® Mmp13 Assay Kit. (C) The relative fluorescence units (RFUs) and (D) the reaction velocity of Mmp13 were dose-dependent increased 30 days post-MWCNT instillation. The mean ± SEM of six mice per group are shown, $^{\#}$ $p < 0.05$ and $^{\#\#}$ $p < 0.01$ compared with the vehicle control mice.

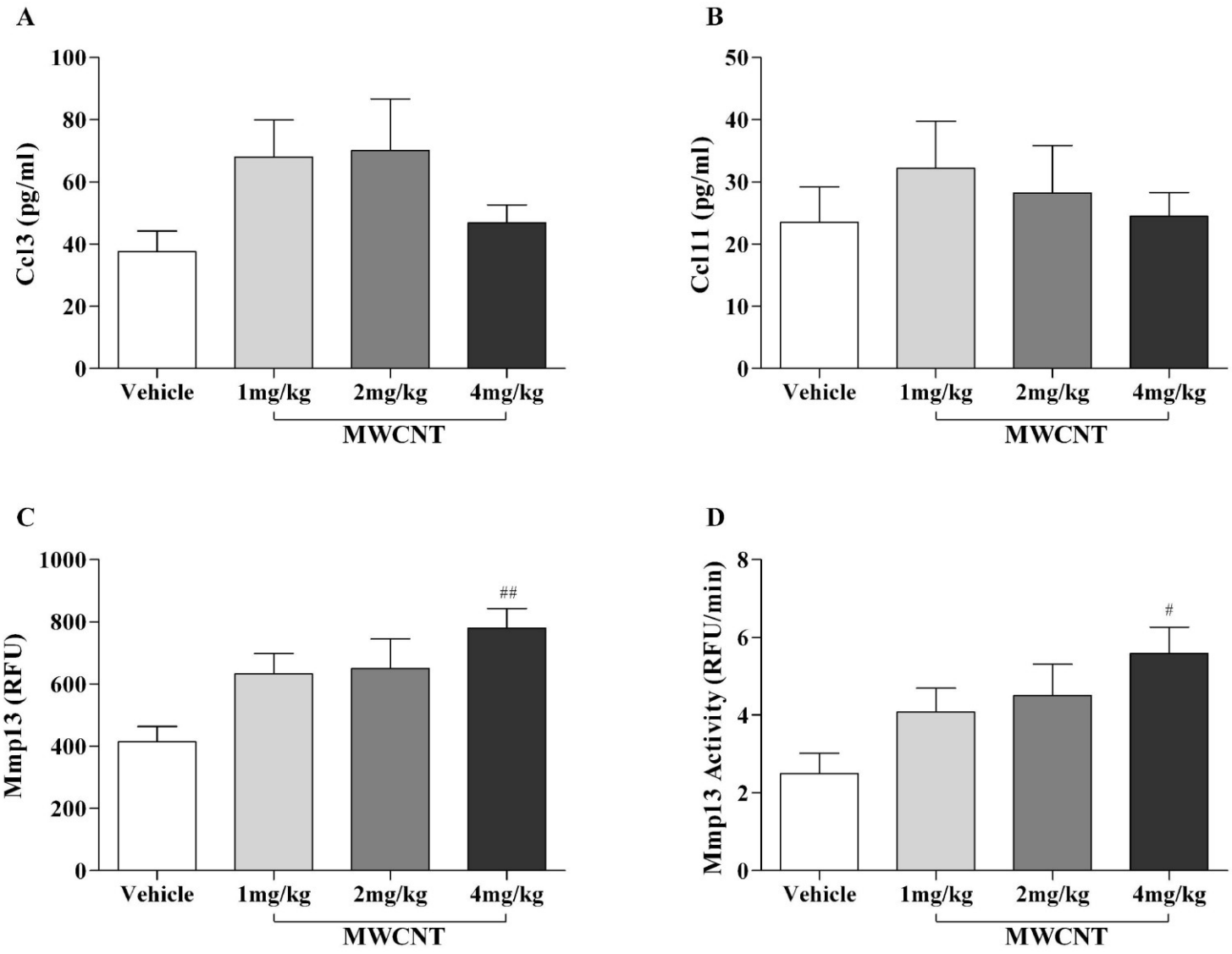
A
Ccl3 (pg/ml)
100
80
60
40
20
0
Vehicle
1mg/kg
2mg/kg
4mg/kg
MWCNT
B
Ccl11 (pg/ml)
50
40
30
20
10
0
Vehicle
1mg/kg
2mg/kg
4mg/kg
MWCNT
C
Mmp13 (RFU)
1000
800
600
400
200
0
##
Vehicle
1mg/kg
2mg/kg
4mg/kg
MWCNT
D
Mmp13 Activity (RFU/min)
8
6
4
2
0
#
Vehicle
1mg/kg
2mg/kg
4mg/kg
MWCNT

Figure 2.11 Induction of IL-33 gene and protein expression in C57BL/6 lung tissue and BALF 30 days post-exposure to MWCNTs

Gene expression of IL-33 (A), determined by Real-Time PCR, demonstrated an approximate three-fold increase in left lung tissue of mice instilled with MWCNTs compared to vehicle control mice. Correspondingly, ELISA protein analysis (B) of IL-33 in BALF of mice exposed to MWCNTs was also significantly increased at all doses (1, 2, and 4 mg/kg) compared to vehicle control (10% surfactant in saline). All values are expressed as mean ± SEM (n=6-11). $^{\#}p < 0.05$ compared to vehicle control mice and $^{\#\#\#}$ $p < 0.001$ compared with the vehicle control mice.

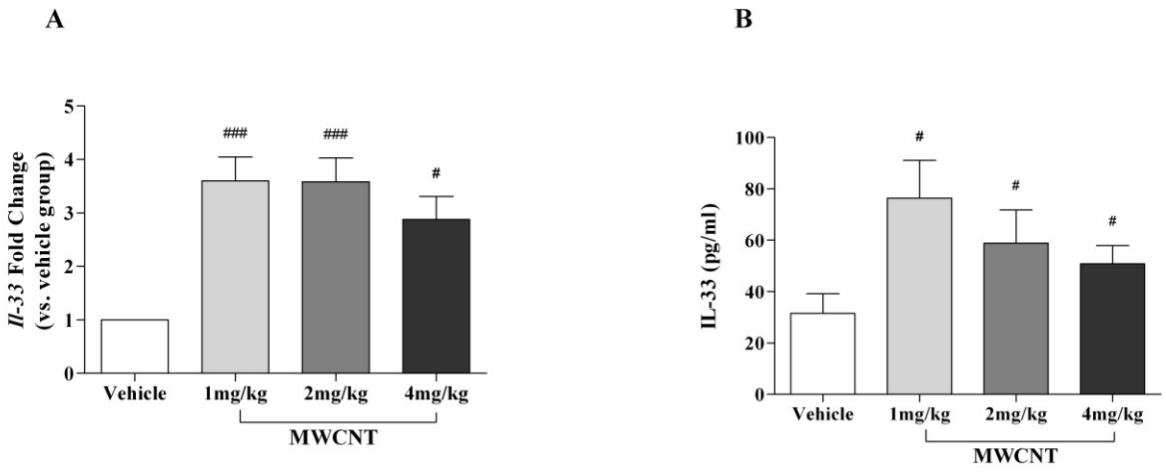
A
Il-33 Fold Change
(vs. vehicle group)
5
4
3
2
1
0
###
###
#
Vehicle
1mg/kg
2mg/kg
4mg/kg
MWCNT
B
IL-33 (pg/ml)
100
80
60
40
20
0
#
#
#
Vehicle
1mg/kg
2mg/kg
4mg/kg
MWCNT

DISCUSSION

Pulmonary toxicity of MWCNTs has been reported in both mouse and rat models (Han et al., 2010; Muller et al., 2005; Reddy et al., 2012). Instillation of MWCNT into the lungs of mice and rats has been shown to induce fibrosis (Mitchell et al., 2007); however, extensive evaluation of pulmonary function changes in animals instilled with MWCNTs has not been reported. In this study, we demonstrated that 30 days following MWCNT instillation, C57BL/6 mice exhibited changes in pulmonary function that were consistent with pulmonary inflammation, increased collagen deposition and granuloma formation. Additionally, increased levels of Ccl3, Ccl11, and Mmp13 were observed in C57BL/6 mice instilled with different doses of MWCNTs. Taken together, these results suggest that MWCNT exposure could lead to impaired pulmonary function due to inflammatory and fibrotic remodeling of lung tissue.

Due to the implication that MWCNTs may adversely affect human health and safety, appropriate dosing of animals was essential to evaluate the pertinence of these findings in regard to human exposure levels. Studies conducted in industrial plants indicated nanoparticle exposure levels up to 0.5 mg/m^3 for an 8-hour work day and 40-hour work week (Demou et al., 2008). Additional evaluations of carbon nanotubes in manufacturing and research facilities, found airborne levels during handling to be as low as 53 $\mu g/m^3$ (Maynard et al., 2004) and as high as 400 $\mu g/m^3$ (Han et al., 2010; Porter et al., 2010). Shvedova *et al*., report that human occupational exposure levels of 5 mg/m^3 over the course of an 8-hour day and 40-hour work week equate to approximately 20 µg of MWCNT aspiration in a mouse model (Shvedova et al., 2005). Current proposed guidelines by the National Institute for Occupational Safety and

Health (NIOSH) limits exposure to 7 μg/m^3, the lowest detectable level of airborne CNT using the latest analytical methods (2010). The doses used in this study, 1, 2 and 4 mg/kg MWCNTs (equivalent to 27, 54, and 108 μg of MWCNT in the average 27 g mouse used in this study), were selected based on these limited exposure studies and doses previously reported in the literature for rodent studies (Porter et al., 2010). Furthermore, the MWCNTs were dispersed in 10% surfactant in saline, a physiologically relevant medium, shown to effectively reduce aggregation of nanotubes in solution (Wang et al., 2011b). Data from this study demonstrated a persistent inflammatory response and the development of granulomatous and collagen-rich fibrotic tissue in C57BL/6 mice, similar to previously reported findings (Porter et al., 2010; Ryman-Rasmussen et al., 2009b). Post-exposure to MWCNTs at 90 days exhibited granulomatous foci similar to those found in chronic human granulomatous disorders (Huizar et al., 2011). In fact, due to their ability to produce a robust granulomatous response, the use of MWCNTs has been proposed as a novel murine model to study chronic granulomatous disease (Huizar et al., 2011). In the present study, we demonstrated that focal aggregates of MWCNTs were present at the core of the granulomas and surrounding fibrotic tissue (Fig 2.6D). In addition, our data indicated that intact MWCNTs do not congregate to form airway granulomas, but are dispersed throughout the lung tissue (Fig 2.6B) contrary to reports from previous investigators (Muller et al., 2005). Furthermore, studies have shown that MWCNTs are not only found in the periphery of the lungs post-exposure, but have also been found to translocate to the pleural space (Ryman-Rasmussen et al., 2009b). Data from this study are consistent with previous reports that MWCNTs induce pulmonary

inflammation and fibrosis, and are widely distributed through the lung following exposure. Further, we have now shown that these severe adverse pulmonary responses have a negative impact on pulmonary function.

In this study, pulmonary functional variables were evaluated in C57BL/6 mice exposed to different doses of MWCNTs using the FlexiVent system. The Snapshot perturbation was imposed to measure resistance (R), dynamic compliance (C), and elastance (E) of the whole respiratory system (including airways, lung, and chest wall). Our data showed that R was significantly increased at the highest dose of MWCNT with a concomitant declined in dynamic compliance (C). The decrease in C is consistent with findings in a bleomycin-induced model of pulmonary fibrosis in mice (Vanoirbeek et al., 2010). However, that study did not demonstrate an increase in R. This discrepancy is likely due to the fact that inflammation was attenuated by use of cyclophosphamide. Thus, in our study, the consistent elevation in numbers of inflammatory cells may have contributed to the increased R observed. Because R reflects the combined resistance contributed by both the airways and lung parenchyma, we employed the constant-phase model to distinguish between central and peripheral respiratory mechanics and to provide information about the heterogeneity of the respiratory response (Shalaby et al., 2010).

Tissue damping (G), which reflects parenchymal distortion, showed a dose-dependent increase in MWCNT instilled mice which was likely due to inflammatory infiltrates, as well as granuloma formation in the peribronchiolar and alveolar regions of the lung. Since these structures account for a major portion of the cross-sectional area of the lung, any obstruction in the distal airways and/or alveolar spaces could contribute

to an increase in R. Furthermore, the decrease in C may suggest that the alveoli are not fully expanding as a result of alveolar volume reduction which is likely due to inflammation and/or granuloma formation. This would reduce the traction normally exerted on the conducting airways at high lung volume and thereby also contribute to changes in resistance (R). Similar to Rn, H, a measure of tissue elastance, also displayed a non-significant trend towards increased elastance with increasing doses of MWCNT (data not shown). Tissue elastance is typically elevated with fibrotic lung disease; but the patchy nature of the granulomatous/fibrotic lesions seen in this model may account for the lack of significance. However, eta (G/H) was dose-dependently increased with MWCNT instillation and was significantly elevated at the highest dose, indicating heterogeneity in the combined inflammatory and fibrotic responses to MWCNTs. On the other hand, Rn showed a trend toward dose-dependent increases that did not reach significance, suggesting that MWCNTs may have a minor effect on central airways. In support of this, we observed only minor inflammation within the central airways. However, this effect, while small with MWCNTs alone, may explain enhancement of airway responses to methacholine in models of allergic airway disease by exposure to air pollution (North et al., 2011) observed in other studies. Along the same line, our study showed a MWCNT-induced increase in eosinophil numbers and eotaxin levels (Ccl11) which may also contribute to MWCNT enhancement of allergic airway disease.

Static compliance (Cst) and the upper portion of the deflation PV curve (K), parameters derived from PVr-P maneuvers, declined significantly at the highest dose of MWCNTs which is typical of fibrotic lung disease. In contrast to our findings, Kamata et

al. (Kamata et al., 2011) reported that carbon black nanoparticles had no effect on lung compliance. This might be due to the physicochemical differences between carbon black nanoparticles and MWCNTs. A decrease in Cst was also observed in the vehicle treated mice suggesting that the administration of high doses of pulmonary surfactant reduces lung compliance.

Taken together, our pulmonary function findings suggest that MWCNT exposure results predominantly in peripheral respiratory disease as a result of combined inflammatory infiltrates and granulomatous/fibrotic parenchymal responses, reflected by a decline in pulmonary function. Consistent with other reports, we observed significant granuloma formation with fibrotic content which likely contributed to restrictive changes in pulmonary function (Huizar et al., 2011). Translocation and penetration of MWCNTs into pleural space, as previously shown, may also contribute to peripheral respiratory injury and subsequent structural changes (Mercer et al., 2010; Ryman-Rasmussen et al., 2009b).

To begin examining potential molecular mechanisms by which MWCNT instillation mediates impaired pulmonary function, gene and protein expression of cytokines and chemokines were examined to identify fibrotic and inflammatory responses. PCR arrays were utilized to identify changes in gene expression related to the development of fibrosis. We identified *Mmp13*, *Ccl3*, and *Ccl11* as three highly upregulated gene products. Mmps can be divided by structure and substrate specificity into several subgroups including collagenases, gelatinases, stromelysins, and membrane-type (MT) Mmps (Selman et al., 2000). Imbalanced expression of MMPs has been associated with fibrosis (Kim et al., 2011). Mmp13, an interstitial collagenase,

is considered a key activator in the cascade of proinflammatory reactions leading to pulmonary fibrosis (Flechsig et al., 2010). Furthermore, activation of Mmp13 enhances the process of macrophage chemoattraction and infiltration of other inflammatory cells following tissue injury. MWCNT instilled mice exhibited a dose dependent increase in Mmp13 production and activity in BAL fluid. Additionally, Ccl3 (also named MIP-1α) is a critical macrophage chemoattractant in murine wound repair (DiPietro et al., 1998). In our study, increased Ccl3 expression in the lung and Mmp13 activity in BAL fluid following MWCNT exposure are likely associated with the collagen deposition and granuloma formation in mouse lung exposed to MWCNT. Lastly, Ccl11, involved in eosinophil recruitment, was significantly increased in the lung following MWCNT instillation. This likely contributed to the increasing trend in eosinophils in the BALF seen with increasing doses of MWCNT. Consistent with previous studies (Emad and Emad, 2007), an influx of eosinophils into the lungs by a variety of eosinophil chemoattractants, such as Ccl11, was observed. This classic Th2 driven inflammatory response may contribute to the subsequent fibrotic outcome and change in resistance that was observed in response to MWCNT exposure.

Finally, IL-33 was examined for its potential role in inflammatory cell recruitment and Th2 immune responses following MWCNT exposure. IL-33 is a member of the IL-1 cytokine family and the only known ligand for the ST2 receptor (Schmitz et al., 2005). The ST2 receptor is most highly expressed on mast cells and Th2 lymphocytes, and is known to exist in at least two isoforms; a transmembrane form and a soluble form which is cleaved after activation by IL-33 (Lloyd, 2010). Haraldsan *et al.* describe IL-33, as a potential alarmin, or immune stimulating danger signal during trauma or infection

(Haraldsen et al., 2009; Oppenheim and Yang, 2005). Studies have confirmed IL-33 as a chemoattractant for human and murine Th2 cells (Komai-Koma et al., 2007). Furthermore, IL-33 has recently been shown to polarize macrophages to a M2 phenotype (or alternatively activated macrophages), resulting in enhanced production of pro-inflammatory and pro-fibrotic cytokines and chemokines in Th2 driven pathologies (Kurowska-Stolarska et al., 2009). The IL-33/ST2 axis, known to influence these Th2 cell types including mast cells, macrophages and eosinophils, has been recognized in modulating disease pathologies such as anaphylaxis and allergic asthma (Liew et al., 2010). A study by Mangan et al. demonstrates that expression of transmembrane ST2 on Th2 cells negatively impacts both pulmonary physiologic and pathologic responses in an OVA-induced pulmonary inflammation mouse model. Changes in airways resistance measures, such as PenH, along with pathologic alterations of pulmonary cell infiltrates and cytokine profiles in ST2 knock-out mice indicate a role for IL-33 and ST2 receptor in regulating allergic inflammatory responses (Mangan et al., 2007). Further, airway hyper-reactivity following allergen challenge can be attenuated by blockade of the transmembrane ST2 receptor in BALB/c mice (Kearley et al., 2009). Thus, during injury or insult to the lung, IL-33 upregulation and activation of ST2 receptors may significantly impact Th2 driven cell types resulting inflammatory, fibrotic and physiological changes.

Our data show significant increases in IL-33 expression with MWCNT exposure compared to vehicle control, demonstrating a potential role in inflammation and fibrosis. Mechanistically, the release of chemokines (CCL3 and CCL11), cytokines (IL-33) and the activation of MMP13, help to amplify pro-inflammatory and pro-fibrotic mediators, as

well as recruit macrophages, neutrophils, and eosinophils into the lung, thereby contributing not only to the pathologic inflammatory and fibrotic responses, but also the physiologic and functional changes induced by MWCNTs.

CONCLUSION

In this study, we have demonstrated that MWCNT instillation results in increased immune cell infiltration, increased collagen deposition, and a granulomatous response. Further, we provide evidence of detrimental lung remodeling exhibited by impaired pulmonary function; and begin to identify mechanisms of MWCNT-induced lung remodeling through increased expression of CCL3, CCL11, MMP13 and IL-33. Given these data and the increased use of MWCNTs and other nanomaterials, we believe further investigation into the toxicity of these materials is warranted.

CHAPTER 3: A CARBON NANOTUBE TOXICITY PARADIGM DRIVEN BY MAST CELLS AND THE IL-33/ST2 AXIS

PUBLISHED: Katwa et al. Small 2012, DOI:10.1002/smll.201200873

SUMMARY

Concern about the use of nanomaterials has increased significantly in recent years due to potentially hazardous impacts on human health. Mast cells are critical for innate and adaptive immune responses, often modulating allergic and pathogenic conditions. Mast cells are well known to act in response to danger signals through a variety of receptors and pathways including IL-33 and the IL-1 like receptor ST2. Here, we examined the involvement of mast cells and the IL-33/ST2 axis in the pulmonary and cardiovascular responses to MWCNT exposure. The toxicological effects of MWCNTs were observed only in mice with a sufficient population of mast cells and were not observed when mast cells were absent or incapable of responding to IL-33. Our findings establish for the first time that mast cells and the IL-33/ST2 axis orchestrate adverse pulmonary and cardiovascular responses to an engineered nanomaterial, giving insight into a previously unknown mechanism of toxicity. This novel mechanism of toxicity could be used for assessing the safety of engineered nanomaterials and provides a realistic therapeutic target for potential nanoparticle induced toxicities.

INTRODUCTION

Carbon nanotubes (CNTs) have great versatility in physical and chemical properties leading to increased use in biomedical and technological applications. Their unique properties, including high electrical and thermal conductance, high-strength to weight ratios, and additional novel physico-chemical properties, have led to significantly increased use of CNTs over the past decade (Endo et al., 2008a). Functionalization of CNTs with amino acids, peptides and other molecules has been an important factor in providing greater stability and lower cellular toxicity compared to non-functionalized or pristine CNTs, making them a promising platform for drug delivery, gene delivery and other biomedical applications (Bianco et al., 2005; Dumortier et al., 2006; Liu et al., 2009). While the novel applications of CNTs are advantageous, there is increased concern about their potentially hazardous effects on human health. Despite limited research on direct effects of CNTs on humans, research in animals has demonstrated pristine CNT exposure leads to adverse pulmonary and cardiovascular outcomes. Due to their high aspect ratio characteristics, multi-walled carbon nanotubes (MWCNTs), in particular, have been compared to asbestos fibers and as a result, have been suggested to induce asbestos-like toxicities (Poland et al., 2008). Inhalation of MWCNTs in animal models elicits detrimental pulmonary responses including inflammation, granulomatous disease, fibrosis, and altered lung function (Huizar et al., 2011; Inoue et al., 2009; Ryman-Rasmussen et al., 2009b; Wang et al., 2011a). In addition, MWCNTs exacerbate cardiac ischemia/reperfusion (IR) injury in mice which occurs as early as 1 day post-exposure (Urankar, *In Submission* 2012b).

Mast cells are critical for innate and adaptive immune responses, often modulating allergic and pathogenic conditions. Described as key sensors of cell injury, mast cells are well known to act in response to danger signals through a variety of receptors and pathways including pathogen associated molecular pattern (PAMP) receptors, scavenger receptors and the IL-1-like receptor ST2 (Abraham and St John, 2010; Enoksson et al., 2011). The ST2 receptor, which can be activated by its ligand interleukin-33, is highly expressed on the surface of mast cells and is pivotal in response to pathogenic and, as suggested, xenobiotic insult (Moritz et al., 1998).

IL-33, a novel cytokine that is a member of the IL-1 family, has recently been termed an “alarmin” to describe its potential role in alerting the immune system of tissue injury or trauma (Moussion et al., 2008). Alarmins, also known as endogenous danger signals, have been shown to activate receptors on immune cells in order to initiate inflammatory responses to cell necrosis (Kono and Rock, 2008). IL-33 can induce the release of Th2 pro-inflammatory cytokines, including IL-6 and IL-13 through the ST2 receptor in a variety of immune cells including mast cells (Enoksson et al., 2011; Ho et al., 2007; Moulin et al., 2007). As an alarmin, IL-33 has a dual role in not only initiating immune responses, but modulating them as well.

Our understanding of mast cells in disease has been elucidated through the use of mast cell deficient mice (*Kit*$^{W\text{-}sh}$ mice). Indeed, *Kit*$^{W\text{-}sh}$ mice reconstituted with cultured bone marrow derived mast cells (BMMCs) have been utilized as a model for investigating the role of mast cells in numerous conditions (Grimbaldeston et al., 2005; Wolters et al., 2005). Through the use of this model, our understanding of mast cells now includes their importance in host immune responses to bacterial infections, airway

reactivity in asthma, as well as toxicity of Gila monster and scorpion venoms as examples (Akahoshi et al., 2011; Sutherland et al., 2011; Yu et al., 2006).

In the current study, we examined the contribution of mast cells and the IL-33/ST2 axis to multi-walled carbon nanotube (MWCNT) directed pulmonary and cardiovascular toxicity. As will be shown, MWCNT exposure resulted in adverse pulmonary and cardiovascular responses in mice with sufficient mast cell populations, while these effects were largely absent in mice deficient in mast cells or mice with mast cells unable to respond to IL-33. Our findings establish for the first time that mast cells and the IL-33/ST2 axis modulate adverse pulmonary and cardiovascular responses to an engineered nanomaterial, giving insight into a previously unknown mechanism of toxicity.

METHODS

MWCNT Characterization

Multi-walled carbon nanotubes were generously provided by NanoTechLabs, Inc (Yadkinville, NC). The dry powder form of MWCNTs was characterized using transmission and scanning electron microscopy to obtain length, diameter distribution and elemental composition. Raman spectra, surface area, pore volume, pore size distribution, hydrodynamic size, zeta potential and isoelectric point of the MWCNTs were obtained as previously described (Wang et al., 2011a). A summary of the MWCNT characterization is presented in Tables 3.1 & 3.2.

Cell Culture

Bone marrow derived mast cells (BMMCs) were generated from femoral bone marrow of 4 week old female C57BL/6 or $ST2^{-/-}$ mice and grown at 37°C with 5% CO_2. BMMCs and $ST2^{-/-}$ BMMCs were cultured in RPMI 1640 medium supplemented with (10%) FBS, (100µg/mL) streptomycin, (100 U/mL) penicillin, (1 M) sodium pyruvate, non-essential amino acids (Sigma-Aldrich, St. Louis, MO), (25 mM) Hepes, (0.0035%) 2-mercaptoethanol, and (300 µg/mL) recombinant murine IL-3 (Peprotech, Rocky Hill, NJ). FcεRI expression was determined at 4 weeks, at which time >95% of cells were mature BMMCs. In addition, absence of ST2 receptor expression was determined in $ST2^{-/-}$ BMMCs by flow cytometry and IL-33 activation studies. Upon reaching maturity, cells were used for reconstitution of B6.Cg-$kit^{W\text{-}sh}$ mast cell deficient mice or *in vitro* experiments. C57BL/6 or $ST2^{-/-}$ BMMCs used for *in vitro* experiments were exposed to BALF acquired from C57BL/6 mice 1 day post-exposure to MWCNT. C57BL/6 or $ST2^{-/-}$

BMMCs were collected for qPCR analysis of IL-6, IL-33 and OPN, following the 2 hour BALF incubation period.

Experimental Animals

C57BL/6J and B6.Cg-*kit*$^{W\text{-}sh}$ mast cell deficient mice were acquired from Jackson Laboratories (Bar Harbor, ME, USA) at 4-10 weeks of age. ST2$^{-/-}$ mice were generously provided by Merck, Inc. and breeding colonies were maintained at East Carolina University. In addition, B6.Cg-*kit*$^{W\text{-}sh}$ mice were reconstituted with wild type (C57BL/6) or ST2$^{-/-}$ BMMCs. They were further divided into 2 treatment groups (6-8 mice/group): vehicle (10% surfactant in saline) or (4 mg/kg) MWCNTs. C57BL/6J, B6.Cg-*kit*$^{W\text{-}sh}$ (without reconstitution) and ST2$^{-/-}$ mice were also assigned to the same treatment groups. The dose was determined based on previously published MWCNT dose response data (Wang et al., 2011a). Mice were lightly anesthetized with isofluorane and received a single dose of MWCNTs (4 mg/kg body weight) or vehicle (10% surfactant) by oropharyngeal aspiration (Wang et al., 2011b). Clinical grade pulmonary surfactant (Infasurf®) was kindly provided by ONY, Inc (Amherst, NY, USA). Mice were sacrificed at 1 or 30 days post-exposure. Animal protocols and procedures were conducted in accordance with the National Institutes of Health guidelines and approved by the East Carolina University Institutional Animal Care and Use Committee.

Mast Cell Reconstitution of B6.Cg-kit$^{W\text{-}sh}$ Mast Cell Deficient Mice

C57BL/6J and ST2$^{-/-}$ BMMCs were centrifuged at 1200 rpm for 5 min and resuspended in sterile saline. Wild type (C57BL/6J) or ST2$^{-/-}$ BMMCs (5 x 10^6 cells in

200 µL of sterile saline) were intravenously injected into 4 week old B6.Cg-*kit*$^{W\text{-}sh}$ mice. BMMCs were allowed to reconstitute for 8 weeks at which time reconstituted B6.Cg-*kit*$^{W\text{-}sh}$ mice were instilled with vehicle or MWCNT and sacrificed 1 or 30 days post-exposure for pulmonary and cardiovascular endpoints.

Pulmonary Function Testing

Elastance (E), compliance (C), and Newtonian resistance (Rn) were measured by forced oscillatory technique using the FlexiVent system (SCIREQ, Montreal, QC, Canada.(Wang et al., 2011a) Briefly, 30 days following instillation of MWCNTs, mice were anesthetized with tribromoethanol (TBE) (400 mg/kg), tracheostomized, and placed on the FlexiVent system. Mice were ventilated with a tidal volume of 10 mL/kg at a frequency of 150 breaths/min and a positive end expiratory pressure of 3 cm H_2O to prevent alveolar collapse. In addition, mice were paralyzed with pancuronium bromide (1 mg/kg) to prevent spontaneous breathing. EKG was monitored for all mice to determine anesthetic depth and potential complications that could have arisen during testing. Total lung capacity (TLC), Snapshot, Quickprime-3, and pressure-volume (PV) loops with constant increasing pressure (PVr-P) were consecutively performed using the Flexivent system. All perturbations were executed until three acceptable measurements with coefficient of determination (COD) ≥ 0.9 were recorded in each individual subject.

BAL and Differential Cell Counts

Following pulmonary function testing, mice underwent *in situ* bronchoalveolar lavage (BAL). The right lung was lavaged four times (26.25 mL/kg body weight) with ice-cold Hanks balanced salt solution (HBSS). Bronchoalveolar lavage fluid (BALF) was collected separately for the first lavage and pooled for the remaining 3 lavages. BALF samples were then centrifuged at 1000 g for 10 min at 4^{o}C and supernatant from the first lavage was snap frozen for cytokine analysis, while cell pellets from all lavage samples were combined and counted, followed by resuspension in (1 mL) HBSS. In order to obtain differential cell counts, 20,000 cells from each BALF sample were centrifuged using a Cytospin IV (Shandon Scientific Ltd., Cheshire, UK) and stained with a three-step hematology stain (Richard Allan Scientific, Kalamazoo, MI, USA). Cell differential counts were determined by morphology with evaluation of 300 cells per slide.

Lung Histopathology

Left lungs from mice were perfused with 10% neutral buffered formalin fixative and stored for 24 hrs, then processed and embedded in paraffin. Samples were then sectioned at a thickness of 5 μM and were mounted on slides for staining with hematoxylin and eosin (H&E) or Masson's trichrome stain to detect morphological changes and collagen deposition. MWCNT aggregates localized within the tissue sections were confirmed by Raman spectroscopy.(Wang et al., 2011a)

Immunofluorescence

Unstained histological lung sections from C57BL/6 mice were used for immunofluorescence detection of IL-33. Sections were deparrafinized and

subsequently underwent microwave irradiation in citrate buffer for antigen retrieval. Sections were then blocked in (5%) filtered fetal bovine serum in Tris buffer saline (TBS) with (0.2%) Tween and sodium azide for 2 hours, following which IL-33 primary antibody was applied at 1:100 (Novus Biologicals, Littleton, CO) for 48 hours at 4°C. Sections were washed 3 times with TBS and incubated in a PE (R-phycoerythrin) conjugated secondary antibody at 1:100 (Fitzgerald Industries International, Concord, MA) for 2 hours at room temperature. Following additional washes in TBS with (0.1%) Triton X, sections were coverslipped using Prolong gold anti-fade containing a DAPI stain (Molecular Probes, Eugene, OR). Dry sections were imaged using DAPI and TRITC filters for nuclear and IL-33 specific staining.

Sircol Collagen Assay

Sircol Collagen Assay (Biocolor, Belfast, UK) was used to detect soluble collagen content within the lung homogenate. Lavaged right lung was homogenized in 2 mL of RIPA buffer containing protease inhibitors and the protocol was conducted according to manufacturer's specifications. In addition, a BCA protein quantification analysis was used to determine total protein content for each sample, of which 100 µg of protein used for collagen quantification.

Myocardial Ischemia/Reperfusion (I/R) Injury

At 1 day post-instillation of MWCNT, mice were anesthetized *i.p.* (intraperitoneally) with 0.005 mL/gram body weight of Ketamine/Xylazine mix (18:2 mg/mL) to measure ischemia/reperfusion injury in accordance with an established

protocol (Weir et al., 2010). In short, following a midline tracheostomy, mice were intubated and ventilated with (100%) oxygen at 115 strokes/min and tidal volume of 0.25 mL, using a Harvard Inspira Ventilator (Harvard Apparatus, Holliston, MA, USA). The pericardium stripped following a thoracotomy to allow for ligation of the left anterior descending coronary artery (LAD). A 06 prolene ligature was used to occlude blood flow for 20 minutes, after which the ligature was released and the myocardium was allowed to reperfuse for 2 hours. The myocardium not subjected to IR injury was determined by infusion of (1%) Evans Blue dye into the aortic arch after which the heart was excised and cut into 1 mm transverse sections. Staining of the sections with 2,3,5-triphenyltetrazolium chloride delineated the area at risk from the infarcted tissue. The area of infarct, expressed as % of area at risk (AAR) was determined Computer Planimetry analysis.

qPCR

Reverse transcription of total lung RNA was performed using a QuantiTect reverse transcription kit (Qiagen). QuantiTect primer assays and SYBR green master mix were utilized for Quantitative real-time PCR to examine mRNA expression levels of IL-33, OPN and IL-6. Cycle threshold (Ct) values and internal reference cDNA levels for the target genes were determined by an Applied Biosystems StepOnePlus Real-Time PCR System (ABI). The cDNA levels were then normalized to GAPDH, used as an internal reference, by the equation $2^{-[\Delta Ct]}$, where ΔCt is defined as Ct_{target}- $Ct_{internal\ reference}$. Values are reported for an average of 4 independent experiments.

ELISA Assays

IL-33 and sST2 levels were measured in BALF using DuoSet ELISA kits (R&D Systems, Minneapolis, MN) in accordance with the manufacturer's instructions. Values are reported as pg/mL.

Statistical Analyses

All data were analyzed by one-way ANOVA, with differences between groups assessed using Bonferroni *post hoc* tests or t-tests and are presented as means ± SEM, where statistically significant differences were identified with $p < 0.05$. All statistical analysis and graphs were generated using GraphPad Prism 5 software (GraphPad, San Diego, CA).

RESULTS AND DISCUSSION

Mast Cells and the IL-33/ST2 Axis Direct MWCNT Induced Lung Fibrosis

The extent and means by which MWCNTs are able to impact pulmonary toxicity was tested by oropharyngeal aspiration of vehicle or MWCNTs (4 mg/kg) in C57BL/6 mice, $Kit^{W\text{-}sh}$ mice, $Kit^{W\text{-}sh}$ mice reconstituted with BMMCs, $Kit^{W\text{-}sh}$ mice reconstituted with $ST2^{-/-}$ BMMCs and $ST2^{-/-}$ mice. The dose used to elucidate mechanisms of MWCNT toxicity was based upon dose response studies published earlier (Wang et al., 2011a). In addition, the characteristics of the MWCNTs used in this study have been previously described (Wang et al., 2011a) and are further detailed in Tables 3.1 & 3.2 and Figure 3.1. As indicated in Table 3.2, the MWCNTs were characterized in suspension (10% Infasurf® pulmonary surfactant in saline), which also serves as our vehicle control, and best exemplifies non-agglomerated MWCNTs in a dispersal medium suited for animal studies. Suspension of MWCNTs in surfactants has been shown to increase dispersal and allow for greater stability of the particles, inhibiting aggregate formation and producing greater toxicity (Wang et al., 2011b). A high zeta potential, as displayed in Table 3.2, is indicative of a stable suspension, which results in well-dispersed MWCNT.

In distinguishing the specific underlying mechanism(s) of MWCNT induced pulmonary toxicities, we first examined the expression levels of IL-33 in lung tissue. At 30 days post-exposure, all groups of mice exposed to MWCNTs demonstrated a significant increase in IL-33 mRNA levels in lung tissue homogenate compared to vehicle controls (Figure 3.2a). Protein levels of IL-33 were also significantly elevated in bronchoalveolar lavage fluid (BALF) of C57BL/6 mice 30 days following MWCNT instillation (Figure 3.2b). Similarly, IL-33 staining of lung tissue sections from MWCNT

exposed C57BL/6 mice was notably increased and not co-localized to the nucleus (Figure 3.2c). Contradictory reports regarding IL-33 function have led to more recent perspectives of IL-33 as a dual-function cytokine; acting as a traditional cytokine and as an intra-nuclear cytokine to regulate gene expression (Haraldsen et al., 2009). The extracellular release of IL-33 has also been debated; however, more recent studies demonstrate IL-33 is released by cells following injury and necrosis, unlike apoptotic cells that retain IL-33 intracellularly (Luthi et al., 2009). Induction of both cellular apoptosis and necrosis can occur with exposure to MWCNTs in cell types such as macrophages and lung epithelial cells (Cavallo et al., 2012; Di Giorgio et al., 2011). In addition, it has been established that there is an increase in IL-33 expression in lung epithelial cells during inflammation (Pichery et al., 2012; Talabot-Ayer et al., 2012). Therefore, it is possible that our data, displaying increased levels of IL-33 released from lung epithelial cells into the BALF and subsequent mast cell activation, are a result of cytotoxicity due to MWCNT exposure.

Additionally, we conducted *in vitro* studies to confirm the activation of mast cells by IL-33 found within the BALF. It has been reported that IL-33 activation of mast cells occurs independent of the FcεRI pathway (Ho et al., 2007). In our study, BMMCs that were treated in culture with BALF collected from C57BL/6 mice instilled with MWCNT display significant elevation in IL-6 and osteopontin (OPN) mRNA expression compared to BALF from vehicle exposed mice (Figure 3.3). Increased expression of these two genes was not observed when $ST2^{-/-}$ BMMCs were exposed to BALF from MWCNT instilled mice (Figure 3.3). These findings validate that the increase in IL-33 found in the lungs of mice treated with MWCNTs is capable of inducing mast cell activation

through the ST2 receptor and that IL-33 appears to be the major soluble factor in the BALF capable of mast cell activation.

To further elucidate an IL-33/ST2 axis mechanism in pulmonary inflammation, differential cell counts were obtained from BALF following MWCNT instillation. IL-33 has been identified as a major determinant in the inflammatory processes of the lung (Yagami et al., 2010). In fact, over expression of IL-33 in transgenic mice demonstrated increased levels of cleaved, mature IL-33, resulting in spontaneous pulmonary inflammation consisting of increased pro-inflammatory cytokines such as IL-5, IL-8 and IL-13, as well as inflammatory cell infiltrates, including neutrophils, in BALF (Zhiguang et al., 2010). In our study, differential cell counts at 1 day post-exposure also demonstrated a significantly increased inflammatory cell profile, which is sustained out to 30 days following MWCNT instillation (Table 3.3). At 30 days post-exposure to MWCNTs, C57BL/6 mice and $Kit^{W\text{-}sh}$ mast cell deficient mice reconstituted with BMMCs displayed pulmonary inflammation with statistically significant neutrophil recruitment (Figure 3.4a). The infiltration of neutrophils into the lung was absent in $Kit^{W\text{-}sh}$, $ST2^{-/-}$, and $Kit^{W\text{-}sh}$ mice reconstituted with $ST2^{-/-}$ BMMCs (Figure 3.4a). These data therefore suggest the involvement of mast cells, or potentially mast cell derived mediators, in the recruitment of neutrophils. In addition, these data also indicate a role for IL-33 and the ST2 receptor in mediating these responses, as inflammation and neutrophil infiltration is not observed in the absence of ST2 receptors (Figure 3.4a). Neutrophils have been shown to regulate IL-33 activity through the cleavage of IL-33 into its mature form by neutrophil elastase and Cathepsin G (Lefrancais et al., 2012). Neutrophil proteinase 3 (PR3) is also proposed to regulate activity of IL-33 by cleavage into its mature form

(Bae et al., 2012). While full length IL-33 is biologically active, it has been reported that the activity of mature IL-33 is significantly higher. Furthermore, both the full length and mature forms of IL-33 were detected during neutrophilic infiltration in a murine model of acute lung injury (Lefrancais et al., 2012). It is possible that mast cell recruitment of neutrophils along with the capacity of neutrophils in regulating IL-33 activity may impact the inflammatory response induced by MWCNTs. Our data demonstrate a clear role for ST2 receptor mediated mast cell activation in MWCNT induced pulmonary inflammation; however, additional studies may be required to address the potential neutrophil-enhanced IL-33 activity in contributing to these inflammatory responses.

While previous studies have identified pulmonary fibrotic responses induced by MWCNTs, few have examined the underlying mechanisms (Aiso et al., 2010; He et al., 2011; Mercer et al., 2011; Wang et al., 2011a). Studies investigating pro-fibrotic mechanisms, however, have recognized IL-33 as a component in fibrotic responses within the skin, liver and lung (Marvie et al., 2010; Rankin et al., 2010; Yanaba et al., 2011). Furthermore, it has been reported that mast cells can also mediate fibrotic responses, specifically in response to particulate toxicity as observed with silicosis (Brown et al., 2007). Here, we investigated IL-33 in conjunction with its activation of mast cells as an underlying mechanism in MWCNT-specific pulmonary fibrosis. Histopathological changes and collagen deposition, along with quantification of collagen content were examined at 30 days following MWCNT exposure to assess pulmonary fibrotic responses. C57BL/6 mice and $Kit^{W\text{-}sh}$ mice reconstituted with BMMCs exhibited a robust increase in collagen content with MWCNT instillation, while $Kit^{W\text{-}sh}$, $ST2^{-/-}$, and $Kit^{W\text{-}sh}$ mice reconstituted with $ST2^{-/-}$ BMMCs showed a minimal change in collagen

content compared to controls (Figure 3.4b). These data were further substantiated by significantly altered lung histopathology that displayed a wide distribution of collagen deposition and granuloma formation throughout the tissue in C57BL/6 and *Kit*$^{W\text{-}sh}$ mice reconstituted with BMMCs following MWCNT aspiration (Figure 3.4c). As indicated by Masson's Trichrome staining, fibrotic tissue was identified within granulomas, along with the deposition of MWCNTs as depicted by arrows (Figure 3.4c). MWCNT deposition within lung sections was confirmed by Raman spectroscopy (Figure 3.5). In contrast, lung sections from MWCNT instilled *Kit*$^{W\text{-}sh}$ mice did not display any collagen deposition and minimal granulomatous tissue (Figure 3.4c). ST2$^{-/-}$ and *Kit*$^{W\text{-}sh}$ mice reconstituted with ST2$^{-/-}$ BMMCs also had an attenuated fibrotic response, suggesting a role for mast cells -- or more specifically -- the ST2 receptor in MWCNT induced pulmonary toxicity.

MWCNTs Elicit Changes in Pulmonary Function Dependent Upon Mast Cells and IL-33

We have shown that instillation of MWCNTs impairs pulmonary function in C57BL/6 mice due to development of lung inflammation and fibrosis (Wang et al., 2011a). To investigate whether mast cells and the IL-33/ST2 axis participate in the observed decline in lung function induced by MWCNT exposure, we used the invasive forced oscillation technique to measure elastance (E), compliance (C) and Newtonian resistance (Rn) in C57BL/6 mice, *Kit*$^{w\text{-}sh}$ mice, *Kit*$^{w\text{-}sh}$ mice reconstituted with BMMC, *Kit*$^{w\text{-}sh}$ mice reconstituted with ST2$^{-/-}$ BMMC and ST2$^{-/-}$ mice, 30 days following MWCNT exposure. As previously reported, (Wang et al., 2011a) C57BL/6 mice exhibited a significant increase in E, suggesting increased elastic rigidity of the lungs (Figure 3.6a).

Similarly, *Kit*$^{w\text{-}sh}$ mice reconstituted with BMMCs exhibited significantly increased E following MWCNT exposure, while little or no change in E occurred in *Kit*$^{w\text{-}sh}$ mice, *Kit*$^{w\text{-}sh}$ mice reconstituted with ST2$^{-/-}$ BMMC or ST2$^{-/-}$ mice following MWCNT instillation (Figure 3.6a). A similar role for mast cells and the IL-33/ST2 pathway was observed when we measured C, which reflects the elasticity of the lung parenchyma and is also influenced by surface tension, smooth muscle contraction and peripheral airway homogeneity. When compared to vehicle treated mice, a reduction in C was observed only in MWCNT instilled C57BL/6 and *Kit*$^{w\text{-}sh}$ mice reconstituted with BMMC (Figure 3.6b). A decrease in C was not observed when *Kit*$^{w\text{-}sh}$ mice were reconstituted with ST2$^{-/-}$ BMMC or when ST2$^{-/-}$ mice were instilled with MWCNTs. The increased E and the decreased C in C57BL/6 mice and *Kit*$^{w\text{-}sh}$ mice reconstituted with BMMC reveal the increased stiffness in the fibrotic lung due to MWCNT exposure, which is consistent with findings in other models of pulmonary fibrosis (Phillips et al., 2011). These results indicate that the decline in pulmonary function as a physiological endpoint induced by MWCNT instillation is largely dependent on the presence of mast cells. In addition, our data suggest that the critical mast cell-dependent effects of MWCNT induced pulmonary fibrosis require the ability of mast cells to respond to IL-33 via the ST2 receptor.

A significant increase in Rn following MWCNT exposure was observed in C57BL/6 and *Kit*$^{w\text{-}sh}$ mice reconstituted with BMMC, with little to no change in Rn in *Kit*$^{w\text{-}sh}$ mice, *Kit*$^{w\text{-}sh}$ mice reconstituted with ST2$^{-/-}$ BMMC or ST2$^{-/-}$ mice (Figure 3.6c). The increased Rn suggests that narrowing of the conducting airways is occurring due to MWCNT exposure. While normal Rn values for mice are around 4.2 $cmH_2O.s/ml$, the *Kit*$^{w\text{-}sh}$ mice in our study displayed abnormally lower values of Rn compared to other

groups (Bates, 2009). However, the lower Rn observed in the *Kit*$^{w\text{-}sh}$ strain was restored to normal values when *Kit*$^{w\text{-}sh}$ mice were reconstituted with C57BL/6 BMMC or ST2$^{-/-}$ BMMC. Studies have shown that *Kit*$^{w\text{-}sh}$ mice reconstituted with BMMCs resulted in notably increased numbers of mast cells in the lung, especially along the central airways, which is similar to the mast cell distribution found in C57BL/6 mice (Cyphert et al., 2011b). This suggests that mast cells, which are located along the main bronchi, have a significant impact on Rn. These findings identify an important role for IL-33, and its receptor ST2, in mast cell mediated changes of Rn. Our observations of increases in E and Rn and a decrease in C in C57BL/6 and *Kit*$^{w\text{-}sh}$ mice reconstituted with BMMC but not in *Kit*$^{w\text{-}sh}$ mice, *Kit*$^{w\text{-}sh}$ mice reconstituted with ST2$^{-/-}$ BMMC or ST2$^{-/-}$ mice support the critical role of mast cell activation via IL-33/ST2 axis in MWCNT mediated impairment of pulmonary function.

MWCNTs Exacerbate Myocardial Ischemia Reperfusion Injury through Mast Cell Activation

Inhalation of ultra-fine, and possibly nano-sized, airborne particulates are well known to elicit adverse cardiovascular events mediated through multiple mechanisms that are largely unclear. We have shown that inhalation of particulates such as cerium oxide nanoparticles can activate mast cells, promoting the release of Th2 pro-inflammatory cytokines and resulting in altered vascular reactivity and exacerbation of an episode of myocardial ischemia/reperfusion injury in C57BL/6 mice, but not *Kit*$^{W\text{-}sh}$ mice (Wingard et al., 2011). Additional studies have established that mast cells and/or mast cell products such as chymase are crucial factors in the regulation of

cardiovascular responses to tissue injury resulting in inflammation, fibrosis, ventricular arrhythmias and myocardial infarction (Nistri et al., 2008; Oyamada et al., 2011).

We propose that mast cells are able to contribute to cardiovascular dysfunction, particularly myocardial IR injury, in part, through activation of the ST2 receptor. Clinical observations have reported increased levels of serum soluble ST2 receptor (sST2) associated with decreased left ventricular function and adverse cardiovascular outcomes in patients following acute myocardial infarction (Weir et al., 2010). It was therefore of interest to examine how the IL-33/ST2 axis in promoting mast cell activation may potentiate cardiovascular toxicities associated with MWCNT exposure. Work in our laboratory has demonstrated that MWCNT instillation in C57BL/6 mice results in exacerbation of IR injury in a dose dependent manner at 1 day post-exposure, which resolves by 30 days post-exposure (Urankar, *In Submission* 2012b). As this cardiovascular response has been shown to occur at an earlier time point, we investigated the role of mast cells and the IL-33/ST2 axis in IR injury responses in mice 1 day following exposure to MWCNTs. Here, we show that instillation of MWCNTs in C57BL/6 mice and $Kit^{W\text{-}sh}$ mice reconstituted with BMMCs exhibit a significant increase in myocardial infarct size following ischemia reperfusion compared to vehicle controls (Figure 3.7). An exacerbation of the infarct size by MWCNTs was not observed in $Kit^{W\text{-}sh}$ mice or $Kit^{W\text{-}sh}$ mice reconstituted with $ST2^{-/-}$ BMMCs (Figure 3.7). Interestingly, $ST2^{-/-}$ mice demonstrated a significant exacerbation of infarct size with MWCNT exposure compared to vehicle controls, however, the augmented response was not as robust as seen in C57BL/6 or $Kit^{W\text{-}sh}$ mice reconstituted with BMMCs. These data, while consistent with the pulmonary data in substantiating an underlying mast cell specific

mechanism associated with MWCNT toxicity, also suggest that the IL-33/ST2 axis may not solely contribute to mast cell activation which appears to be the major contributing factor in mediating myocardial IR injury responses following MWCNT exposure.

Table 3.1 MWCNT Characteristics

MWCNT Characteristics							
	Mean Diameter by TEM (nm)	Length Range by TEM (μm)	Metal Ash Content by TGA (% weight)	Spectral Content (Atomic %)		Surface area by BET (m^2/g)	Pore volume by BJH (cm^3/g)
				C	Fe		
MWCNT	22.5 ± 1.3	10 - 100	4.80	99.6	0.04	113.10	0.69

Table 3.2 MWCNT Suspension Characteristics

MWCNT Suspension Characteristics				
			Hydrodynamic Size	
	Zeta Potential	IEP	Major peak	Minor peak
MWCNT	- 44.6 mV	pH = 3.5	180 ± 50 nm	1100 ± 200 nm

Figure 3.1Transmission electron microscopy (TEM) of MWCNTs

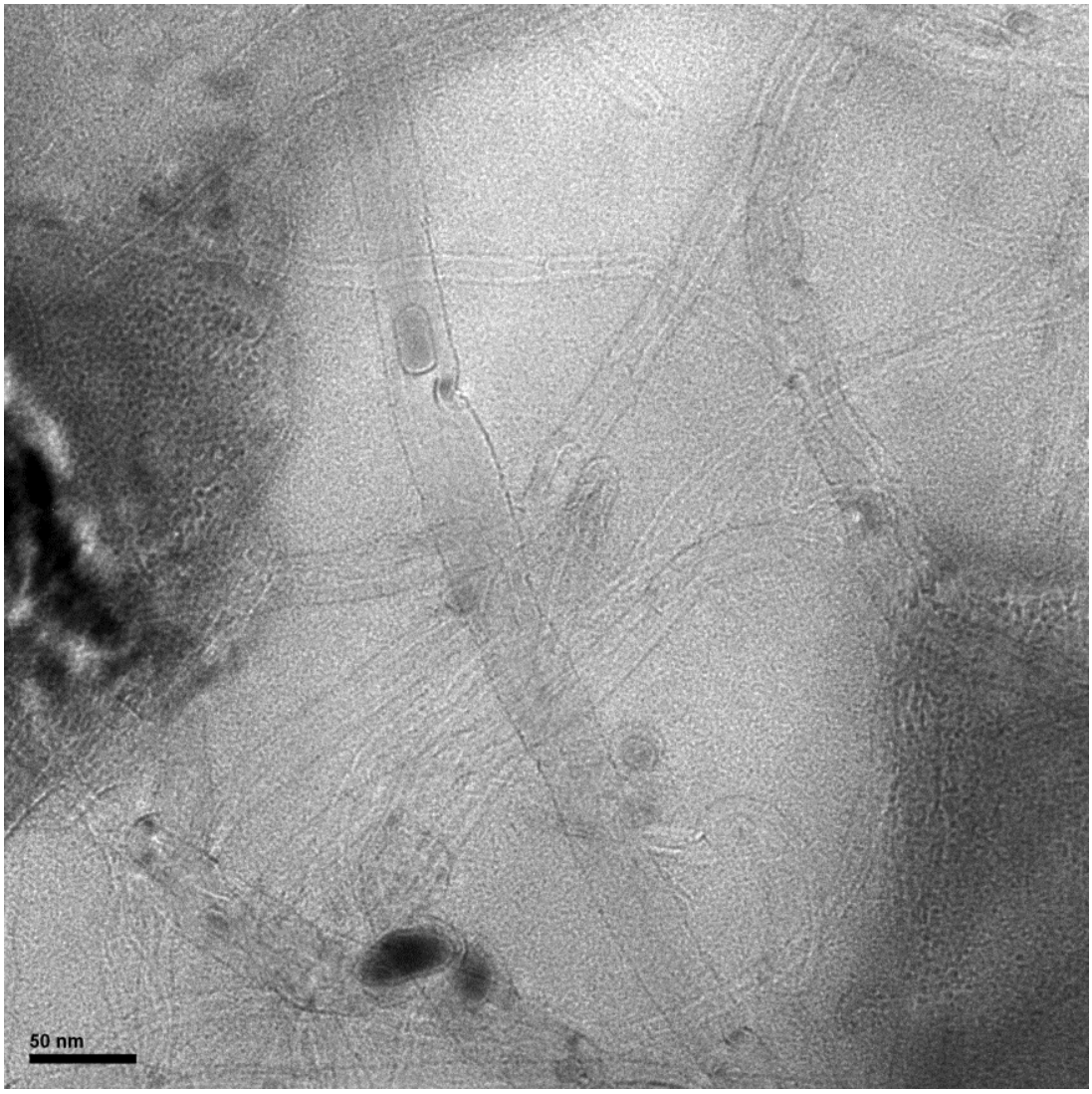
50 nm

Figure 3.2 IL-33 Gene and Protein Expression in Lungs of Mice 30 Days Post-Exposure to MWCNT

a, Gene expression of IL-33 in lung tissue, determined by real-time PCR analysis, displayed a >2 fold increase in all groups 30 days post-exposure to MWCNT compared to vehicle controls. **b, c,** Corresponding protein analysis with ELISA **(b)** and immunofluorescence images taken at a magnification of 20x **(c)**. Values are expressed as mean ± SEM (n=6-11). *$p < 0.05$ compared to strain matched vehicle control.

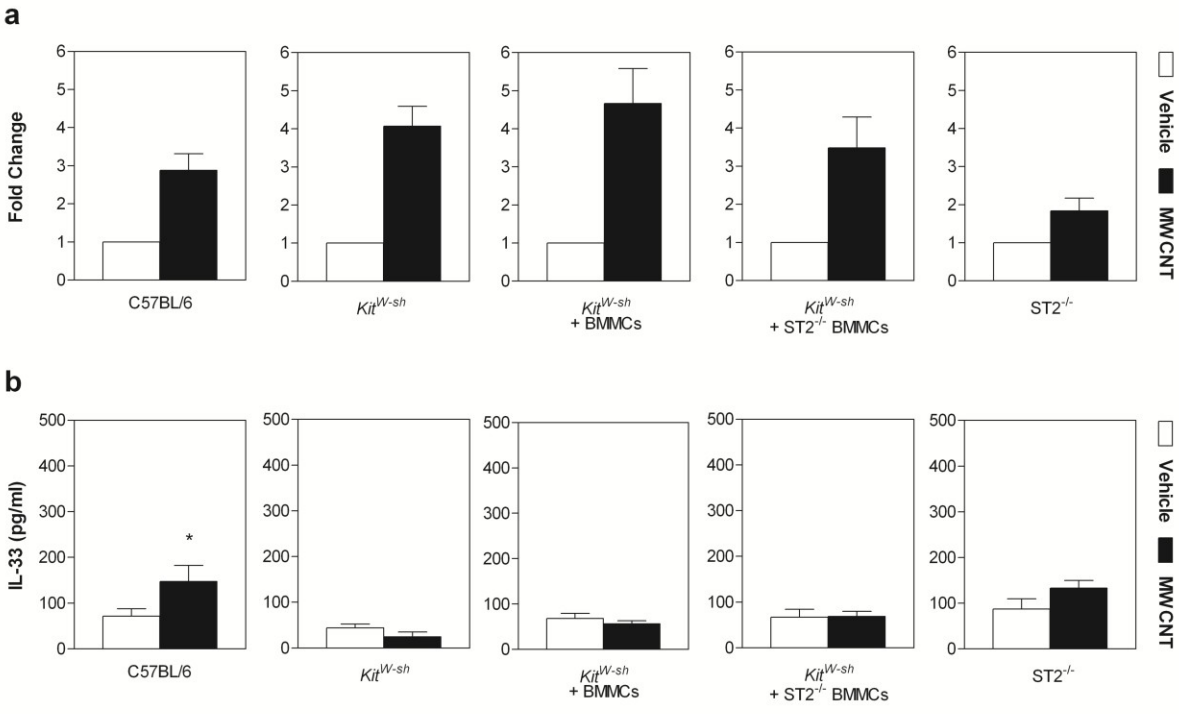
a
Fold Change
C57BL/6
Kit^W-sh
Kit^W-sh + BMMCs
Kit^W-sh + ST2^-/- BMMCs
ST2^-/-
Vehicle
MWCNT
b
IL-33 (pg/ml)
*
C57BL/6
Kit^W-sh
Kit^W-sh + BMMCs
Kit^W-sh + ST2^-/- BMMCs
ST2^-/-
Vehicle
MWCNT

c

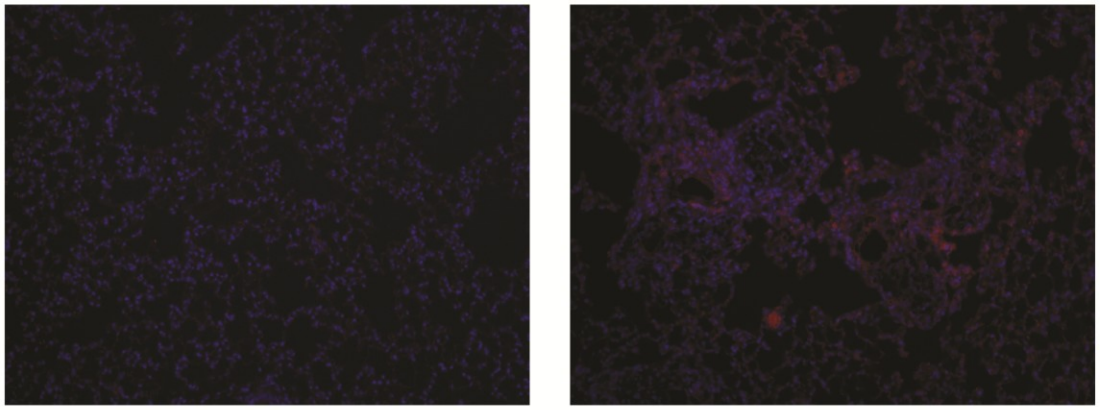

Figure 3.3 BALF from MWCNT Exposed Mice Results in Mast Cell Activation via the IL-33/ST2 Axis

Gene expression of IL-6 and osteopontin (OPN), determined by real-time PCR analysis, in bone marrow derived mast cells (BMMCs) and $ST2^{-/-}$ BMMCs after exposure to bronchoalveolar lavage fluid (BALF) obtained from C57BL/6 1 day following MWCNT instillation. Values are expressed as mean ± SEM (n=3-6).

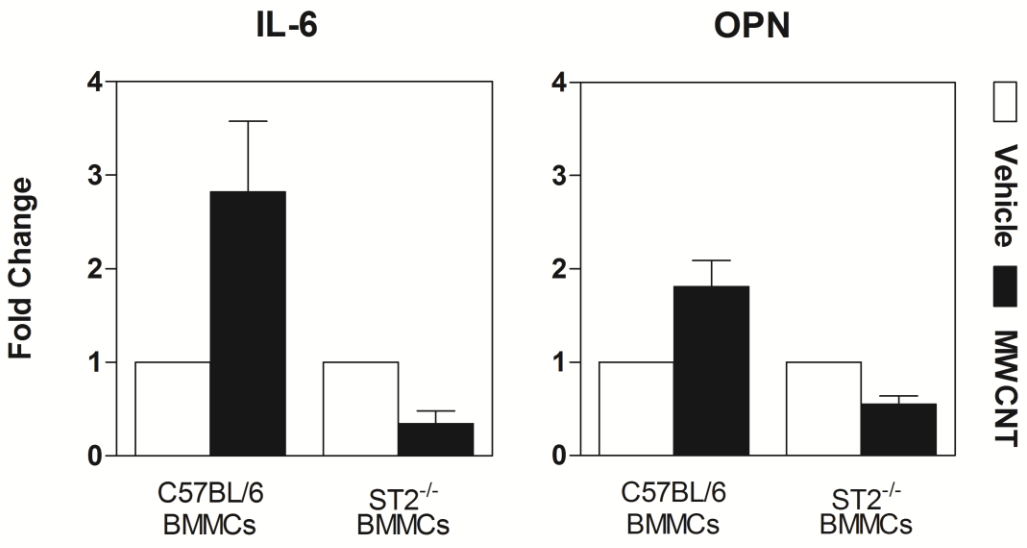
IL-6
OPN
Fold Change
4
3
2
1
0
C57BL/6 BMMCs
ST2-/- BMMCs
Vehicle
MWCNT

Table 3.3 Pulmonary cell populations in mice at 30 days following MWCNT exposure

Strain	Treatment	Macrophages ($x10^3$)	Neutrophils ($x10^3$)	Eosinophils ($x10^3$)	Lymphocytes ($x10^3$)	Total Cells ($x10^3$)
C57BL/6	Vehicle	114.35 ± 8.76	1.55 ± 0.79	0.50 ± 0.16	0.05 ± 0.03	136.77 ± 11.68
C57BL/6	MWCNT	283.39 ± 37.63 Ŧ	16.06 ± 4.56**	3.25 ± 1.16**	0.65 ± 0.34	349.00 ± 42.86 Ŧ
Kit$^{W\text{-}sh}$	Vehicle	207.91 ± 31.61	2.75 ± 2.11	0.00 ± 0.00	0.25 ± 0.25	264.75 ± 38.81
Kit$^{W\text{-}sh}$	MWCNT	370.82 ± 74.85*	51.62 ± 46.41	0.00 ± 0.00	0.00 ± 0.00	509.00 ± 109.19*
Kit$^{W\text{-}sh}$ + BMMCs	Vehicle	183.98 ± 19.93	1.59 ± 0.52	0.00 ± 0.00	2.79 ± 1.10	220.60 ± 21.31
Kit$^{W\text{-}sh}$ + BMMCs	MWCNT	189.49 ± 27.08	112.08 ± 34.45**	38.45 ± 19.04	39.94 ± 26.50*	455.20 ± 90.58*
Kit$^{W\text{-}sh}$ + ST2 $^{-/-}$BMMCs	Vehicle	150.23 ± 21.26	0.00 ± 0.00	0.00 ± 0.00	0.00 ± 0.00	198.00 ± 29.17
Kit$^{W\text{-}sh}$ + ST2 $^{-/-}$BMMCs	MWCNT	286.30 ± 48.56*	7.54 ± 5.84	1.17 ± 0.87	0.00 ± 0.00	375.00 ± 63.26*
ST2 $^{-/-}$	Vehicle	156.73 ± 18.64	3.10 ± 2.32	0.00 ± 0.00	0.93 ± 0.93	180.83 ± 20.86
ST2 $^{-/-}$	MWCNT	186.90 ± 20.63	7.19 ± 3.54	0.35 ± 0.24	2.34 ± 1.24	219.00 ± 24.58

Values are mean ± SEM. N=6/group; *p < 0.05 vs vehicle within strain; **p < 0.01 vs vehicle within strain; Ŧp< 0.001 vs vehicle within strain

Figure 3.4 Neutrophil Cell Counts, Histopathology and Collagen Content in Lungs of Mice Instilled with MWCNT

a, Neutrophil cell counts in mice 30 days following instillation with vehicle or MWCNTs. **b**, Percent collagen change in lung tissue of mice exposed to MWCNT at 30 days compared to vehicle control. **c**, Masson's trichrome staining at 30 days post-exposure to MWCNT. As indicated by the bluish color stain, extensive collagen rich granulomas and fibrotic tissue were identified in C57BL/6 and $Kit^{W\text{-}sh}$ mice reconstituted with BMMCs. $Kit^{W\text{-}sh}$ mice did not display any fibrotic responses, while $Kit^{W\text{-}sh}$ mice reconstituted with $ST2^{-/-}$ BMMCs and $ST2^{-/-}$ mice demonstrated minimal granuloma formation, unlike the robust response displayed by mast cell sufficient mice. Agglomerates of MWCNT were identified by Raman spectroscopy (Wang et al., 2011a) and can be seen within granulomas as indicated by arrows. Images are representative of 6-11 mice per group 30 days post-exposure to MWCNT with original magnifications of 20x. All values are expressed as mean ± SEM. $*p < 0.05$ compared to strain matched vehicle control and $*p < 0.01$ compared to strain matched vehicle control.

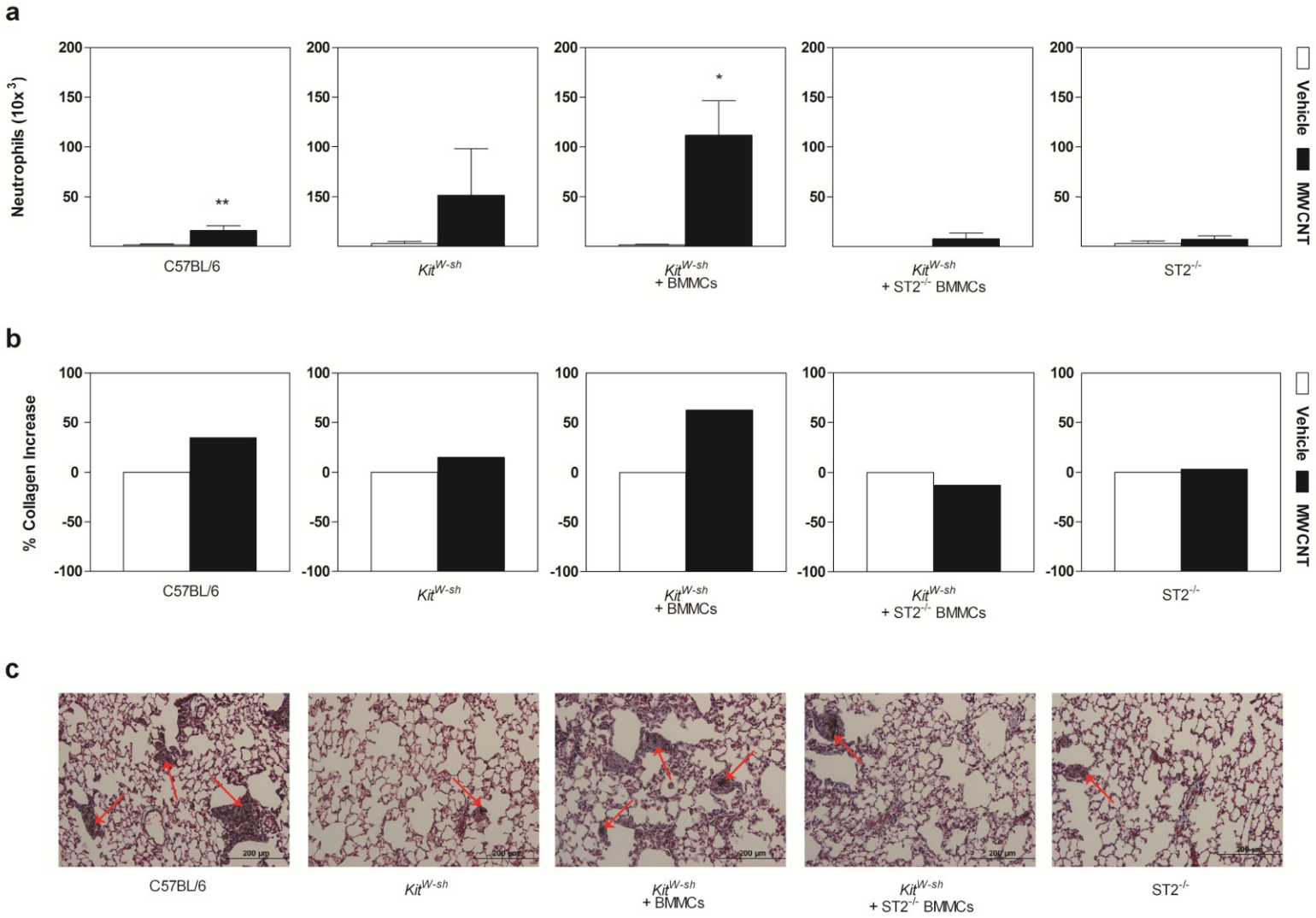
a
Neutrophils (10x 3)
200
150
100
50
**
*
C57BL/6
KitW-sh
KitW-sh + BMMCs
KitW-sh + ST2-/- BMMCs
ST2-/-
Vehicle
MWCNT
b
% Collagen Increase
100
50
0
-50
-100
C57BL/6
KitW-sh
KitW-sh + BMMCs
KitW-sh + ST2-/- BMMCs
ST2-/-
Vehicle
MWCNT
c
200 µm
C57BL/6
KitW-sh
KitW-sh + BMMCs
KitW-sh + ST2-/- BMMCs
ST2-/-

Figure 3.5 Raman Spectroscopy of Lung Histology

a) A representative microscope image for the unstained lung sections shown in Fig. 3c. b) The Raman map for the boxed area shown in a). Mapping measurement were performed using a 514.5 nm Ar+ ion laser coupled to a Dilor XY Raman spectrometer. The red color in the map corresponds to the typical spectroscopic signature of MWCNTs shown in c). Green color indicates the absence of peaks shown in c). c) A representative Raman spectrum of MWCNTs, acquired from the sample shown in a), exhibits the disorder (or D-band) band at ~1450 cm^{-1} and the graphitic (or G-band) at ~1600 cm^{-1}.

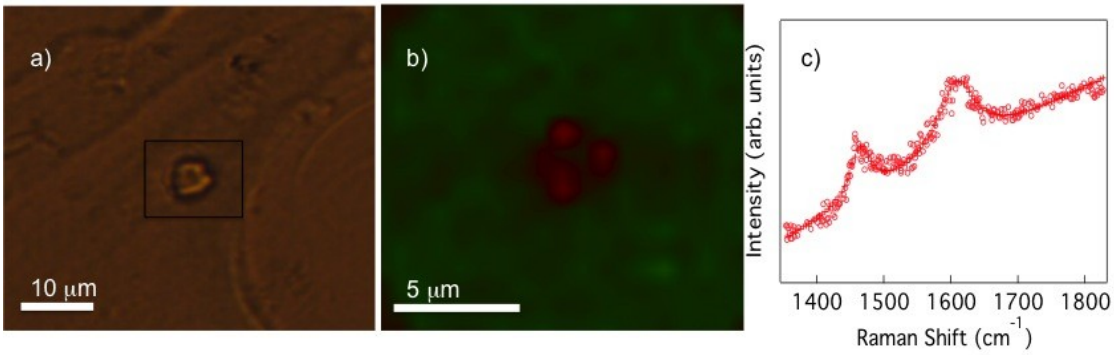
a)
10 μm
b)
5 μm
c)
Intensity (arb. units)
1400 1500 1600 1700 1800
Raman Shift (cm-1)

Figure 3.6 Altered Pulmonary Function Following MWCNT Instillation

The force oscillatory technique was performed on tracheotomized C57BL/6 mice, *Kit*$^{w\text{-}sh}$ mice, *Kit*$^{w\text{-}sh}$ mice reconstituted with BMMC (*Kit*$^{w\text{-}sh}$ + BMMCs), *Kit*$^{w\text{-}sh}$ mice reconstituted with ST2$^{-/-}$ BMMCs (*Kit*$^{w\text{-}sh}$ + ST2$^{-/-}$ BMMCs) and ST2$^{-/-}$ mice 30 days post-instillation with MWCNTs. The perturbation parameters, E (elastance) (**a**), C (compliance) (**b**), and Rn (Newtonian resistance) (**c**) were measured. All values are expressed as mean ± SEM (n=5-6). *$p < 0.05$ compared to strain matched vehicle control (open bar).

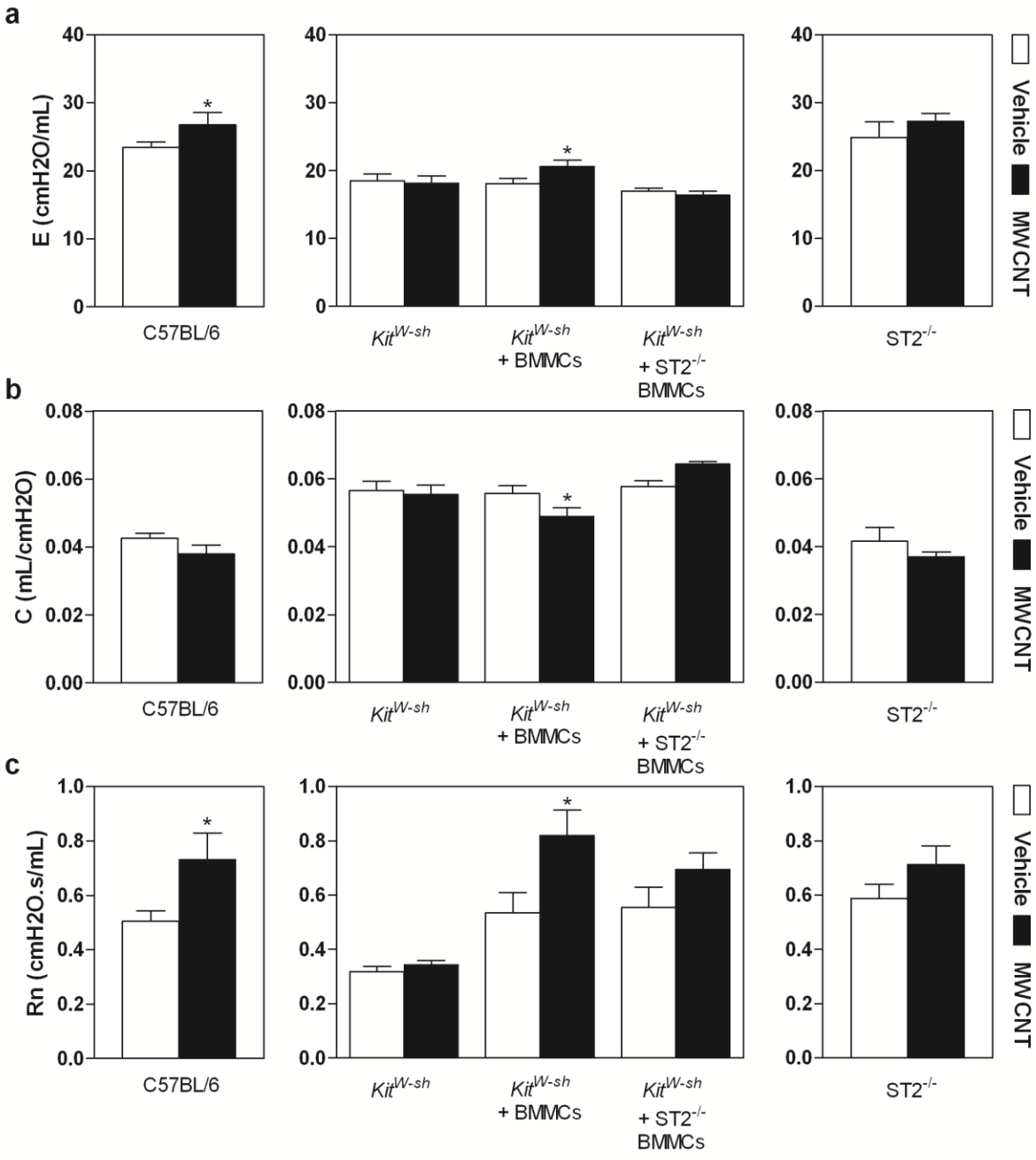
a
E (cmH2O/mL)
40
30
20
10
0
*
C57BL/6
Kit W-sh
Kit W-sh + BMMCs
Kit W-sh + ST2-/- BMMCs
ST2-/-
Vehicle
MWCNT
b
C (mL/cmH2O)
0.08
0.06
0.04
0.02
0.00
c
Rn (cmH2O.s/mL)
1.0
0.8
0.6
0.4
0.2
0.0

Figure 3.7 MWCNT Induced Exacerbation of Myocardial Ischemia Reperfusion Injury

Myocardial ischemia reperfusion injury response was assessed as a comparison of infarct size to total area at risk (%) in C57BL/6 mice, *Kit*$^{w\text{-}sh}$ mice *Kit*$^{w\text{-}sh}$ mice reconstituted with BMMCs (*Kit*$^{w\text{-}sh}$ + BMMCs), *Kit*$^{w\text{-}sh}$ mice reconstituted with ST2$^{-/-}$ BMMC (*Kit*$^{w\text{-}sh}$ + ST2$^{-/-}$ BMMCs) and ST2$^{-/-}$ mice, 1 day following exposure to vehicle or MWCNT. All values are expressed as mean ± SEM (n=4-25). $^{**}p < 0.01$ compared to strain matched vehicle control and $^{***}p < 0.001$ compared to strain matched vehicle control.

Vehicle
MWCNT
Infarct/Risk Area (%)
50
40
30
20
10
0
***
C57BL/6
Kit^W-sh
***
Kit^W-sh
+ BMMCs
Kit^W-sh
+ ST2^-/-
BMMCs
**
ST2^-/-

CONCLUSION

In this study, we proposed that MWCNT aspiration actuates the extracellular release of IL-33 in lung tissue, leading to the activation of mast cells through the ST2 receptor, resulting in an increase in pulmonary inflammation, granuloma and fibrotic tissue formation, altered pulmonary function and exacerbated IR injury responses in the heart (Figure 3.8). We have demonstrated that these MWCNT induced toxicities are mediated by mast cell activation in both the pulmonary and cardiovascular systems, entirely or in part, through the IL-33/ST2 axis. Furthermore, in identifying the mechanism of toxicity, our study provides a crucial insight in delineating efforts to limit exposure to nanoparticles and discerning appropriate means of treatment that could be needed following exposures. There are several routes of exposure to MWCNT. In this study we have examined the toxicity of MWCNT through a respiratory exposure, however, it is important to acknowledge that there is great potential intravenous exposures as MWCNTs are currently display a unique platform for drug delivery. Despite the differences in exposure routes, intravenous injection of MWCNTs may result in similar toxicities. Intravenous exposure may distribute MWCNTs into the lung tissue to display the mast cell mediated pulmonary toxicities reported in this study. In addition, as mast cells are known to reside in many tissue types, there is still a potential for MWCNT to activate mast cells in other areas of the body to produce additional, unreported toxicities (Yong, 1997).

In the current study, we have demonstrated a key role of mast cells as modulators of MWCNT toxicity, therefore, targeting mast cells therapeutically may serve to alleviate the potential toxicities associated with exposure to MWCNTs, and have also provided a

novel screening tool to discern the potential toxicity and concern associated with the rising use of nanomaterials.

Figure 3.8 Mechanism of MWCNT Induced Pulmonary and Cardiovascular Toxicity

MWCNT induced injury to the lung epithelium results in the release of IL-33. In the lung, IL-33 can activate mast cells through the ST2 receptor to induce pulmonary inflammation, granuloma formation and fibrosis, as well as altered lung function. A similar mechanism in the heart may influence the activation of mast cells by IL-33 via ST2 receptors to exacerbate ischemia reperfusion injury responses.

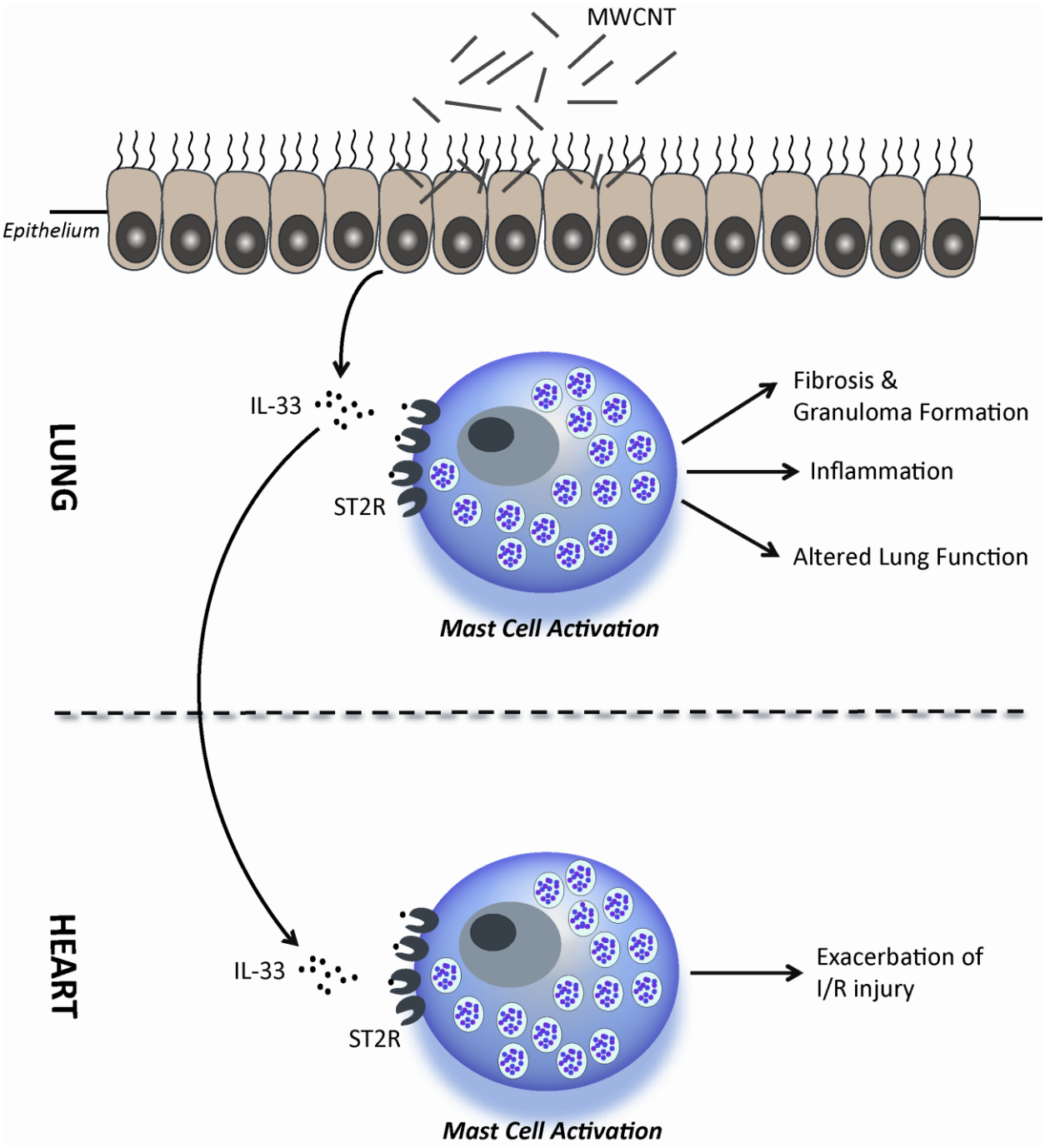
MWCNT
Epithelium
LUNG
IL-33
ST2R
Fibrosis &
Granuloma Formation
Inflammation
Altered Lung Function
Mast Cell Activation
HEART
IL-33
ST2R
Exacerbation of
I/R injury
Mast Cell Activation

CHAPTER 4: ADDITIONAL RESULTS

C57BL/6 Mice Display Normal Pulmonary Function 30 Days Following Carbon Black Exposure

In order to corroborate our pulmonary function data and to ensure that the results were specific to MWCNT exposure and not a generalized response to particulate inhalation, we used carbon black as a reference particle. Although carbon black is not a true negative control as it is not entirely inert, it is often considered to be a more inert nanoparticle compared to MWCNTs and does not display the profound toxicities associated with MWCNTs and other nanomaterials. Further, while carbon black consists of similar elemental composition, it does not display the same important physicochemical properties that potentially contribute to MWCNT toxicity such as high aspect ratio and surface area.

Age matched (9-10 weeks) C57BL/6 mice were exposed to vehicle or 4 mg/kg carbon black particles (in vehicle or 10% surfactant/saline) via oropharyngeal aspiration and utilized for pulmonary function testing 30 days post-exposure. The total lung resistance (R), compliance (C) and elastance (E) parameters, measured by the FlexiVent snapshot perturbation, do not exhibit any statistically significant changes between vehicle control or treatment groups with one exception (Figure 4.1). Mice exposed to carbon black did display an increase in R (Figure 4.1a). This may be due to a mild inflammatory response observed in carbon black exposed mice. The BAL differential cell counts of carbon black exposed mice did not show significant increases in macrophage or eosinophil counts, but demonstrated slightly elevated numbers of

neutrophils and total cells, though not as robust a response as seen with mice instilled with MWCNTs (Figure 4.3). These data confirm carbon black as an appropriate reference particle which does not induce robust pulmonary inflammation or impaired pulmonary function in parameters associated with pulmonary fibrosis (E and C) 30 days following exposure.

Additional pulmonary function parameters, tissue damping or energy dissipation (G), tissue elastance or energy conservation (H), hysteresivity (eta or G/H) of the lung parenchyma and Area within the PV loop were also measured with a Quickprime-3 or PVr-P loop perturbation. The increases in G and eta were not observed in mice exposed to carbon black and values were similar to mice instilled with vehicle control (Figure 4.2). The increase in G, a parameter that accounts for parenchymal distortion, was also absent in carbon black instilled mice, suggesting that these mice may not have altered lung morphology and therefore may not elicit adverse pulmonary responses that translate into physiologically meaningful changes (Figure 4.2a). As there are no significant changes in H, eta, representative of the G to H ratio, or the ratio of energy dissipation to energy conservation in the cycle of inhalation and exhalation, is also decreased in carbon black instilled mice, displaying a pattern similar to G (Figure 4.2b and 4.2c). Mice exposed to carbon black most likely lack a significant formation of rigid fibrotic tissue. With less energy required to inflate the lung, there is less energy dissipation into the tissue, decreased tissue elastance and therefore decreased hysteresis or eta. Area of the PV loop, which reflects the energy or pressure required to inflate the lung, displayed no significant difference between carbon black instilled mice when compared to vehicle control mice, as would be expected for normal lung tissue

since there is most likely an absence of fibrotic tissue which is much stiffer than normal lung tissue (Figure 4.2d).

These data indicate that exposure to carbon black does not alter pulmonary function 30 days following instillation, and that the pulmonary toxicity and impaired lung function associated with MWCNT exposure is specific to this particular nanomaterial.

Low Gene and Protein Expression Levels of IL-33 in *in vitro* Lung Epithelial and Fibroblast Cell Culture Models

In order to fully understand the proposed underlying mechanism of MWCNT induced pulmonary and cardiovascular toxicity, we attempted to establish an *in vitro* model that would allow us to test the hypothesis using IL-33 specific antibodies, ST2 receptor antagonists or even examining interactions between cells types implicated in MWCNT associated pulmonary toxicity.

As mentioned previously, animals exposed *in vivo* to MWCNT exhibited significant amounts of IL-33 protein in BALF and lung tissue as well as IL-33 expression throughout the lung parenchyma and alveolar epithelial cells as indicated by immunofluorescence. *In vitro*, we first examined mast cells, but were unable detect IL-33 expression in BMMCs or bone marrow derived macrophages (BMDMs) with exposure to MWCNTs (data not shown). Based on our *in vivo* data, we also examined several pulmonary epithelial cell lines including a transformed murine lung epithelial (MLE-12) cell line and the C10 lung epithelial cell line. Cell lines were grown in either supplemented RPMI 1640 or DMEM medium with 5% FBS at 37°C and 5% CO_2 until 70% confluence was reached. Cells were then treated and collected to assess a variety

of endpoints. As shown in figure 4.4, MWCNTs failed to induce IL-33 gene expression in MLE-12 cells at 2, 4 or 24 hours post-exposure (Figure 4.4). C10 lung epithelial cells also demonstrated a lack of IL-33 induction at similar time points of 2, 4, or 8 hours following treatment with several different MWCNT doses (Figure 4.5). Interestingly, a high dose 100 ng/mL of LPS was unable to effectively elicit a significant response from either MLE-12 or C10 lung epithelial cells. As such, C10 cells were primed and stimulated with a low dose of LPS (20 ng/mL), known to enhance responses and activation of numerous cell types, 30 minutes prior to MWCNT exposure. However, neither group of cells, primed or unprimed, demonstrated IL-33 mRNA induction at any dose of MWCNT (4.6). We also investigated the possibility that IL-33 was an intracellular cytokine in healthy tissues, which may not be released in the absence of tissue damage or necrosis (Haraldsen et al., 2009; Luthi et al., 2009). We examined protein levels of IL-33 in C10 cell culture supernatant collected following 24 hours of treatment with 0.1, 1, 10 $\mu g/cm^2$ MWCNT or 100 ng/mL LPS, but were still unable to discern a significant increase in IL-33 protein following exposure to MWCNTs (Figure 4.7). Concurrent data were obtained when C10 cell lysate from the same experiment was analyzed for IL-33 protein by ELISA (Figure 4.7). C10 cells were also co-cultured with BMMCs, both in contact and transwell systems, prior to MWCNT exposure to determine if direct contact or proximity to different cell types impacted activation or IL-33 release. Co-cultures with BMMCs and C10 cells were not successful in exacting BMMC activation reflected through IL-6 expression or C10 expression of IL-33, following MWCNT treatment (data not shown). Several additional lung epithelial cell lines, including human A549 (ATTC, Manassas, VA) cells and human primary small airway

epithelial cells (SAEC, ATTC, Manassas, VA), were also explored for use as potential *in vitro* models, but yielded analogous outcomes (data not shown).

Alternatively, a primary murine lung fibroblast (MLF) cell, was also investigated as fibroblasts drive the adverse pulmonary fibrotic responses induced by MWCNTs, and may contribute to IL-33 production. However, MLF cells were not responsive to 100 ng/mL LPS or to different doses of MWCNT treatment and did not enhance IL-33 mRNA or protein expression (Figures 4.8 and 4.9).

Despite an array of negative data in establishing a relevant cell culture model, we were able to utilize *in vivo* models, specifically murine receptor knock out and mast cell reconstitution models for the ST2 receptor to address the validity of our proposed mechanism, ST2 receptor activation of mast cells by IL-33 in mediating MWCNT toxicity. Our negative data emphasizes the complexity of an organ system response and its associated cellular interactions. *In vitro* studies are limited by several factors as they lack certain microenvironments that may be essential in modulating cell function, activation or even phenotype. While this study has validated an IL-33 and mast cell specific mechanism of MWCNT induced toxicity, it is important to acknowledge that several presently unknown factors may modulate mast cells and mast cell phenotypes to produce a unique response following activation.

Figure 4.1 Changes in Pulmonary Function as Determined by Snapshot Perturbation After Carbon Black Instillation

The snapshot perturbation was performed in tracheotomized C57BL/6 mice instilled with vehicle (10% surfactant in saline) or 4 mg/kg carbon black. (**a**), total lung resistance (R), (**b**), compliance (C), and (**c**), elastance (E) parameters, indicative of whole lung respiratory mechanics, were measured. The mean ± SEM of 4-16 mice per group are shown. *$p < 0.05$ compared with vehicle control mice.

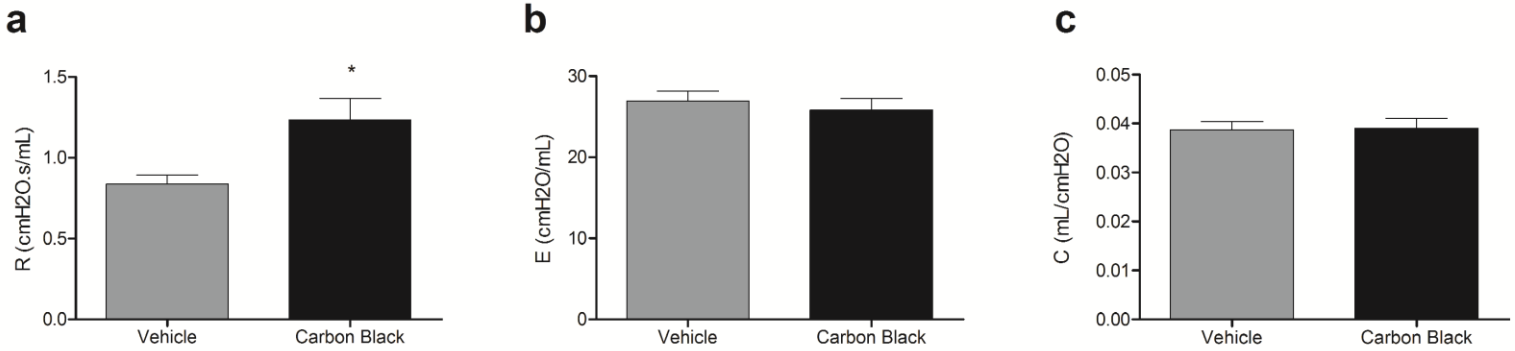
a
b
c
R (cmH2O.s/mL)
E (cmH2O/mL)
C (mL/cmH2O)
1.5
1.0
0.5
0.0
30
20
10
0
0.05
0.04
0.03
0.02
0.01
0.00
*
Vehicle
Carbon Black
Vehicle
Carbon Black
Vehicle
Carbon Black

Figure 4.2 Changes in Pulmonary Function as Determined by Quicktime-3 and PVr-P Perturbation Following Carbon Black Instillation

Quick-prime 3 and PVr-P perturbations were imposed on C57BL/6 mice 30 days following exposure to vehicle or 4 mg/kg carbon black. Quick-prime 3 parameters can differentiate specific lung compartments, enabling measurements of (**a**), tissue damping (G), (**b**) tissue elastance (H) and (**c**), hysteresivity or eta. From PV loops, the Area (**d**) perturbation parameter was determined. The mean ± SEM of 4-16 mice per group are shown and differences between vehicle and treatment groups were not significant

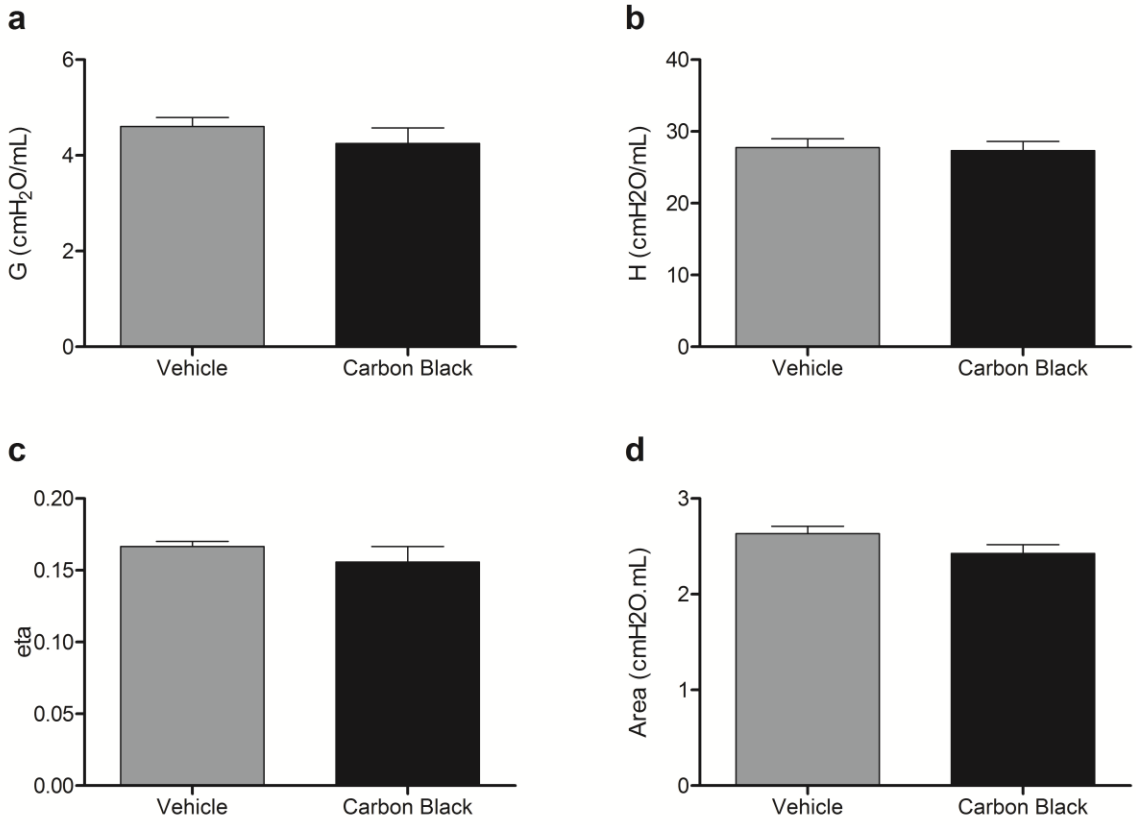
a
G (cmH2O/mL)
6
4
2
0
Vehicle
Carbon Black
b
H (cmH2O/mL)
40
30
20
10
0
Vehicle
Carbon Black
c
eta
0.20
0.15
0.10
0.05
0.00
Vehicle
Carbon Black
d
Area (cmH2O.mL)
3
2
1
0
Vehicle
Carbon Black

Figure 4.3 Differential Cell Counts in C57BL/6 mice 30 Days Following Carbon Black Exposure

C57BL/6 mice were exposed to vehicle or 4 mg/kg carbon black and underwent bronchoalveolar lavage 30 days following exposure. Differential cell counts for macrophages, neutrophils and eosinophils, along with total cell counts, were obtained from cytospins of bronchoalveolar lavage fluid. The mean ± SEM of 4-9 mice per group are shown. *$p < 0.05$ compared with vehicle control mice.

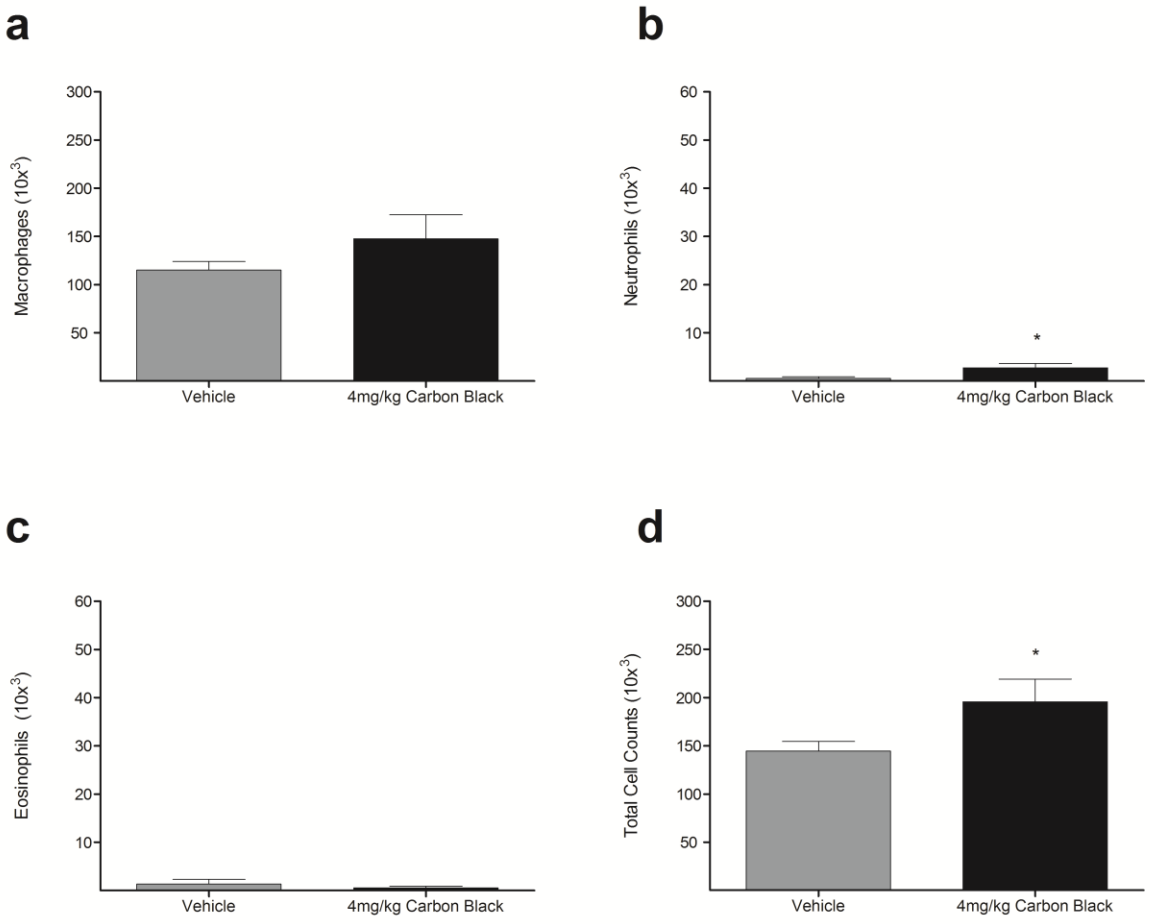
a
Macrophages (10x3)
300
250
200
150
100
50
Vehicle
4mg/kg Carbon Black
b
Neutrophils (10x3)
60
50
40
30
20
10
*
Vehicle
4mg/kg Carbon Black
c
Eosinophils (10x3)
60
50
40
30
20
10
Vehicle
4mg/kg Carbon Black
d
Total Cell Counts (10x3)
300
250
200
150
100
50
*
Vehicle
4mg/kg Carbon Black

Figure 4.4 Expression of IL-33 mRNA in MLE-12 Murine Lung Epithelial Cells at 2, 4, and 24 Hours Following MWCNT Exposure

MLE-12, a transformed murine lung epithelial cell line (ATCC, Manassas, VA) was cultured in FBS supplemented DMEM medium until 70% confluence was reached. Cells were then exposed to vehicle, 0.1, 1 or 10 μg/cm^2 MWCNT, 63 μg/cm^2 silica, or 100 ng/mL LPS. Samples were collected 2 (**a**), 4 (**b**) and 24 (**c**) hours after exposure for real-time PCR analysis to determine IL-33 mRNA expression. All values are expressed as fold changes compared to vehicle control. (n=3)

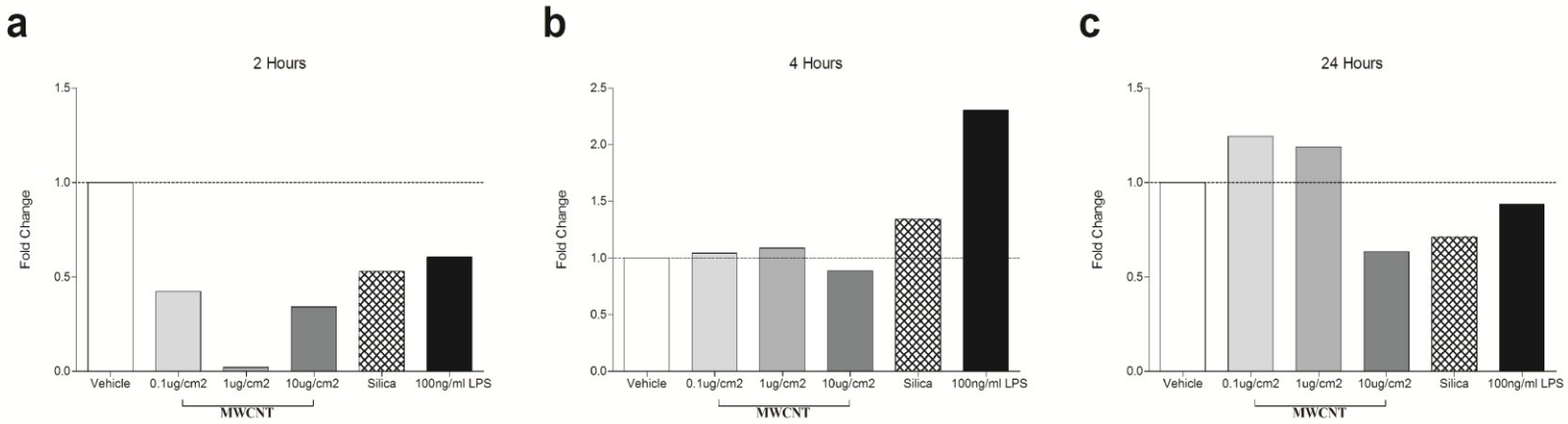
a
2 Hours
Fold Change
1.5
1.0
0.5
0.0
Vehicle
0.1ug/cm2
1ug/cm2
10ug/cm2
Silica
100ng/ml LPS
MWCNT
b
4 Hours
Fold Change
2.5
2.0
1.5
1.0
0.5
0.0
Vehicle
0.1ug/cm2
1ug/cm2
10ug/cm2
Silica
100ng/ml LPS
MWCNT
c
24 Hours
Fold Change
1.5
1.0
0.5
0.0
Vehicle
0.1ug/cm2
1ug/cm2
10ug/cm2
Silica
100ng/ml LPS
MWCNT

Figure 4.5 Expression of IL-33 mRNA in C10 Lung Epithelial Cells at 2, 4, and 8 Hours Post-Exposure to MWCNTs

Real-Time PCR analysis was performed on C10 lung epithelial cells collected from culture 2 (left panel), 4 (middle panel) or 8 (right panel) hours following vehicle or increasing doses of MWCNT to determine mRNA levels of IL-33, expressed as fold changes compared to vehicle control samples. C10 cells collected at the 2 hour time point were treated with vehicle, 0.1, 1, 3, or 10 μg/cm^2 MWCNT, while cells collected at the 4 and 8 hour time points were exposed to vehicle, 0.1, 1, or 10 μg/cm^2 MWCNT and an additional treatment group exposed to 100 ng/mL LPS, serving as a positive control.

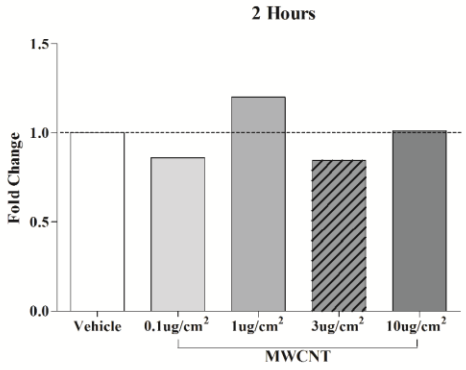
2 Hours
Fold Change
1.5
1.0
0.5
0.0
Vehicle
0.1ug/cm2
1ug/cm2
3ug/cm2
10ug/cm2
MWCNT

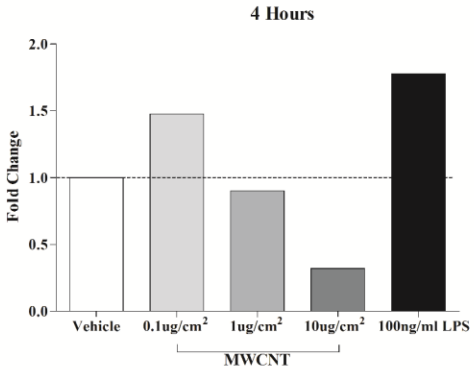
4 Hours
Fold Change
2.0
1.5
1.0
0.5
0.0
Vehicle
0.1ug/cm2
1ug/cm2
10ug/cm2
100ng/ml LPS
MWCNT

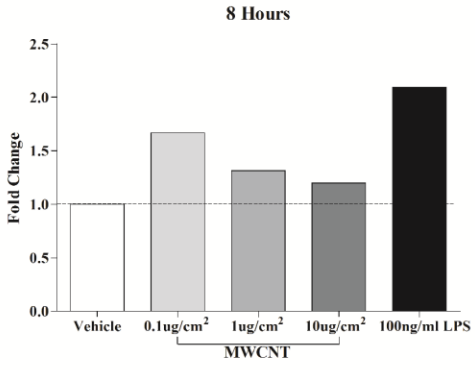
8 Hours
Fold Change
2.5
2.0
1.5
1.0
0.5
0.0
Vehicle
0.1ug/cm2
1ug/cm2
10ug/cm2
100ng/ml LPS
MWCNT

Figure 4.6 IL-33 mRNA Expression at 4 Hours Following MWCNT Treatment in C10 Cells Primed with LPS

C10 lung epithelial cells, cultured to 70% confluence, were primed 20 ng/mL LPS 30 minutes prior to treatment. Primed cells were exposed to 0.1, 1, or 10 μg/cm^2 MWCNT suspended in culture medium, for 4 hours. Cells that were not primed with 20 ng/mL LPS were simultaneously exposed to the same doses of MWCNT, with three additional control groups: untreated cells only, 20 ng/mL LPS and 100 ng/mL LPS. All samples were collected 4 hours later for real-Time PCR analysis to quantify IL-33 mRNA expression as fold changes compared to vehicle control samples.

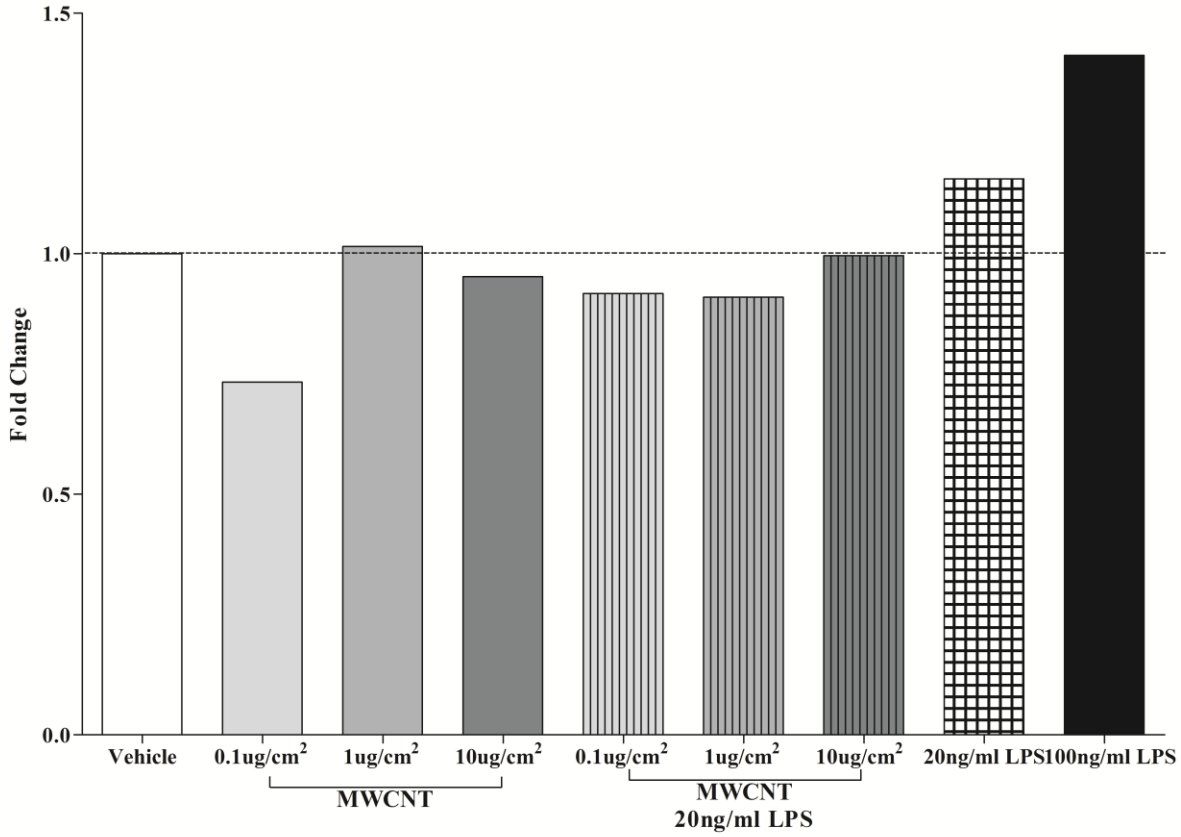
1.5
1.0
0.5
0.0
Fold Change
Vehicle
0.1ug/cm2
1ug/cm2
10ug/cm2
0.1ug/cm2
1ug/cm2
10ug/cm2
20ng/ml LPS
100ng/ml LPS
MWCNT
MWCNT
20ng/ml LPS

Figure 4.7 IL-33 Protein Levels in C10 Lung Epithelial Cells 24 Hours Following MWCNT Exposure

C10 cells, untreated or exposed to vehicle, 0.1, 1, 10 μg/cm^2 MWCNTs (in 10% surfactant/saline), or 100 ng/mL LPS were obtained 24 hours following exposure. Cell supernatant was removed from culture chamber for an ELISA, IL-33 cytokine protein analysis (left panel). The adherent C10 cells were then lysed using a lysis buffer to extract protein from within the cell for an additional IL-33 ELISA (right panel).

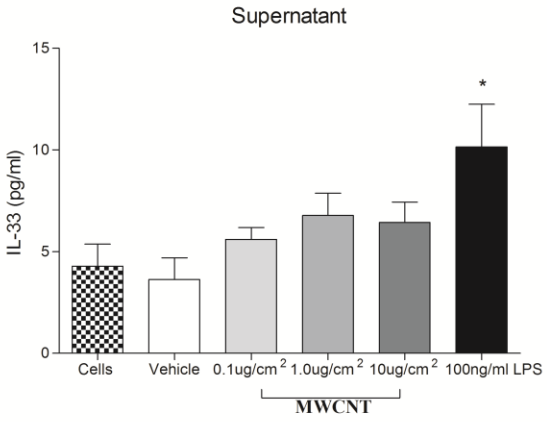
Supernatant
IL-33 (pg/ml)
15
10
5
0
*
Cells
Vehicle
0.1ug/cm 2
1.0ug/cm 2
10ug/cm 2
100ng/ml LPS
MWCNT

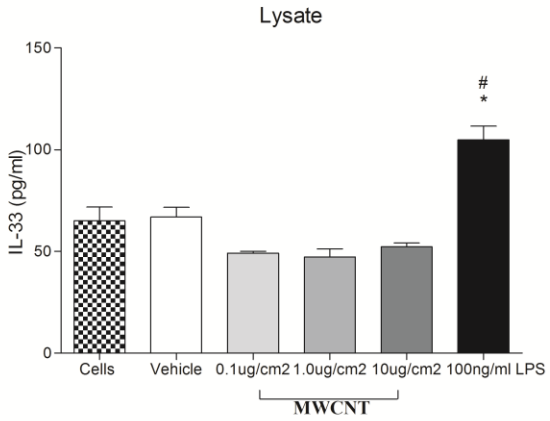
Lysate
IL-33 (pg/ml)
150
100
50
0
#
*
Cells
Vehicle
0.1ug/cm2
1.0ug/cm2
10ug/cm2
100ng/ml LPS
MWCNT

Figure 4.8 IL-33 mRNA Expression in Murine Lung Fibroblasts Following MWCNT Exposure

Primary murine lung fibroblasts (MLFs) were grown in a 6 well plate to 70% confluence exposed to 0.1, 1 or 10 μg/cm^2 MWCNT or 100 ng/mL LPS as a positive control. MWCNTs were suspended directly into culture medium instead of a vehicle. Cells were obtained at 2 (left panel) and 4 (right panel) hour time points for real-time PCR analysis to determine gene expression of IL-33 (expressed as fold change compared to control cells only group).

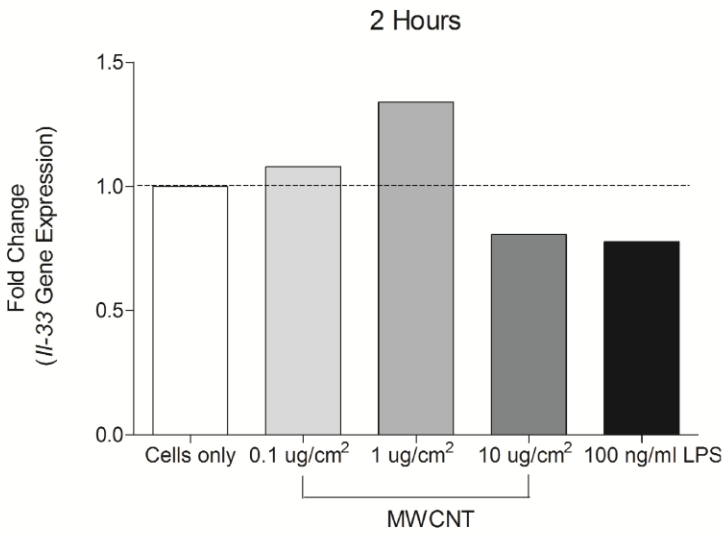
2 Hours
Fold Change
(Il-33 Gene Expression)
1.5
1.0
0.5
0.0
Cells only
0.1 ug/cm2
1 ug/cm2
10 ug/cm2
100 ng/ml LPS
MWCNT

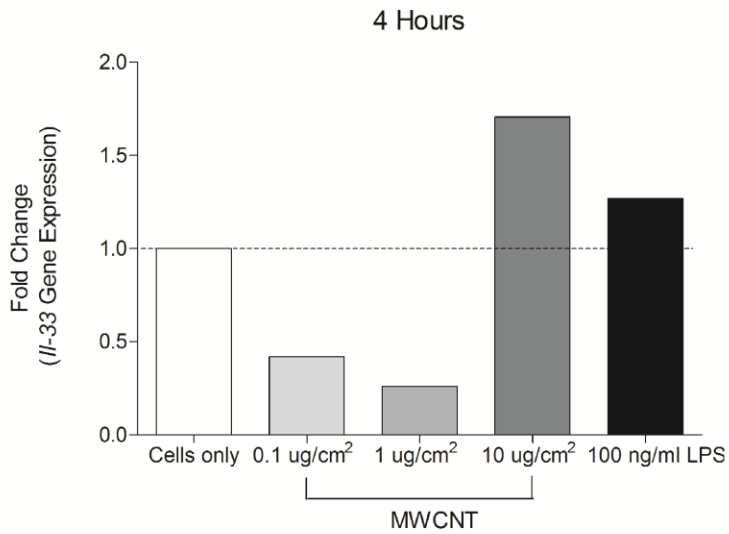
4 Hours
Fold Change
(Il-33 Gene Expression)
2.0
1.5
1.0
0.5
0.0
Cells only
0.1 ug/cm2
1 ug/cm2
10 ug/cm2
100 ng/ml LPS
MWCNT

Figure 4.9 IL-33 Protein Expression in Murine Lung Fibroblasts 24 Hours After MWCNT Treatment

Primary MLFs, exposed to 1 or 10 μg/cm^2 MWCNTs suspended in culture medium, were collected at 24 hours following exposure for ELISA analysis to quantify IL-33 protein within the cells.

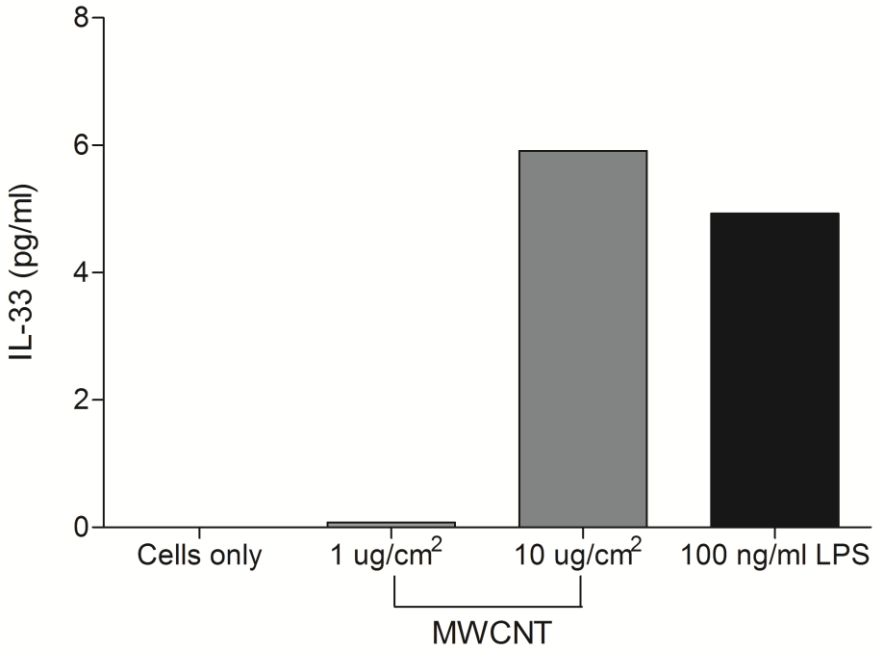
8
6
4
2
0
IL-33 (pg/ml)
Cells only
1 ug/cm2
10 ug/cm2
100 ng/ml LPS
MWCNT

CHAPTER 5: GENERAL DISCUSSION

The present study was undertaken to identify the potential role of mast cells and the IL-33/ST2 axis as an underlying mechanism in the pulmonary and cardiovascular toxicity induced by MWCNT exposure.

In Aim 1, we examined the role of mast cells in the pulmonary inflammation and fibrosis induced by oropharyngeal aspiration of MWCNTs. To accurately assess the pulmonary toxicity, we investigated a dose response with vehicle, 1, 2, and 4 mg/kg MWCNT. At 30 days following MWCNT instillation, C57BL/6 mice displayed an altered inflammatory cell profile with significantly increased neutrophil numbers at all doses (Table 2.1), associated with increased collagen deposition (Figure 2.5), granulomas and fibrotic tissue development at the high dose (Figure 2.6). Additional analyses supporting the observed altered lung morphology demonstrated upregulation in gene expression levels of *Mmp13*, *Ccl3* (also known as MIP-1α) and *Ccl11* (eotaxin) in BALF of mice instilled with the high dose of MWCNT (Figure 2.9). MMP13, a matrix metalloproteinase (MMP), belongs to a group of proteases that can be further categorized into collagenases, gelatinases, stromelysins, and membrane-type MMPs, known for ability to degrade extracellular matrix proteins (Selman et al., 2000). MMP13 in particular has been implicated as a key player in the development of pulmonary fibrosis (Flechsig et al., 2010). Enhanced expression of CCL3 and CCL11, macrophage and eosinophil chemoattractants, was also evident following MWCNT exposure, and most likely led to the recruitment of macrophages and eosinophils, contributing to the observed granuloma formation (Table 2.1). Together, the imbalance of the extracellular

matrix resulting from increased MMP13 activity, along with CCL3 and CCL11 chemokine induced immune cell infiltration may play an important role in the development of pulmonary fibrosis following MWCNT instillation.

In contrast, investigation of mast cell deficient *Kit*$^{W\text{-}sh}$ mice 30 days following MWCNT exposure revealed normal lung collagen content and morphology compared to vehicle controls (Figure 3.4). While MWCNT aggregates were still visible throughout the lung parenchyma and peribronchiolar spaces, inflammatory cell infiltrates, granulomas and fibrotic tissue were not present in the lung tissue of MWCNT instilled *Kit*$^{W\text{-}sh}$ mice (Figure 3.4). Our data confirmed previous reports of MWCNT induced pulmonary toxicity and provided crucial insight into the potential for mast cells in modulating the observed adverse pulmonary responses (Huizar et al., 2011; Ma-Hock et al., 2009; Porter et al., 2010). In addition, we were interested in the physiological ramifications of the severe pulmonary toxicities that were observed. We conducted additional studies to evaluate pulmonary function in C57BL/6 mice exposed to varying doses MWCNT (1, 2, or 4 mg/kg).

The forced oscillation technique (FOT) was used to ascertain values for all parameters by imposing small pressure oscillations to record pressure and flow following various preprogrammed maneuvers, resulting in detailed measurements of pulmonary mechanics (Glaab et al., 2007; Shalaby et al., 2010; Vanoirbeek et al., 2010). Analysis of pulmonary function parameters demonstrated a significant increase in resistance (R) with high dose instillation of MWCNT compared to vehicle controls (Figure 2.7). The R parameter accounts for both conducting airway resistance and resistance in the lung parenchyma, while conducting airway resistance alone is

distinguished as the Newtonian resistance (Rn) parameter (Shalaby et al., 2010). Additional experiments with MWCNT instilled C57BL/6 mice exhibited an increase in Rn compared to vehicle controls (Figure 3.6). The increases in R and Rn are likely to reflect the heightened inflammation due to elevated numbers of neutrophils. The presence of granulomas through the parenchyma and peribronchial regions of the lung (Figure 2.6) may also contribute to increases in R as airway obstruction hinders airflow, thus generating greater resistance through the tissues and airways. The formation of granulomas and fibrotic tissue can also attribute to the significant increase of tissue damping or energy dissipation in the lung (G), reflected by increased hysteresivity (eta). Fibrotic tissue originates through the process of wound healing, which becomes dysregulated, resulting in the development of thicker, more rigid scar tissue (or fibrotic tissue) (Wynn, 2011). The rigidity of fibrotic tissue results in greater energy dissipation, G, (or tissue damping) throughout the lung tissue during inhalation; however, it should also have enhanced recoil in the release of air, which would be evident in the H or tissue elastance parameter. Although C57BL/6 mice instilled with MWCNT do not mirror this increase in H, overall increases in G, as well as eta (ratio of tissue damping to tissue elastance, G/H) strongly suggest the impairment of lung function is due to the presence of fibrotic tissue (Figures 2.7 and 4.2).

Kit$^{W\text{-}sh}$ exposed to 4 mg/kg MWCNTs did not demonstrate any significant changes in pulmonary function parameters compared to strain matched vehicle controls (Figure 3.6 and data not shown), reinforcing the hypothesis that the presence of mast cells as key players in pulmonary inflammation, fibrosis and altered lung function incited by MWCNTs.

The focus of aims 2 and 3 was to determine whether IL-33 activation of mast cells via the ST2 receptor attributed to the underlying mechanism of MWCNT induced toxicity. While we were not able to fully investigate this aim *in vitro*, due to insufficient cell culture models, we were able to incite mast cell activation and release of IL-6 and OPN in BMMCs exposed to BALF taken from MWCNT exposed C57BL/6 mice. To ensure the mast cell activation was IL-33 mediated, we cultured BMMCs from $ST2^{-/-}$ mice and exposed them to the same BALF, but were unable to induce IL-6 or OPN expression. *In vivo*, we were able to thoroughly examine IL-33 activation of mast cells through the ST2 receptor. As mast cell deficient mice did not display pulmonary inflammation, fibrosis or impaired lung function, a mast cell reconstitution animal model was used. $Kit^{W\text{-}sh}$ reconstituted with cultured, mature BMMCs demonstrated results similar to C57BL/6 mice. They exhibited increased pulmonary cell infiltrates, collagen deposition, granuloma formation and impaired lung function 30 days following MWCNT exposure. While these data confirmed a role for mast cells in MWCNT induced toxicity, they did not address the involvement of the IL-33/ST2 axis in the underlying mechanism. To examine the role of the IL-33/ST2 axis, we utilized a global $ST2^{-/-}$ mouse model in conjunction with mast cell deficient mice reconstituted with $ST2^{-/-}$ BMMCs cultured from the $ST2^{-/-}$ mouse model. As with any global knock out model, results could not be attributed only to mast cell specific ST2 receptors as several cell types, including Th2 cells have been shown to express the receptor (Yagami et al., 2010). However, the reconstitution of the $Kit^{W\text{-}sh}$ with BMMCs from ST2-/- mice was able to provide a more direct approach for assessing the deficiency of ST2 on mast cells.

Investigation of pulmonary inflammation demonstrated no significant increases in inflammatory cell types in *Kit*$^{W\text{-}sh}$, ST2$^{-/-}$ mice and *Kit*$^{W\text{-}sh}$ reconstituted with ST2$^{-/-}$ BMMCs. Interestingly, C67BL/6 and *Kit*$^{W\text{-}sh}$ reconstituted with wild type BMMCs display significant elevations in neutrophils within the lung following MWCNT exposure (Table 3.3 and Figure 3.4). This may indicate an important role for neutrophils in IL-33 modulation of the resulting pulmonary inflammation. As increased neutrophils were only observed in animals possessing mast cells with fully functional ST2 receptors, it is possible that activation of mast cells through the ST2 receptor leads to the release of inflammatory cytokines which act to recruit neutrophils into the lungs. Furthermore, neutrophils have been shown to regulate the activity of IL-33 through the release of neutrophil elastase, cathepsin G and neutrophil PR3, all of which act to cleave IL-33 into a more mature form with greater biological activity then full length IL-33 (Bae et al., 2012; Lefrancais et al., 2012). This may greatly enhance mast cell activation and subsequent cytokine release facilitating greater inflammation similar to a positive feedback cycle. However, the abundant release of myeloperoxidase by neutrophils may also act as a compensatory mechanism in response to MWCNTs. Myeloperoxidase is suggested to play a role in the clearance and oxidative degradation of CNTs through an H_2O_2 reaction yielding reactive intermediates that produce hypochlorous acid (HOCl) (Shvedova et al., 2012). Further investigation is required to elucidate the complex functions of immune cell mediators to determine the true nature of the neutrophilic response in MWCNT-induced pulmonary inflammation.

As with the pulmonary inflammatory responses, MWCNT induced fibrotic outcomes including collagen deposition and granuloma formation were only observed in

C57BL/6 and *Kit*$^{W\text{-}sh}$ reconstituted with BMMCs. MWCNT instilled *Kit*$^{W\text{-}sh}$, *Kit*$^{W\text{-}sh}$ reconstituted with ST2$^{-/-}$ BMMCs, and ST2$^{-/-}$ mice did not exhibit significant increase in collagen content (Figure 3.4). While *Kit*$^{W\text{-}sh}$ displayed normal lung morphology, lung sections from *Kit*$^{W\text{-}sh}$ reconstituted with ST2$^{-/-}$ BMMCs, and ST2$^{-/-}$ mice did show normal lung tissue with areas of minimal granulomatous tissue (Figure 3.4). Altogether, these data validate a role for mast cells and the IL-33/ST2 axis in mediating the observed pulmonary fibrosis following MWCNT exposure. As anticipated, the changes in lung morphology evident in C57BL/6 and *Kit*$^{W\text{-}sh}$ reconstituted with BMMCs exposed to MWCNT also translated into physiological changes with significant increases in elastance (E) potentially due to the more pronounced recoil or rigidity of fibrotic tissue (Figure 3.6). Classically, fibrotic tissue exhibits increases in E coupled with decreases in compliance (C), which reflects elasticity or the resistance of recoil in the lung tissue. While C57BL/6 mice did not demonstrate a statistically significant increase in C, a slight elevation was seen in MWCNT instilled mice. However, in *Kit*$^{W\text{-}sh}$ reconstituted with BMMCs and exposed to MWCNT, the presence of mast cells resulted in increased C values compared to strain matched vehicle control mice or mice completely deficient of mast cells. In addition, increases in the Newtonian resistance (Rn), a measure accounting for the narrowing of conducting airways, were evident in both the C57BL/6 and *Kit*$^{W\text{-}sh}$ reconstituted with BMMCs, demonstrating the clear involvement of mast cells in modulating these pulmonary function parameters (Figure 3.6). The increase in Rn may be due to the fact that mast cells are ideally located in close proximity to bronchial epithelial cells of the conducting airways, reported to produce IL-33, thus possibly activating mast cells and resulting in subsequent release of mediators that may

impact resistance of the conducting airways (Cyphert et al., 2011a; Kurowska-Stolarska et al., 2009). Mice that lacked mast cells or lacked functional ST2 receptors on mast cells did not have any impairment in pulmonary function following MWCNT exposure, suggesting that mast cell activation through the ST2 receptor is essential in actuating MWCNT induced pulmonary inflammation, fibrosis and altered lung function (Figure 3.6).

In addition to the proposed aims in this dissertation, the cardiovascular toxicity of MWCNTs was also investigated to determine if the proposed underlying mechanism involving mast cells and the IL-33/ST2 axis also governed the adverse cardiovascular effects associated with MWCNTs. Several studies have implicated particulate exposure such as cerium oxide in adverse cardiovascular events and previous studies from our lab and others have established a role for mast cells in modulating the induced changes in vascular reactivity and exacerbating myocardial IR injury through the release of Th2 cytokines (Nistri et al., 2008; Wingard et al., 2011). Given the complexity of mediators that may be released by mast cells, it is important to consider the cardiac mast cell phenotype. Mast cell phenotypes can impact mast cell function through a variety of means. The presence of the MC_{TC} mast cell phenotype in cardiac tissue has been reported, but is further supported by a study which implicates mast cell chymase in acute myocardial ischemia reperfusion (IR) injury and subsequent increases in activation of mediators such as MMP-9, shown to be associated with exacerbation of infarct size, and SCF, known to induce mast cell proliferation (Oyamada et al., 2011; Sperr et al., 1994). In a porcine survival model of IR injury response, mast cell numbers in the infarct area were significantly increased at 1 and 21 days following IR injury

(Kwon et al., 2011). Our data, also examining myocardial IR injury response, exhibit significant exacerbation of IR injury in C57BL/6 and mast cell deficient mice reconstituted with wild types BMMCs post-exposure to MWCNT, suggesting the involvement of mast cells and the IL-33/ST2 axis in modulating the response (Figure 3.7). Mast cell deficient mice and mast cell deficient mice reconstituted with $ST2^{-/-}$ BMMCs did not show any exacerbation of the IR injury compared controls after MWCNT instillation (Figure 3.7). Interestingly $ST2^{-/-}$ mice exposed to MWCNT demonstrated a slight exacerbation, though significantly attenuated compared to C57BL/6 and mast cell deficient mice, suggesting that our proposed mechanism of cardiovascular toxicity mediated by mast cells may not be solely dictated by activation through the ST2 receptor (Figure 3.7).

In this study, the proposed mechanism of MWCNT induced toxicity was validated through the use of the $Kit^{W\text{-}sh}$ and the $Kit^{W\text{-}sh}$ reconstitution model wherein cultured mast cells were injected back into the mast cell deficient mouse. The use of $Kit^{W\text{-}sh}$ mice, evolving from a spontaneously occurring inversion mutation in the c-kit transcriptional regulatory region of mouse chromosome 5, is a relatively recent occurrence, but is largely favored over the use of previous mast cell deficient mouse models for several reasons (Wolters et al., 2005). Unlike the previous WBB6F1-$Kit^{W/W\text{-}v}$ mouse model, $Kit^{W\text{-}sh}$ mice do not display profound phenotypic abnormalities including sterility, macrolytic anemia, gastric ulcers, spontaneous dermatitis, and many other conditions (Grimbaldeston et al., 2005). In fact, $Kit^{W\text{-}sh}$ mice only demonstrate an impairment of skin pigmentation, making them appear white in color, but otherwise display normal mouse phenotypes with normal levels of lymphoid cells and hematopoietic cells, with

the exception of mast cells (Grimbaldeston et al., 2005). Additionally, this model has responded well to adoptive transfer or reconstitution of normal, c-Kit expressing, cultured mast whether by intravenous, intradermal or other means of transplantation (Grimbaldeston et al., 2005; Wolters et al., 2005). Indeed, this makes the *Kit*$^{W\text{-}sh}$ mouse a very attractive model for investigating mast cell function; however, the model does display limitations due to the lack of c-kit expression. The c-Kit receptor is not only central in the development of mast cells, it is also important for other hematopoietic and immune cell lineages. While *Kit*$^{W\text{-}sh}$ mice demonstrate normal immune cell counts, the extent of immune function in various cell types is not fully understood. Along with mast cells, dendritic cells and natural killer cells have been shown to retain expression of the c-Kit receptor, suggesting that it may play numerous roles in different facets of the immune system. In dendritic cells, it has been shown that c-Kit and SCF expression is upregulated in the presence of Th2 or Th17 inducing stimuli (Ray et al., 2010). The c-Kit receptor has also been shown to influence generation of natural killer cells, impacting survival, proliferation and lytic function once maturity has been reached (Ray et al., 2010). These mast cell-independent functions of c-Kit in the immune system demonstrate the potential for altered and compensatory immune responses in *Kit*$^{W\text{-}sh}$ mice. Therefore, the use of *Kit*$^{W\text{-}sh}$ mice adds a layer of complexity in delineating the effects observed following MWCNT exposure and whether they are due to mast cell deficiency or the lack of c-Kit expression. Though evidence for our proposed mast cell mediated mechanism is compelling, it is important to acknowledge the limitations of this animal model.

Interestingly, a recent study has investigated the interaction of signaling mechanisms between the c-kit receptor and the IL-33 receptor. In both human and murine mast cells, cross activation of the IL-33 receptor, ST2, and the c-kit receptor has been reported to occur through trimerization of ST2 with IL-1RAcP and c-kit, the latter of which are constitutively complexed (Drube et al., 2010). Therefore, the trimerization of ST2 results in integrated IL-33 and c-Kit signal transduction pathways, enhanced activation of signaling molecules and robust cellular responses (Drube et al., 2010). In the presence of SCF, a ligand for c-Kit, the activation of the ST2 receptor by IL-33 yields a synergistic response, which may have yielded weak responses with IL-33 activation alone or a complete lack of response in the SCF activation of c-Kit alone (Drube et al., 2010). The implications of this study on the current body of work are significant. It is possible that the lack of IL-33 and ST2 mediated pulmonary and cardiovascular toxicity induced by MWCNT in $Kit^{W\text{-}sh}$ mice may be influenced by a lack of integrated ST2 and c-Kit signaling to induce the level of response observed in C57BL/6 mice. At present the direct impact of these integrated signaling pathways beyond the cellular level, particularly on mast cell function in immune responses and disease pathology, is unknown.

Overall, the data generated from this study has contributed greatly to our understanding of the underlying mechanisms of MWCNT toxicity. Figure 5.1, a detailed schematic of our proposed mechanism of MWCNT-toxicity, illustrates how MWCNT exposure may damage and incite lung epithelial cells to release IL-33. IL-33 activation of mast cells through the ST2 receptor initiates a cascade of downstream effects leading to MWCNT induced pulmonary and cardiovascular toxicity. Mast cell activation

can result in the release of a variety of mediators and engage effector cells in contributing to the immune response. However, many of cytokines released by activated mast cells and downstream effector cells following MWCNT still remain to be investigated, though other studies have implicated a host of mediators that could potentially be released by mast cells and are involved in the pathophysiology of conditions similar to those observed with MWCNT pulmonary toxicity. Several cytokines released by mast cells, including TNF-α and IL-8 act to recruit neutrophils to the site of inflammation, wherein neutrophils produce additional pro-inflammatory cytokines contributing to total lung inflammation (Zhang et al., 1992). As depicted in figure 5.1, neutrophil proteases (elastase, cathepsin G and PR3) may then act on IL-33 cleaving it to its more active mature form, enhancing mast cell activation (Bae et al., 2012; Lefrancais et al., 2012). Additionally, mast cells can act on macrophages through the release of IL-4, IL-6, IL-13, MCP-1 and other cytokines, involving recruitment of macrophage precursors and activation of macrophages to produce additional Th2 pro-inflammatory and pro-fibrotic cytokines such as TGF-β (Lee et al., 2001). Several Th2 cytokines and growth factors also drive fibroblast activation or proliferation, including TGF-β, IL-13, bFGF, and PDGF-AA (Inoue et al., 1996; Ryman-Rasmussen et al., 2009b). Many of these mediators, such as TGF-β, have enhanced activation *in vivo* due to release of mast cell proteases, specifically chymase. The release of chymase, typically associated with the MC_{TC} mast cell phenotype, suggests a shift in phenotype in pulmonary fibrotic pathologies (Hamada et al., 2000; Lang et al., 2010; Orito et al., 2004). It is possible that MWCNT exposure may lead to an induction of mediators like TGF-β, known to promote a shift in mast cell phenotype from MC_T to MC_{TC}. The

immune response following mast cell activation in lungs exposed to MWCNTs has been shown to induce significant pulmonary inflammation and fibrosis, manifesting physiologically with impairment of pulmonary function. In the heart, mast cell activation by IL-33 through the ST2 receptor may result in the release of chymase, again, from mast cells with the MC_{TC} phenotypes, found abundantly through heart tissue (Oyamada et al., 2011). Further studies need to be conducted to determine the release of specific cytokines, which may impact exacerbation of myocardial IR injury responses. Thus far, we have established a role for IL-33 activation of mast cells via the ST2 receptor in mediating adverse pulmonary and cardiovascular resulting from MWCNT exposure. This novel mechanism may prove to highlight potential mast cell specific therapeutics to alleviate toxicity of nanoparticle exposure or adverse effects to nanomedicines. More importantly, distinguishing critical underlying mechanisms of nanomaterial toxicity may enable the development of better, more efficient screening tools to address heightened concerns regarding the risks of nanoparticle exposure to human health.

Future Studies

Given the minor drawbacks of our animal models, an additional model may be used to support the findings of our study. One model that may potentially transcend the shortcomings of $Kit^{W\text{-}sh}$ mice is the "Cre-mediated mast cell eradication" (Cre-Master) mouse model, established through the insertion of a Cre recombinase into the mast cell carboxypeptidase A3 gene locus (Feyerabend et al., 2011). The use of this particular Cre-Lox system resulted in a serious deficiency of mast cells with Cre recombinase

expression. As the Cre-Lox recombination system specifically targets carboxypeptidase A3, which is largely expressed in mast cells and perhaps only minimally expressed in basophils, Cre-Master mice do not display any other abnormalities with the exception of slightly decreased basophil numbers (Feyerabend et al., 2011). Unlike *Kit*$^{W\text{-}sh}$ mice, Cre-Master mice are not impacted by a lack of c-Kit function in other hematopoietic cell types, enabling them to display completely normal immune systems (Feyerabend et al., 2011). In the context of this study, the Cre-Master mouse model may prove to further delineate the exact role of IL-33/ST2 axis activation of mast cells and their downstream responses from the potential c-Kit receptor interactions. Furthermore, Cre-Master mice provide another major advantage in that these mice are not limited to the C57BL/6 genetic background. Strain controls for *Kit*$^{W\text{-}sh}$ mice are generally C57BL/6 mice or mice that share a similar genetic background, but as the Cre-Lox system is an inducible expression of Cre resulting in mast cell deficiency, no strain controls would be required and mice with the other genetic backgrounds could be utilized. Future studies involving the Cre-Master mice would be highly advantageous.

Several additional studies may be conducted in the future to validate and address more specific aspects of this mast cell mediated mechanism of MWCNT toxicity. In order to establish the mast cell as realistic target for therapeutics to treat side effects of nanomedicines or hazardous occupational exposures to nanomaterials, it is essential to investigate the potential of mast cell specific drugs in alleviating MWCNT induced pulmonary and cardiovascular toxicity. Utilizing our current wild type murine model, several mast cell stabilizers, such as cromolyn sodium (Intal ®) or Nedocromil (Tilade ®) could be administered following exposure to MWCNTs. Currently, mast cell

stabilizers in an aerosol or inhaler formulation are indicated for the prevention of asthma symptoms and other allergic conditions. To optimize the effectiveness of the drug, a dose and time course study would be required in delineating a therapeutic window. It would also be prudent to consider a mast cell stabilizer as a preventative measure of MWCNT toxicity, especially in occupational settings where nanomaterials may pose greater health hazards as the risks of exposure are constant. Alternatively, another therapeutic possibility would be the use of an IL-33 specific monoclonal antibody to inhibit MWCNT toxicity. Though other monoclonal antibodies like TNF-α, indicated for autoimmune diseases, are currently available on the market, no therapeutic IL-33 antibody has been FDA-approved. Pre-treatment of animals with a specific IL-33 antibody prior to MWCNT exposure may attenuate the subsequent pulmonary and cardiovascular responses, providing a feasible means of reducing the risks and toxicity associated with MWNCTs.

In our study, we demonstrate that IL-33 activation of mast cells through the ST2 receptor is crucial in modulating MWCNT induced toxicity through the release of pro-inflammatory or pro-fibrotic mediators. While we have established a previously unknown mechanism of toxicity, we have yet to explore the effects downstream of mast cell activation. As previously mentioned, mast cells exhibit extraordinary phenotypic plasticity, enabling them to effectively actuate differential immune responses in a variety of conditions. Changes in mast cell phenotype have been documented in the pathology of conditions such as asthma (Balzar et al., 2011). To determine how changes in phenotypes are implicated in mast cell and IL-33/ST2 axis mediated MWCNT toxicity, we would need to characterize mast cell phenotypes within the lung, alterations of

phenotypes following MWCNT exposure, and identify the specific mediators released. Mast cell phenotypes are also known to be inherently distinct in different tissues types. In this study, mast cells and the IL-33/ST2 axis were determined to be important in the adverse cardiovascular responses elicited by MWCNTs. As previously mentioned, the majority of cardiac mast cells are reported to maintain a MC_{TC} phenotype and though their exact role cardiovascular pathophysiology is currently unknown, chymase, tryptase and other mediators of cardiac mast cells, are important factors in a variety of pathological conditions (Oyamada et al., 2011; Sperr et al., 1994). Elucidating the complexities of mast cell function regulated by phenotype within the confines of our recently established mechanism of MWCNT induced toxicity could greatly add to our understanding of mast cell involvement in disease pathologies as well as environmental toxicities.

In this study, we have not yet established whether the MWCNT induced cardiovascular toxicities result directly from the IL-33 activation of cardiac mast cells or indirectly from the mediators released by IL-33 activation of pulmonary mast cells into cardiovascular tissues. To address this question, an effective technique would be the use of the Langendorff perfused isolated heart system. This type of experiment would require an excision of the heart from the animal following MWCNT exposure and perfusion in a chamber with physiologically relevant medium. This system would enable us to investigate an endpoint similar to the *in vivo* IR injury model used in this study. By using a global or regional IR model in the Langendorff heart system, we would be able to ascertain if the observed MWCNT-induced cardiovascular toxicity was a direct result of IL-33 activation of cardiac mast cells, as pulmonary mast cells would not be present

(Skrzypiec-Spring et al., 2007). These results could be validated through the use of IL-33 antibodies, ST2 receptor antagonists, cromolyn sodium or nedocromil directly into the isolated heart perfusion chamber. Furthermore, additional cardiovascular studies may be conducted with the Langendorff heart system to examine alterations in physiological functions resulting from MWCNT exposure, including biochemical analysis with the release of cytokines and chemokines from the heart, and electrocardiographs to assess abnormal cardiac rhythms.

Although the main focus of this study has been on a respiratory exposure to MWCNTs, the use of MWCNTs in a variety of biomedical applications has assuredly increased the potential for other routes of exposures. As drug delivery and nanomedicine remain a key topic of interest in the nanotechnology area, exposure through an intravenous route is an important field of study (Baughman et al., 2002; Martin and Kohli, 2003). While some studies have reported the toxicity of intravenous MWCNT exposure, few have yet to examine the implications of mast cells in the subsequently observed toxicities (Jain et al., 2011; Ji et al., 2009). Intravenous administration will likely distribute MWCNTs to numerous areas of the body. Distribution of MWCNTs to the lungs may result in some of the mast cell and IL-33/ST2 axis driven pulmonary toxicities reported in this study. However, as mast cells are known to reside in numerous tissues types, it is possible for MWCNTs to impact mast cell activation and induce toxicities in several areas of the body through the IL-33/ST2 pathway or additional mechanisms of mast cell activation. Thus, the route of MWCNT exposure may be a key factor in determining the associated mast cell mediated toxicities.

Future Directions in Nanotoxicology

The field of nanotechnology has expanded enormously over the past decade, thanks to significant advances in analytical techniques enabling manipulation of materials at the nano-scale. In the creation of CNTs, newer discoveries were made highlighting structural configurations that enabled unique thermal, electrical and mechanical properties, making them attractive options for numerous applications (Bethune, 1993). The incredible diversity in the properties and subsequent applications of nanoparticles places a huge burden on safety regulations. Currently, the National Institute for Occupational Safety and Health (NIOSH) has issued a bulletin on occupational exposures to carbon nanotubes, nanofibers and other nanomaterials, detailing concentrations levels of nanomaterials suggested to be safer and present minimal risks to exposed workers (NIOSH, 2010). The recommended exposure level for CNTs is suggested not to exceed 7 $\mu g/cm^3$, the lowest detectable value using the current analytical method, suggesting even lower exposures may still pose a threat to human health (NIOSH, 2010). While this report has indicated the gravity of nanomaterial exposures, no current regulations are in place to govern the means by which nanoparticles are used or the threat they pose, not only to human health, but also to the environment.

Further study of nanomaterial toxicity will provide support for instituting regulations and accurately assessing the risks of nanomaterial exposure. Therein lies a great challenge as nanoparticle toxicity is dictated by a multitude of facets and characteristics that constitute any single type of nanoparticle. The distinguishing

characteristics of each type of nanomaterial, including chemical composition, shape, size, surface area and function groups, may result in distinctly unique toxicities, making it difficult to apply generalized means of therapy or risk assessments to all nanomaterial exposures (Luo et al., 2012; Zhao and Castranova, 2011). Establishing appropriate therapeutics for nanoparticle exposure is, in and of itself, a formidable task. Unlike other toxicological exposures, the size of nanomaterials enables greater surface areas and heightened potential for biological interactions within the body.

The toxicological studies that have been conducted to assess the toxicity of nanomaterials provide data in support of establishing nanoparticle regulation. These studies have yet to effectively set a no observable effect level (NOEL) or the level at which a given nanoparticle does not display toxic effects, suggesting any amount exposure to a nanoparticle may be detrimental. Assessing and characterizing the hazards of nanoparticles is crucial in understanding the potential risks to human health. The margin of exposure, or the ratio of the NOEL to estimated exposure dose, is often used as a tool in risk assessments as a means of establishing the toxicity level of a given nanomaterial. The NOEL for CNTs, however, is unknown and the estimated human exposure levels remain ambiguous, therefore making it difficult to identify the margin of exposure. This study has reported important mechanistic findings of MWCNT toxicity at an exposure dose that is comparable to a high human exposure level. While MWCNT exposure in humans may not necessarily reach such high levels, lower levels of exposure may still result in toxicities following inhalation, many of which have been detailed in this study. The doses utilized in this animal study are relevant and comparable to potential human exposures and outline toxicological endpoints that may

be meaningful in humans. However, it is clear that there is a need for additional studies regarding CNT toxicity, particularly in assessing current exposures and toxicities in humans, so that we may better assess the risks these nanomaterials pose.

Current toxicological means for assessing nanomaterial toxicity are costly and time consuming, requiring the use of appropriate animal models and targeted *in vitro* systems to adequately address certain toxicities. The sheer volume of distinct nanomaterials currently produced makes it impractical to utilize traditional toxicological means as a screening platform for nanotoxicity. There is a profound need for better toxicity testing tools and the use of high throughput screening may provide an effective alternate to animal studies and high yield of data, imparting greater insight to how engineered nanoparticle properties are associated with certain toxicity responses (Damoiseaux et al., 2011). While traditional animal studies remain central to investigating mechanisms of toxicity, high throughput screening will enable efficient identification of known toxicities and toxicological mechanisms, given the high potential for many novel nanomaterials to revolutionize biomedical applications and nanomedicines. In this study, the mast cell serves as a crucial cell type in modulating MWCNT toxicity, and thus may be an invaluable source of information for the development of high throughput screening systems for future studies in nanotoxicology.

Figure 5.1 Schematic Representation of an IL-33/ST2 Axis and Mast Cell Mediated Mechanism of MWCNT Induced Toxicity

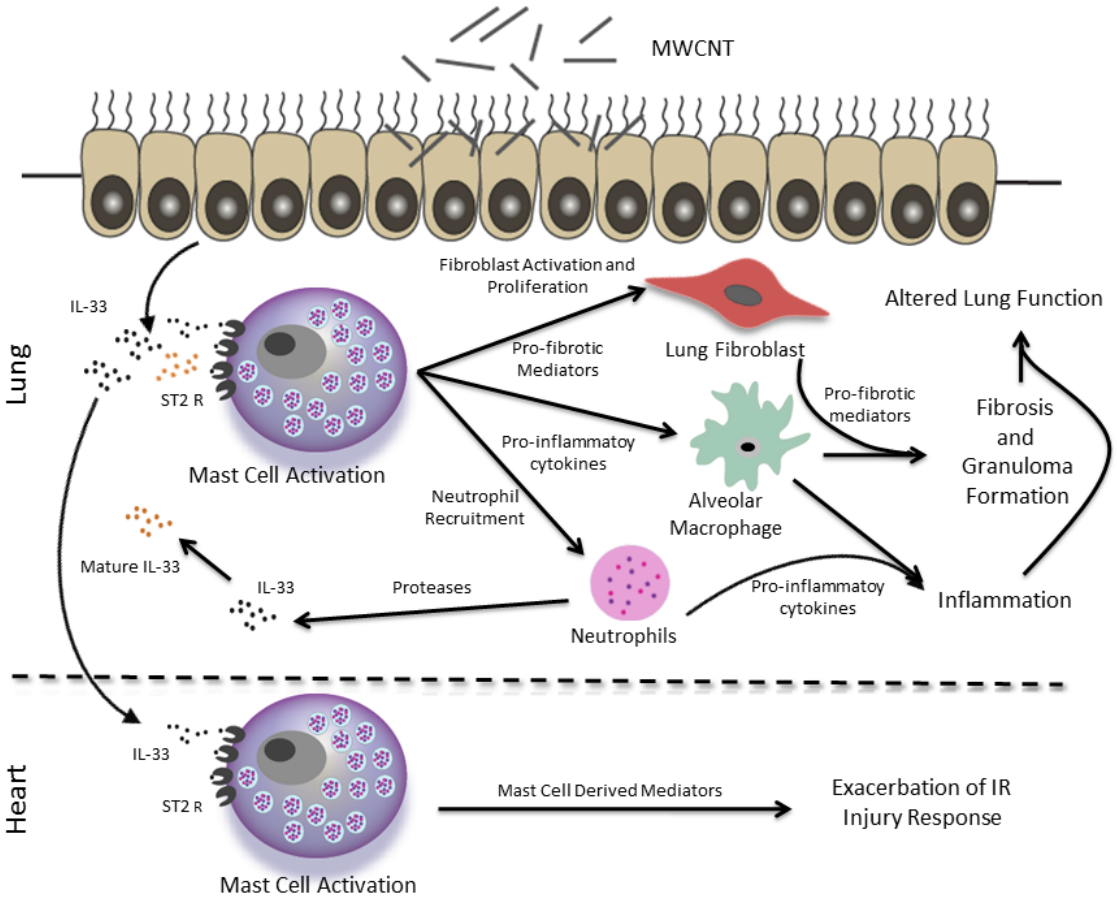
MWCNT
Lung
IL-33
ST2 R
Mast Cell Activation
Fibroblast Activation and Proliferation
Pro-fibrotic Mediators
Lung Fibroblast
Altered Lung Function
Pro-fibrotic mediators
Fibrosis and Granuloma Formation
Pro-inflammatoy cytokines
Neutrophil Recruitment
Alveolar Macrophage
Mature IL-33
IL-33
Proteases
Neutrophils
Pro-inflammatoy cytokines
Inflammation
Heart
IL-33
ST2 R
Mast Cell Activation
Mast Cell Derived Mediators
Exacerbation of IR Injury Response

REFERENCES

Abonia, J.P., J. Hallgren, T. Jones, T. Shi, Y. Xu, P. Koni, R.A. Flavell, J.A. Boyce, K.F. Austen, and M.F. Gurish. 2006. Alpha-4 integrins and VCAM-1, but not MAdCAM-1, are essential for recruitment of mast cell progenitors to the inflamed lung. *Blood*. 108:1588-1594.

Abraham, S.N., and A.L. St John. 2010. Mast cell-orchestrated immunity to pathogens. *Nature reviews. Immunology*. 10:440-452.

Aiso, S., K. Yamazaki, Y. Umeda, M. Asakura, T. Kasai, M. Takaya, T. Toya, S. Koda, K. Nagano, H. Arito, and S. Fukushima. 2010. Pulmonary toxicity of intratracheally instilled multiwall carbon nanotubes in male Fischer 344 rats. *Industrial health*. 48:783-795.

Ajayan, P.M., J. Charlier, and A.G. Rinzler. 1999. Carbon nanotubes: from macromolecules to nanotechnology. *Proceedings of the National Academy of Sciences of the United States of America*. 96:14199-14200.

Akahoshi, M., C.H. Song, A.M. Piliponsky, M. Metz, A. Guzzetta, M. Abrink, S.M. Schlenner, T.B. Feyerabend, H.R. Rodewald, G. Pejler, M. Tsai, and S.J. Galli. 2011. Mast cell chymase reduces the toxicity of Gila monster venom, scorpion venom, and vasoactive intestinal polypeptide in mice. *The Journal of clinical investigation*. 121:4180-4191.

Akers, I.A., M. Parsons, M.R. Hill, M.D. Hollenberg, S. Sanjar, G.J. Laurent, and R.J. McAnulty. 2000. Mast cell tryptase stimulates human lung fibroblast proliferation via protease-activated receptor-2. *Am J Physiol Lung Cell Mol Physiol*. 278:L193-201.

Alfaro-Moreno, E., T.S. Nawrot, B.M. Vanaudenaerde, M.F. Hoylaerts, J.A. Vanoirbeek, B. Nemery, and P.H. Hoet. 2008. Co-cultures of multiple cell types mimic pulmonary cell communication in response to urban PM10. *Eur Respir J*. 32:1184-1194.

Ali, H., J. Ahamed, C. Hernandez-Munain, J.L. Baron, M.S. Krangel, and D.D. Patel. 2000. Chemokine production by G protein-coupled receptor activation in a human mast cell line: roles of extracellular signal-regulated kinase and NFAT. *J Immunol*. 165:7215-7223.

Alkhouri, H., F. Hollins, L.M. Moir, C.E. Brightling, C.L. Armour, and J.M. Hughes. 2011. Human lung mast cells modulate the functions of airway smooth muscle cells in asthma. *Allergy*. 66:1231-1241.

Andersson, C.K., M. Mori, L. Bjermer, C.G. Lofdahl, and J.S. Erjefalt. 2009. Novel site-specific mast cell subpopulations in the human lung. *Thorax*. 64:297-305.

Atkinson, R.W., H.R. Anderson, J. Sunyer, J. Ayres, M. Baccini, J.M. Vonk, A. Boumghar, F. Forastiere, B. Forsberg, G. Touloumi, J. Schwartz, and K. Katsouyanni. 2001. Acute effects of particulate air pollution on respiratory admissions: results from APHEA 2 project. Air Pollution and Health: a European Approach. *American journal of respiratory and critical care medicine*. 164:1860-1866.

Bae, S., J. Choi, J. Hong, H. Jhun, K. Hong, T. Kang, K. Song, S. Jeong, H. Yum, and S. Kim. 2012. Neutrophil proteinase 3 induces diabetes in a mouse model of glucose tolerance. *Endocrine research*. 37:35-45.

Balzar, S., M.L. Fajt, S.A. Comhair, S.C. Erzurum, E. Bleecker, W.W. Busse, M. Castro, B. Gaston, E. Israel, L.B. Schwartz, D. Curran-Everett, C.G. Moore, and S.E. Wenzel. 2011. Mast cell phenotype, location, and activation in severe asthma. Data from the Severe Asthma Research Program. *American journal of respiratory and critical care medicine*. 183:299-309.

Barrett, E.P., Joyner, L.G., and P.P. Halenda. 1951. The determination of pore volume and area distributions in porous substances. I. Computations from nitrogen isotherms. *J. Am. Chem. Soc.* 73:373-380.

Bates, J.H.T. 2009. Pulmonary mechanics: A system identification perspective. *In* Engineering in Medicine and Biology Society, 2009. EMBC 2009. Annual International Conference of the IEEE. 170-172.

Baughman, R.H., A.A. Zakhidov, and W.A. de Heer. 2002. Carbon nanotubes--the route toward applications. *Science*. 297:787-792.

Baumann, U., N. Chouchakova, B. Gewecke, J. Kohl, M.C. Carroll, R.E. Schmidt, and J.E. Gessner. 2001. Distinct tissue site-specific requirements of mast cells and complement components C3/C5a receptor in IgG immune complex-induced injury of skin and lung. *J Immunol*. 167:1022-1027.

Beaven, M.A. 2009. Our perception of the mast cell from Paul Ehrlich to now. *Eur. J. Immunol.* 39:11-25.

Behndig, A.F., I.S. Mudway, J.L. Brown, N. Stenfors, R. Helleday, S.T. Duggan, S.J. Wilson, C. Boman, F.R. Cassee, A.J. Frew, F.J. Kelly, T. Sandstrom, and A. Blomberg. 2006. Airway antioxidant and inflammatory responses to diesel exhaust exposure in healthy humans. *Eur Respir J*. 27:359-365.

Bethune, D.S., C. H. Kiang, M. S. de Vires, G. Gorman, R. Savoy, J. Vazquez, and R. Beyers. 1993. Cobalt-catalysed growth of carbon nanotubes with single-atomic-layer walls. *Nature (London, U. K.)*. 363:605-607.

Bianco, A., K. Kostarelos, C.D. Partidos, and M. Prato. 2005. Biomedical applications of functionalised carbon nanotubes. *Chem Commun (Camb)*:571-577.

Bot, I., S.C. de Jager, A. Zernecke, K.A. Lindstedt, T.J. van Berkel, C. Weber, and E.A. Biessen. 2007. Perivascular mast cells promote atherogenesis and induce plaque destabilization in apolipoprotein E-deficient mice. *Circulation*. 115:2516-2525.

Bradding, P., Y. Okayama, P.H. Howarth, M.K. Church, and S.T. Holgate. 1995. Heterogeneity of human mast cells based on cytokine content. *J Immunol*. 155:297-307.

Brightling, C.E., A.J. Ammit, D. Kaur, J.L. Black, A.J. Wardlaw, J.M. Hughes, and P. Bradding. 2005. The CXCL10/CXCR3 axis mediates human lung mast cell migration to asthmatic airway smooth muscle. *American journal of respiratory and critical care medicine*. 171:1103-1108.

Brightling, C.E., P. Bradding, F.A. Symon, S.T. Holgate, A.J. Wardlaw, and I.D. Pavord. 2002. Mast-cell infiltration of airway smooth muscle in asthma. *N. Engl. J. Med.* 346:1699-1705.

Brightling, C.E., F.A. Symon, S.S. Birring, P. Bradding, A.J. Wardlaw, and I.D. Pavord. 2003a. Comparison of airway immunopathology of eosinophilic bronchitis and asthma. *Thorax*. 58:528-532.

Brightling, C.E., F.A. Symon, S.T. Holgate, A.J. Wardlaw, I.D. Pavord, and P. Bradding. 2003b. Interleukin-4 and -13 expression is co-localized to mast cells within the airway smooth muscle in asthma. *Clinical and experimental allergy : journal of the British Society for Allergy and Clinical Immunology*. 33:1711-1716.

Brown, J.M., E.J. Swindle, N.M. Kushnir-Sukhov, A. Holian, and D.D. Metcalfe. 2007. Silica-directed mast cell activation is enhanced by scavenger receptors. *American journal of respiratory cell and molecular biology*. 36:43-52.

Brown, J.M., T.M. Wilson, and D.D. Metcalfe. 2008. The mast cell and allergic diseases: role in pathogenesis and implications for therapy. *Clinical and experimental allergy : journal of the British Society for Allergy and Clinical Immunology*. 38:4-18.

Brunauer, S., Emmett, P. H., and E. Teller. 1938. Adsorption of Gases in Multimolecular Layers. *J. Am. Chem. Soc.* 60:309-319.

Caron, G., Y. Delneste, E. Roelandts, C. Duez, N. Herbault, G. Magistrelli, J.Y. Bonnefoy, J. Pestel, and P. Jeannin. 2001. Histamine induces CD86 expression and chemokine production by human immature dendritic cells. *J Immunol*. 166:6000-6006.

Carriere, V., L. Roussel, N. Ortega, D.A. Lacorre, L. Americh, L. Aguilar, G. Bouche, and J.P. Girard. 2007. IL-33, the IL-1-like cytokine ligand for ST2 receptor, is a chromatin-associated nuclear factor in vivo. *Proceedings of the National Academy of Sciences of the United States of America*. 104:282-287.

Cavallo, D., C. Fanizza, C.L. Ursini, S. Casciardi, E. Paba, A. Ciervo, A.M. Fresegna, R. Maiello, A.M. Marcelloni, G. Buresti, F. Tombolini, S. Bellucci, and S. Iavicoli.

2012. Multi-walled carbon nanotubes induce cytotoxicity and genotoxicity in human lung epithelial cells. *Journal of applied toxicology : JAT*.

Cesta, M.F., J.P. Ryman-Rasmussen, D.G. Wallace, T. Masinde, G. Hurlburt, A.J. Taylor, and J.C. Bonner. 2010. Bacterial lipopolysaccharide enhances PDGF signaling and pulmonary fibrosis in rats exposed to carbon nanotubes. *American journal of respiratory cell and molecular biology*. 43:142-151.

Chackerian, A.A., E.R. Oldham, E.E. Murphy, J. Schmitz, S. Pflanz, and R.A. Kastelein. 2007. IL-1 receptor accessory protein and ST2 comprise the IL-33 receptor complex. *J Immunol*. 179:2551-2555.

Choi, Y.S., H.J. Choi, J.K. Min, B.J. Pyun, Y.S. Maeng, H. Park, J. Kim, Y.M. Kim, and Y.G. Kwon. 2009. Interleukin-33 induces angiogenesis and vascular permeability through ST2/TRAF6-mediated endothelial nitric oxide production. *Blood*. 114:3117-3126.

Cumberbatch, M., R.J. Dearman, C. Antonopoulos, R.W. Groves, and I. Kimber. 2001. Interleukin (IL)-18 induces Langerhans cell migration by a tumour necrosis factor-alpha- and IL-1beta-dependent mechanism. *Immunology*. 102:323-330.

Cyphert, J.M., M. Kovarova, and B.H. Koller. 2011a. Unique populations of lung mast cells are required for antigen-mediated bronchoconstriction. *Clinical and experimental allergy : journal of the British Society for Allergy and Clinical Immunology*. 41:260-269.

Cyphert, J.M., M. Kovarova, and B.H. Koller. 2011b. Unique populations of lung mast cells are required for antigen-mediated bronchoconstriction. *Clinical & Experimental Allergy*. 41:260-269.

Dacre, K.J., B.C. McGorum, D.J. Marlin, L.R. Bartner, J.K. Brown, D.J. Shaw, N.E. Robinson, C. Deaton, and A.D. Pemberton. 2007. Organic dust exposure increases mast cell tryptase in bronchoalveolar lavage fluid and airway epithelium of heaves horses. *Clinical and experimental allergy : journal of the British Society for Allergy and Clinical Immunology*. 37:1809-1818.

Damoiseaux, R., S. George, M. Li, S. Pokhrel, Z. Ji, B. France, T. Xia, E. Suarez, R. Rallo, L. Madler, Y. Cohen, E.M. Hoek, and A. Nel. 2011. No time to lose--high throughput screening to assess nanomaterial safety. *Nanoscale*. 3:1345-1360.

Delgado, L., E.R. Parra, and V.L. Capelozzi. 2006. Apoptosis and extracellular matrix remodelling in human silicosis. *Histopathology*. 49:283-289.

Dellinger, A., Z. Zhou, S.K. Norton, R. Lenk, D. Conrad, and C.L. Kepley. 2010. Uptake and distribution of fullerenes in human mast cells. *Nanomedicine*. 6:575-582.

Demou, E., P. Peter, and S. Hellweg. 2008. Exposure to manufactured nanostructured particles in an industrial pilot plant. *Ann Occup Hyg*. 52:695-706.

Dhillon, O.S., H.K. Narayan, P.A. Quinn, I.B. Squire, J.E. Davies, and L.L. Ng. 2011. Interleukin 33 and ST2 in non-ST-elevation myocardial infarction: comparison with Global Registry of Acute Coronary Events Risk Scoring and NT-proBNP. *Am Heart J*. 161:1163-1170.

Di Giorgio, M.L., S. Di Bucchianico, A.M. Ragnelli, P. Aimola, S. Santucci, and A. Poma. 2011. Effects of single and multi walled carbon nanotubes on macrophages: cyto and genotoxicity and electron microscopy. *Mutation research*. 722:20-31.

DiPietro, L.A., M. Burdick, Q.E. Low, S.L. Kunkel, and R.M. Strieter. 1998. MIP-1alpha as a critical macrophage chemoattractant in murine wound repair. *The Journal of clinical investigation*. 101:1693-1698.

Drube, S., S. Heink, S. Walter, T. Lohn, M. Grusser, A. Gerbaulet, L. Berod, J. Schons, A. Dudeck, J. Freitag, S. Grotha, D. Reich, O. Rudeschko, J. Norgauer, K. Hartmann, A. Roers, and T. Kamradt. 2010. The receptor tyrosine kinase c-Kit controls IL-33 receptor signaling in mast cells. *Blood*. 115:3899-3906.

Dumortier, H., S. Lacotte, G. Pastorin, R. Marega, W. Wu, D. Bonifazi, J.P. Briand, M. Prato, S. Muller, and A. Bianco. 2006. Functionalized carbon nanotubes are non-cytotoxic and preserve the functionality of primary immune cells. *Nano Lett.* 6:1522-1528.

Dvorak, A.M. 1986. Mast-cell degranulation in human hearts. *N. Engl. J. Med.* 315:969-970.

El-Shazly, A., P. Berger, P.O. Girodet, O. Ousova, M. Fayon, J.M. Vernejoux, R. Marthan, and J.M. Tunon-de-Lara. 2006. Fraktalkine produced by airway smooth muscle cells contributes to mast cell recruitment in asthma. *J Immunol*. 176:1860-1868.

Emad, A., and Y. Emad. 2007. Relationship between eosinophilia and levels of chemokines (CCL5 and CCL11) and IL-5 in bronchoalveolar lavage fluid of patients with mustard gas-induced pulmonary fibrosis. *J Clin Immunol*. 27:605-612.

Endo, M., M. Strano, and P. Ajayan. 2008a. Potential Applications of Carbon Nanotubes. Vol. 111. Springer Berlin / Heidelberg. 13-61.

Endo, M., S. Tsuruoka, and G. Ichihara. 2008b. Carbon Nanotubes in historical and future perspective Summary of an Extended Session at Carbon 2008 in Nagano (JP). *Particle and fibre toxicology*. 5:21.

Enoksson, M., K. Lyberg, C. Moller-Westerberg, P.G. Fallon, G. Nilsson, and C. Lunderius-Andersson. 2011. Mast cells as sensors of cell injury through IL-33 recognition. *J Immunol*. 186:2523-2528.

Feyerabend, T.B., A. Weiser, A. Tietz, M. Stassen, N. Harris, M. Kopf, P. Radermacher, P. Moller, C. Benoist, D. Mathis, H.J. Fehling, and H.R. Rodewald. 2011. Cre-mediated cell ablation contests mast cell contribution in models of antibody- and T cell-mediated autoimmunity. *Immunity*. 35:832-844.

Flechsig, P., B. Hartenstein, S. Teurich, M. Dadrich, K. Hauser, A. Abdollahi, H.J. Grone, P. Angel, and P.E. Huber. 2010. Loss of matrix metalloproteinase-13 attenuates murine radiation-induced pulmonary fibrosis. *Int J Radiat Oncol Biol Phys*. 77:582-590.

Folkman, J. 1995. Angiogenesis in cancer, vascular, rheumatoid and other disease. *Nat Med*. 1:27-31.

Frandji, P., C. Tkaczyk, C. Oskeritzian, B. David, C. Desaymard, and S. Mecheri. 1996. Exogenous and endogenous antigens are differentially presented by mast cells to CD4+ T lymphocytes. *Eur. J. Immunol.* 26:2517-2528.

Frossi, B., G. Gri, C. Tripodo, and C. Pucillo. 2010. Exploring a regulatory role for mast cells: 'MCregs'? *Trends in immunology*. 31:97-102.

Gadina, M., and C.A. Jefferies. 2007. IL-33: a sheep in wolf's clothing? *Sci STKE*. 2007:pe31.

Gauchat, J.F., S. Henchoz, G. Mazzei, J.P. Aubry, T. Brunner, H. Blasey, P. Life, D. Talabot, L. Flores-Romo, J. Thompson, and et al. 1993. Induction of human IgE synthesis in B cells by mast cells and basophils. *Nature*. 365:340-343.

Ghanem, N.S., E.S. Assem, K.B. Leung, and F.L. Pearce. 1988. Cardiac and renal mast cells: morphology, distribution, fixation and staining properties in the guinea pig and preliminary comparison with human. *Agents Actions*. 23:223-226.

Gilles, S., S. Zahler, U. Welsch, C.P. Sommerhoff, and B.F. Becker. 2003. Release of TNF-alpha during myocardial reperfusion depends on oxidative stress and is prevented by mast cell stabilizers. *Cardiovasc. Res.* 60:608-616.

Glaab, T., C. Taube, A. Braun, and W. Mitzner. 2007. Invasive and noninvasive methods for studying pulmonary function in mice. *Respir Res*. 8:63.

Grimbaldeston, M.A., C.C. Chen, A.M. Piliponsky, M. Tsai, S.Y. Tam, and S.J. Galli. 2005. Mast cell-deficient W-sash c-kit mutant Kit W-sh/W-sh mice as a model for investigating mast cell biology in vivo. *The American journal of pathology*. 167:835-848.

Hallgren, J., T.G. Jones, J.P. Abonia, W. Xing, A. Humbles, K.F. Austen, and M.F. Gurish. 2007. Pulmonary CXCR2 regulates VCAM-1 and antigen-induced recruitment of mast cell progenitors. *Proceedings of the National Academy of Sciences of the United States of America*. 104:20478-20483.

Hamada, H., V. Vallyathan, C.D. Cool, E. Barker, Y. Inoue, and L.S. Newman. 2000. Mast cell basic fibroblast growth factor in silicosis. *American journal of respiratory and critical care medicine*. 161:2026-2034.

Hamilton, R.F., Jr., S.A. Thakur, and A. Holian. 2008. Silica binding and toxicity in alveolar macrophages. *Free Radic Biol Med*. 44:1246-1258.

Han, S.G., R. Andrews, and C.G. Gairola. 2010. Acute pulmonary response of mice to multi-wall carbon nanotubes. *Inhal Toxicol*. 22:340-347.

Haraldsen, G., J. Balogh, J. Pollheimer, J. Sponheim, and A.M. Kuchler. 2009. Interleukin-33 - cytokine of dual function or novel alarmin? *Trends in immunology*. 30:227-233.

Hayakawa, H., M. Hayakawa, A. Kume, and S. Tominaga. 2007. Soluble ST2 blocks interleukin-33 signaling in allergic airway inflammation. *The Journal of biological chemistry*. 282:26369-26380.

He, X., S.H. Young, D. Schwegler-Berry, W.P. Chisholm, J.E. Fernback, and Q. Ma. 2011. Multiwalled carbon nanotubes induce a fibrogenic response by stimulating reactive oxygen species production, activating NF-kappaB signaling, and promoting fibroblast-to-myofibroblast transformation. *Chemical research in toxicology*. 24:2237-2248.

Ho, L.H., T. Ohno, K. Oboki, N. Kajiwara, H. Suto, M. Iikura, Y. Okayama, S. Akira, H. Saito, S.J. Galli, and S. Nakae. 2007. IL-33 induces IL-13 production by mouse mast cells independently of IgE-FcepsilonRI signals. *Journal of leukocyte biology*. 82:1481-1490.

Hsieh, F.H., P. Sharma, A. Gibbons, T. Goggans, S.C. Erzurum, and S.J. Haque. 2005. Human airway epithelial cell determinants of survival and functional phenotype for primary human mast cells. *Proceedings of the National Academy of Sciences of the United States of America*. 102:14380-14385.

Huizar, I., A. Malur, Y.A. Midgette, C. Kukoly, P. Chen, P.C. Ke, R. Podila, A.M. Rao, C.J. Wingard, L. Dobbs, B.P. Barna, M.S. Kavuru, and M.J. Thomassen. 2011. Novel murine model of chronic granulomatous lung inflammation elicited by carbon nanotubes. *American journal of respiratory cell and molecular biology*. 45:858-866.

Ichinose, T., H. Takano, Y. Miyabara, K. Sadakaneo, M. Sagai, and T. Shibamoto. 2002. Enhancement of antigen-induced eosinophilic inflammation in the airways of mast-cell deficient mice by diesel exhaust particles. *Toxicology*. 180:293-301.

Iikura, M., H. Suto, N. Kajiwara, K. Oboki, T. Ohno, Y. Okayama, H. Saito, S.J. Galli, and S. Nakae. 2007. IL-33 can promote survival, adhesion and cytokine production in human mast cells. *Lab. Invest.* 87:971-978.

Ingram, J.L., A.B. Rice, K. Geisenhoffer, D.K. Madtes, and J.C. Bonner. 2004. IL-13 and IL-1beta promote lung fibroblast growth through coordinated up-regulation of PDGF-AA and PDGF-Ralpha. *FASEB J.* 18:1132-1134.

Inoue, K., E. Koike, R. Yanagisawa, S. Hirano, M. Nishikawa, and H. Takano. 2009. Effects of multi-walled carbon nanotubes on a murine allergic airway inflammation model. *Toxicology and applied pharmacology*. 237:306-316.

Inoue, K., H. Takano, E. Koike, R. Yanagisawa, M. Sakurai, S. Tasaka, A. Ishizaka, and A. Shimada. 2008. Effects of pulmonary exposure to carbon nanotubes on lung and systemic inflammation with coagulatory disturbance induced by lipopolysaccharide in mice. *Exp Biol Med (Maywood)*. 233:1583-1590.

Inoue, Y., T.E. King, Jr., S.S. Tinkle, K. Dockstader, and L.S. Newman. 1996. Human mast cell basic fibroblast growth factor in pulmonary fibrotic disorders. *The American journal of pathology*. 149:2037-2054.

Ishii, H., S. Hayashi, J.C. Hogg, T. Fujii, Y. Goto, N. Sakamoto, H. Mukae, R. Vincent, and S.F. van Eeden. 2005. Alveolar macrophage-epithelial cell interaction following exposure to atmospheric particles induces the release of mediators involved in monocyte mobilization and recruitment. *Respir Res*. 6:87.

Jain, S., V.S. Thakare, M. Das, C. Godugu, A.K. Jain, R. Mathur, K. Chuttani, and A.K. Mishra. 2011. Toxicity of multiwalled carbon nanotubes with end defects critically depends on their functionalization density. *Chemical research in toxicology*. 24:2028-2039.

Janssens, S., and R. Beyaert. 2002. A universal role for MyD88 in TLR/IL-1R-mediated signaling. *Trends Biochem. Sci.* 27:474-482.

Ji, Z., D. Zhang, L. Li, X. Shen, X. Deng, L. Dong, M. Wu, and Y. Liu. 2009. The hepatotoxicity of multi-walled carbon nanotubes in mice. *Nanotechnology*. 20:445101.

Jin, C., C.P. Shelburne, G. Li, E.N. Potts, K.J. Riebe, G.D. Sempowski, W.M. Foster, and S.N. Abraham. 2011. Particulate allergens potentiate allergic asthma in mice through sustained IgE-mediated mast cell activation. *The Journal of clinical investigation*. 121:941-955.

Kabashima, K., D. Sakata, M. Nagamachi, Y. Miyachi, K. Inaba, and S. Narumiya. 2003. Prostaglandin E2-EP4 signaling initiates skin immune responses by promoting migration and maturation of Langerhans cells. *Nat Med*. 9:744-749.

Kalinski, P., C.M. Hilkens, A. Snijders, F.G. Snijdewint, and M.L. Kapsenberg. 1997. Dendritic cells, obtained from peripheral blood precursors in the presence of PGE2, promote Th2 responses. *Adv. Exp. Med. Biol.* 417:363-367.

Kamata, H., S. Tasaka, K. Inoue, K. Miyamoto, Y. Nakano, H. Shinoda, Y. Kimizuka, H. Fujiwara, M. Ishii, N. Hasegawa, R. Takamiya, S. Fujishima, H. Takano, and A. Ishizaka. 2011. Carbon black nanoparticles enhance bleomycin-induced lung inflammatory and fibrotic changes in mice. *Exp Biol Med (Maywood)*. 236:315-324.

Kashiwakura, J., H. Yokoi, H. Saito, and Y. Okayama. 2004. T cell proliferation by direct cross-talk between OX40 ligand on human mast cells and OX40 on human T cells: comparison of gene expression profiles between human tonsillar and lung-cultured mast cells. *J Immunol*. 173:5247-5257.

Katwa, P., Wang, X., Urankar R. N., Podila, R., Hilderbrand, S. C., Fick, R. B., Rao, A. M., Ke, P. C., Wingard, C. J., & Brown, J. M. in submission 2012. A Novel Carbon Nanotube Toxicity Paradigm Driven by Mast Cells and the IL-33/ST2 Axis.

Kearley, J., K.F. Buckland, S.A. Mathie, and C.M. Lloyd. 2009. Resolution of allergic inflammation and airway hyperreactivity is dependent upon disruption of the T1/ST2-IL-33 pathway. *American journal of respiratory and critical care medicine*. 179:772-781.

Keith, I., R. Day, S. Lemaire, and I. Lemaire. 1987. Asbestos-induced fibrosis in rats: increase in lung mast cells and autacoid contents. *Exp Lung Res*. 13:311-327.

Kim, E.J., H.J. Cho, D. Park, J.Y. Kim, Y.B. Kim, T.G. Park, C.K. Shim, and Y.K. Oh. 2011. Antifibrotic effect of MMP13-encoding plasmid DNA delivered using polyethylenimine shielded with hyaluronic acid. *Molecular therapy : the journal of the American Society of Gene Therapy*. 19:355-361.

Kim, J.E., H.T. Lim, A. Minai-Tehrani, J.T. Kwon, J.Y. Shin, C.G. Woo, M. Choi, J. Baek, D.H. Jeong, Y.C. Ha, C.H. Chae, K.S. Song, K.H. Ahn, J.H. Lee, H.J. Sung, I.J. Yu, G.R. Beck, Jr., and M.H. Cho. 2010. Toxicity and clearance of intratracheally administered multiwalled carbon nanotubes from murine lung. *Journal of toxicology and environmental health. Part A*. 73:1530-1543.

Kirshenbaum, A.S., S.W. Kessler, J.P. Goff, and D.D. Metcalfe. 1991. Demonstration of the origin of human mast cells from CD34+ bone marrow progenitor cells. *J Immunol*. 146:1410-1415.

Komai-Koma, M., D. Xu, Y. Li, A.N. McKenzie, I.B. McInnes, and F.Y. Liew. 2007. IL-33 is a chemoattractant for human Th2 cells. *Eur. J. Immunol.* 37:2779-2786.

Konig, A., S. Corbacioglu, M. Ballmaier, and K. Welte. 1997. Downregulation of c-kit expression in human endothelial cells by inflammatory stimuli. *Blood*. 90:148-155.

Kono, H., and K.L. Rock. 2008. How dying cells alert the immune system to danger. *Nature reviews. Immunology*. 8:279-289.

Kurowska-Stolarska, M., B. Stolarski, P. Kewin, G. Murphy, C.J. Corrigan, S. Ying, N. Pitman, A. Mirchandani, B. Rana, N. van Rooijen, M. Shepherd, C. McSharry, I.B. McInnes, D. Xu, and F.Y. Liew. 2009. IL-33 amplifies the polarization of

alternatively activated macrophages that contribute to airway inflammation. *J Immunol*. 183:6469-6477.

Kwon, J.S., Y.S. Kim, A.S. Cho, H.H. Cho, J.S. Kim, M.H. Hong, S.Y. Jeong, M.H. Jeong, J.G. Cho, J.C. Park, J.C. Kang, and Y. Ahn. 2011. The novel role of mast cells in the microenvironment of acute myocardial infarction. *J. Mol. Cell. Cardiol.* 50:814-825.

Lang, Y.D., S.F. Chang, L.F. Wang, and C.M. Chen. 2010. Chymase mediates paraquat-induced collagen production in human lung fibroblasts. *Toxicol. Lett.* 193:19-25.

Lee, C.G., R.J. Homer, Z. Zhu, S. Lanone, X. Wang, V. Koteliansky, J.M. Shipley, P. Gotwals, P. Noble, Q. Chen, R.M. Senior, and J.A. Elias. 2001. Interleukin-13 induces tissue fibrosis by selectively stimulating and activating transforming growth factor beta(1). *J. Exp. Med.* 194:809-821.

Lefrancais, E., S. Roga, V. Gautier, A. Gonzalez-de-Peredo, B. Monsarrat, J.P. Girard, and C. Cayrol. 2012. IL-33 is processed into mature bioactive forms by neutrophil elastase and cathepsin G. *Proceedings of the National Academy of Sciences of the United States of America*. 109:1673-1678.

Lewis, R.A., N.A. Soter, P.T. Diamond, K.F. Austen, J.A. Oates, and L.J. Roberts, 2nd. 1982. Prostaglandin D2 generation after activation of rat and human mast cells with anti-IgE. *J Immunol*. 129:1627-1631.

Liew, F.Y., N.I. Pitman, and I.B. McInnes. 2010. Disease-associated functions of IL-33: the new kid in the IL-1 family. *Nature reviews. Immunology*. 10:103-110.

Lin, Y., S. Taylor, H. Li, K.A.S. Fernando, L. Qu, W. Wang, L. Gu, B. Zhou, and Y.-P. Sun. 2004. Advances toward bioapplications of carbon nanotubes. *J. Mater. Chem.* 14:527-541.

Lindberg, B.F., E. Gyllstedt, and K.E. Andersson. 1997. Conversion of angiotensin I to angiotensin II by chymase activity in human pulmonary membranes. *Peptides*. 18:847-853.

Liu, Z., S. Tabakman, K. Welsher, and H. Dai. 2009. Carbon Nanotubes in Biology and Medicine: In vitro and in vivo Detection, Imaging and Drug Delivery. *Nano Res*. 2:85-120.

Lloyd, C.M. 2010. IL-33 family members and asthma - bridging innate and adaptive immune responses. *Curr. Opin. Immunol.* 22:800-806.

Luo, M., X. Deng, X. Shen, L. Dong, and Y. Liu. 2012. Comparison of cytotoxicity of pristine and covalently functionalized multi-walled carbon nanotubes in RAW 264.7 macrophages. *J. Nanosci. Nanotechnol.* 12:274-283.

Luthi, A.U., S.P. Cullen, E.A. McNeela, P.J. Duriez, I.S. Afonina, C. Sheridan, G. Brumatti, R.C. Taylor, K. Kersse, P. Vandenabeele, E.C. Lavelle, and S.J. Martin. 2009. Suppression of interleukin-33 bioactivity through proteolysis by apoptotic caspases. *Immunity*. 31:84-98.

Ma-Hock, L., S. Treumann, V. Strauss, S. Brill, F. Luizi, M. Mertler, K. Wiench, A.O. Gamer, B. van Ravenzwaay, and R. Landsiedel. 2009. Inhalation toxicity of multiwall carbon nanotubes in rats exposed for 3 months. *Toxicol. Sci.* 112:468-481.

Malaviya, R., N.J. Twesten, E.A. Ross, S.N. Abraham, and J.D. Pfeifer. 1996. Mast cells process bacterial Ags through a phagocytic route for class I MHC presentation to T cells. *J Immunol*. 156:1490-1496.

Mangan, N.E., A. Dasvarma, A.N. McKenzie, and P.G. Fallon. 2007. T1/ST2 expression on Th2 cells negatively regulates allergic pulmonary inflammation. *Eur. J. Immunol.* 37:1302-1312.

Marshall, J.S. 2004. Mast-cell responses to pathogens. *Nature reviews. Immunology*. 4:787-799.

Marshall, R.P., R.J. McAnulty, and G.J. Laurent. 2000. Angiotensin II is mitogenic for human lung fibroblasts via activation of the type 1 receptor. *American journal of respiratory and critical care medicine*. 161:1999-2004.

Martin, C.R., and P. Kohli. 2003. The emerging field of nanotube biotechnology. *Nat Rev Drug Discov*. 2:29-37.

Marvie, P., M. Lisbonne, A. L'Helgoualc'h, M. Rauch, B. Turlin, L. Preisser, K. Bourd-Boittin, N. Theret, H. Gascan, C. Piquet-Pellorce, and M. Samson. 2010. Interleukin-33 overexpression is associated with liver fibrosis in mice and humans. *Journal of cellular and molecular medicine*. 14:1726-1739.

Matsuzawa, S., K. Sakashita, T. Kinoshita, S. Ito, T. Yamashita, and K. Koike. 2003. IL-9 enhances the growth of human mast cell progenitors under stimulation with stem cell factor. *J Immunol*. 170:3461-3467.

Maynard, A.D., P.A. Baron, M. Foley, A.A. Shvedova, E.R. Kisin, and V. Castranova. 2004. Exposure to carbon nanotube material: aerosol release during the handling

of unrefined single-walled carbon nanotube material. *Journal of toxicology and environmental health. Part A*. 67:87-107.

McCurdy, J.D., T.J. Olynych, L.H. Maher, and J.S. Marshall. 2003. Cutting edge: distinct Toll-like receptor 2 activators selectively induce different classes of mediator production from human mast cells. *J Immunol*. 170:1625-1629.

Mercer, R.R., A.F. Hubbs, J.F. Scabilloni, L. Wang, L.A. Battelli, S. Friend, V. Castranova, and D.W. Porter. 2011. Pulmonary fibrotic response to aspiration of multi-walled carbon nanotubes. *Particle and fibre toxicology*. 8:21.

Mercer, R.R., A.F. Hubbs, J.F. Scabilloni, L. Wang, L.A. Battelli, D. Schwegler-Berry, V. Castranova, and D.W. Porter. 2010. Distribution and persistence of pleural penetrations by multi-walled carbon nanotubes. *Particle and fibre toxicology*. 7:28.

Metcalfe, D.D., R.D. Peavy, and A.M. Gilfillan. 2009. Mechanisms of mast cell signaling in anaphylaxis. *The Journal of allergy and clinical immunology*. 124:639-646; quiz 647-638.

Mierke, C.T., M. Ballmaier, U. Werner, M.P. Manns, K. Welte, and S.C. Bischoff. 2000. Human endothelial cells regulate survival and proliferation of human mast cells. *J. Exp. Med.* 192:801-811.

Mitchell, L.A., J. Gao, R.V. Wal, A. Gigliotti, S.W. Burchiel, and J.D. McDonald. 2007. Pulmonary and systemic immune response to inhaled multiwalled carbon nanotubes. *Toxicol. Sci.* 100:203-214.

Moritz, D.R., H.R. Rodewald, J. Gheyselinck, and R. Klemenz. 1998. The IL-1 receptor-related T1 antigen is expressed on immature and mature mast cells and on fetal blood mast cell progenitors. *J Immunol*. 161:4866-4874.

Mossman, B.T., M. Lippmann, T.W. Hesterberg, K.T. Kelsey, A. Barchowsky, and J.C. Bonner. 2011. Pulmonary endpoints (lung carcinomas and asbestosis) following inhalation exposure to asbestos. *J Toxicol Environ Health B Crit Rev*. 14:76-121.

Moulin, D., O. Donze, D. Talabot-Ayer, F. Mezin, G. Palmer, and C. Gabay. 2007. Interleukin (IL)-33 induces the release of pro-inflammatory mediators by mast cells. *Cytokine*. 40:216-225.

Moussion, C., N. Ortega, and J.P. Girard. 2008. The IL-1-like cytokine IL-33 is constitutively expressed in the nucleus of endothelial cells and epithelial cells in vivo: a novel 'alarmin'? *PloS one*. 3:e3331.

Muller, J., F. Huaux, N. Moreau, P. Misson, J.F. Heilier, M. Delos, M. Arras, A. Fonseca, J.B. Nagy, and D. Lison. 2005. Respiratory toxicity of multi-wall carbon nanotubes. *Toxicology and applied pharmacology*. 207:221-231.

Murphy, F.A., C.A. Poland, R. Duffin, K.T. Al-Jamal, H. Ali-Boucetta, A. Nunes, F. Byrne, A. Prina-Mello, Y. Volkov, S. Li, S.J. Mather, A. Bianco, M. Prato, W. Macnee, W.A. Wallace, K. Kostarelos, and K. Donaldson. 2011. Length-dependent retention of carbon nanotubes in the pleural space of mice initiates sustained inflammation and progressive fibrosis on the parietal pleura. *The American journal of pathology*. 178:2587-2600.

Murphy, F.A., A. Schinwald, C.A. Poland, and K. Donaldson. 2012. The mechanism of pleural inflammation by long carbon nanotubes: interaction of long fibres with

macrophages stimulates them to amplify pro-inflammatory responses in mesothelial cells. *Particle and fibre toxicology*. 9:8.

Navajas, D., and R. Farre. 2001. Forced oscillation assessment of respiratory mechanics in ventilated patients. *Crit Care*. 5:3-9.

NIOSH: *Current Intelligence Bulletin: Occupation Exposure to Carbon Nanotubes and Nanofibers*. 2010.

Nistri, S., L. Cinci, A.M. Perna, E. Masini, R. Mastroianni, and D. Bani. 2008. Relaxin induces mast cell inhibition and reduces ventricular arrhythmias in a swine model of acute myocardial infarction. *Pharmacological research : the official journal of the Italian Pharmacological Society*. 57:43-48.

North, M.L., H. Amatullah, N. Khanna, B. Urch, H. Grasemann, F. Silverman, and J.A. Scott. 2011. Augmentation of arginase 1 expression by exposure to air pollution exacerbates the airways hyperresponsiveness in murine models of asthma. *Respir Res*. 12:19.

Norton, S.K., A. Dellinger, Z. Zhou, R. Lenk, D. Macfarland, B. Vonakis, D. Conrad, and C.L. Kepley. 2010. A new class of human mast cell and peripheral blood basophil stabilizers that differentially control allergic mediator release. *Clin Transl Sci*. 3:158-169.

Oboki, K., S. Nakae, K. Matsumoto, and H. Saito. 2011. IL-33 and Airway Inflammation. *Allergy Asthma Immunol Res*. 3:81-88.

Ohshima, Y., L.P. Yang, T. Uchiyama, Y. Tanaka, P. Baum, M. Sergerie, P. Hermann, and G. Delespesse. 1998. OX40 costimulation enhances interleukin-4 (IL-4)

expression at priming and promotes the differentiation of naive human CD4(+) T cells into high IL-4-producing effectors. *Blood*. 92:3338-3345.

Okayama, Y., A.S. Kirshenbaum, and D.D. Metcalfe. 2000. Expression of a functional high-affinity IgG receptor, Fc gamma RI, on human mast cells: Up-regulation by IFN-gamma. *J Immunol*. 164:4332-4339.

Oppenheim, J.J., and D. Yang. 2005. Alarmins: chemotactic activators of immune responses. *Curr. Opin. Immunol.* 17:359-365.

Orito, K., Y. Suzuki, H. Matsuda, M. Shirai, and F. Akahori. 2004. Chymase is activated in the pulmonary inflammation and fibrosis induced by paraquat in hamsters. *Tohoku J. Exp. Med.* 203:287-294.

Oshikawa, K., K. Kuroiwa, K. Tago, H. Iwahana, K. Yanagisawa, S. Ohno, S.I. Tominaga, and Y. Sugiyama. 2001. Elevated soluble ST2 protein levels in sera of patients with asthma with an acute exacerbation. *American journal of respiratory and critical care medicine*. 164:277-281.

Oyamada, S., C. Bianchi, S. Takai, L.M. Chu, and F.W. Sellke. 2011. Chymase inhibition reduces infarction and matrix metalloproteinase-9 activation and attenuates inflammation and fibrosis after acute myocardial ischemia/reperfusion. *The Journal of pharmacology and experimental therapeutics*. 339:143-151.

Pacurari, M., Y. Qian, W. Fu, D. Schwegler-Berry, M. Ding, V. Castranova, and N.L. Guo. 2012. Cell permeability, migration, and reactive oxygen species induced by multiwalled carbon nanotubes in human microvascular endothelial cells. *Journal of toxicology and environmental health. Part A*. 75:112-128.

Padilla-Carlin, D.J., M.C. Schladweiler, J.H. Shannahan, U.P. Kodavanti, A. Nyska, L.D. Burgoon, and S.H. Gavett. 2011. Pulmonary inflammatory and fibrotic responses in Fischer 344 rats after intratracheal instillation exposure to Libby amphibole. *Journal of toxicology and environmental health. Part A*. 74:1111-1132.

Palmer, G., B.P. Lipsky, M.D. Smithgall, D. Meininger, S. Siu, D. Talabot-Ayer, C. Gabay, and D.E. Smith. 2008. The IL-1 receptor accessory protein (AcP) is required for IL-33 signaling and soluble AcP enhances the ability of soluble ST2 to inhibit IL-33. *Cytokine*. 42:358-364.

Patterson, R., and I.M. Suszko. 1971. Primate respiratory mast cells. Reactions with Ascaris antigen and anti-heavy chain sera. *J Immunol*. 106:1274-1283.

Peel, J.L., P.E. Tolbert, M. Klein, K.B. Metzger, W.D. Flanders, K. Todd, J.A. Mulholland, P.B. Ryan, and H. Frumkin. 2005. Ambient air pollution and respiratory emergency department visits. *Epidemiology*. 16:164-174.

Pejler, G., S.D. Knight, F. Henningsson, and S. Wernersson. 2009. Novel insights into the biological function of mast cell carboxypeptidase A. *Trends in immunology*. 30:401-408.

Pesci, A., G. Bertorelli, M. Gabrielli, and D. Olivieri. 1993. Mast cells in fibrotic lung disorders. *Chest*. 103:989-996.

Phillips, J.E., R. Peng, L. Burns, P. Harris, R. Garrido, G. Tyagi, J.S. Fine, and C.S. Stevenson. 2011. Bleomycin induced lung fibrosis increases work of breathing in the mouse. *Pulm. Pharmacol. Ther.*

Pichery, M., E. Mirey, P. Mercier, E. Lefrancais, A. Dujardin, N. Ortega, and J.P. Girard. 2012. Endogenous IL-33 Is Highly Expressed in Mouse Epithelial Barrier

Tissues, Lymphoid Organs, Brain, Embryos, and Inflamed Tissues: In Situ Analysis Using a Novel Il-33-LacZ Gene Trap Reporter Strain. *J Immunol*.

Poland, C.A., R. Duffin, I. Kinloch, A. Maynard, W.A. Wallace, A. Seaton, V. Stone, S. Brown, W. Macnee, and K. Donaldson. 2008. Carbon nanotubes introduced into the abdominal cavity of mice show asbestos-like pathogenicity in a pilot study. *Nature nanotechnology*. 3:423-428.

Porter, D.W., A.F. Hubbs, R.R. Mercer, N. Wu, M.G. Wolfarth, K. Sriram, S. Leonard, L. Battelli, D. Schwegler-Berry, S. Friend, M. Andrew, B.T. Chen, S. Tsuruoka, M. Endo, and V. Castranova. 2010. Mouse pulmonary dose- and time course-responses induced by exposure to multi-walled carbon nanotubes. *Toxicology*. 269:136-147.

Prodeus, A.P., X. Zhou, M. Maurer, S.J. Galli, and M.C. Carroll. 1997. Impaired mast cell-dependent natural immunity in complement C3-deficient mice. *Nature*. 390:172-175.

Rankin, A.L., J.B. Mumm, E. Murphy, S. Turner, N. Yu, T.K. McClanahan, P.A. Bourne, R.H. Pierce, R. Kastelein, and S. Pflanz. 2010. IL-33 induces IL-13-dependent cutaneous fibrosis. *J Immunol*. 184:1526-1535.

Ray, P., N. Krishnamoorthy, T.B. Oriss, and A. Ray. 2010. Signaling of c-kit in dendritic cells influences adaptive immunity. *Ann. N. Y. Acad. Sci.* 1183:104-122.

Reddy, A.R., Y.N. Reddy, D.R. Krishna, and V. Himabindu. 2012. Pulmonary toxicity assessment of multiwalled carbon nanotubes in rats following intratracheal instillation. *Environ. Toxicol.* 27:211-219.

Riedl, M., and D. Diaz-Sanchez. 2005. Biology of diesel exhaust effects on respiratory function. *The Journal of allergy and clinical immunology*. 115:221-228; quiz 229.

Ryan, J.J., H.R. Bateman, A. Stover, G. Gomez, S.K. Norton, W. Zhao, L.B. Schwartz, R. Lenk, and C.L. Kepley. 2007. Fullerene nanomaterials inhibit the allergic response. *J Immunol*. 179:665-672.

Ryman-Rasmussen, J.P., M.F. Cesta, A.R. Brody, J.K. Shipley-Phillips, J.I. Everitt, E.W. Tewksbury, O.R. Moss, B.A. Wong, D.E. Dodd, M.E. Andersen, and J.C. Bonner. 2009a. Inhaled carbon nanotubes reach the subpleural tissue in mice. *Nature nanotechnology*. 4:747-751.

Ryman-Rasmussen, J.P., E.W. Tewksbury, O.R. Moss, M.F. Cesta, B.A. Wong, and J.C. Bonner. 2009b. Inhaled multiwalled carbon nanotubes potentiate airway fibrosis in murine allergic asthma. *American journal of respiratory cell and molecular biology*. 40:349-358.

Salvi, S., A. Blomberg, B. Rudell, F. Kelly, T. Sandstrom, S.T. Holgate, and A. Frew. 1999. Acute inflammatory responses in the airways and peripheral blood after short-term exposure to diesel exhaust in healthy human volunteers. *American journal of respiratory and critical care medicine*. 159:702-709.

Satoh, M., and I. Takayanagi. 2006. Pharmacological studies on fullerene (C60), a novel carbon allotrope, and its derivatives. *J Pharmacol Sci*. 100:513-518.

Scaffidi, P., T. Misteli, and M.E. Bianchi. 2002. Release of chromatin protein HMGB1 by necrotic cells triggers inflammation. *Nature*. 418:191-195.

Schmitz, J., A. Owyang, E. Oldham, Y. Song, E. Murphy, T.K. McClanahan, G. Zurawski, M. Moshrefi, J. Qin, X. Li, D.M. Gorman, J.F. Bazan, and R.A.

Kastelein. 2005. IL-33, an interleukin-1-like cytokine that signals via the IL-1 receptor-related protein ST2 and induces T helper type 2-associated cytokines. *Immunity*. 23:479-490.

Schwartz, L.B., A.M. Irani, K. Roller, M.C. Castells, and N.M. Schechter. 1987. Quantitation of histamine, tryptase, and chymase in dispersed human T and TC mast cells. *J Immunol*. 138:2611-2615.

Sekizawa, K., G.H. Caughey, S.C. Lazarus, W.M. Gold, and J.A. Nadel. 1989. Mast cell tryptase causes airway smooth muscle hyperresponsiveness in dogs. *The Journal of clinical investigation*. 83:175-179.

Sellares, J., I. Acerbi, H. Loureiro, R.L. Dellaca, M. Ferrer, A. Torres, D. Navajas, and R. Farre. 2009. Respiratory impedance during weaning from mechanical ventilation in a mixed population of critically ill patients. *Br J Anaesth*. 103:828-832.

Selman, M., V. Ruiz, S. Cabrera, L. Segura, R. Ramirez, R. Barrios, and A. Pardo. 2000. TIMP-1, -2, -3, and -4 in idiopathic pulmonary fibrosis. A prevailing nondegradative lung microenvironment? *Am J Physiol Lung Cell Mol Physiol*. 279:L562-574.

Shalaby, K.H., L.G. Gold, T.F. Schuessler, J.G. Martin, and A. Robichaud. 2010. Combined forced oscillation and forced expiration measurements in mice for the assessment of airway hyperresponsiveness. *Respir Res*. 11:82.

Shvedova, A.A., A.A. Kapralov, W.H. Feng, E.R. Kisin, A.R. Murray, R.R. Mercer, C.M. St Croix, M.A. Lang, S.C. Watkins, N.V. Konduru, B.L. Allen, J. Conroy, G.P. Kotchey, B.M. Mohamed, A.D. Meade, Y. Volkov, A. Star, B. Fadeel, and V.E. Kagan. 2012. Impaired clearance and enhanced pulmonary inflammatory/fibrotic

response to carbon nanotubes in myeloperoxidase-deficient mice. *PloS one*. 7:e30923.

Shvedova, A.A., E.R. Kisin, R. Mercer, A.R. Murray, V.J. Johnson, A.I. Potapovich, Y.Y. Tyurina, O. Gorelik, S. Arepalli, D. Schwegler-Berry, A.F. Hubbs, J. Antonini, D.E. Evans, B.K. Ku, D. Ramsey, A. Maynard, V.E. Kagan, V. Castranova, and P. Baron. 2005. Unusual inflammatory and fibrogenic pulmonary responses to single-walled carbon nanotubes in mice. *Am J Physiol Lung Cell Mol Physiol*. 289:L698-708.

Skrzypiec-Spring, M., B. Grotthus, A. Szelag, and R. Schulz. 2007. Isolated heart perfusion according to Langendorff---still viable in the new millennium. *J. Pharmacol. Toxicol. Methods*. 55:113-126.

Sperr, W.R., H.C. Bankl, G. Mundigler, G. Klappacher, K. Grossschmidt, H. Agis, P. Simon, P. Laufer, M. Imhof, T. Radaszkiewicz, D. Glogar, K. Lechner, and P. Valent. 1994. The human cardiac mast cell: localization, isolation, phenotype, and functional characterization. *Blood*. 84:3876-3884.

Sutherland, R.E., X. Xu, S.S. Kim, E.J. Seeley, G.H. Caughey, and P.J. Wolters. 2011. Parasitic infection improves survival from septic peritonitis by enhancing mast cell responses to bacteria in mice. *PloS one*. 6:e27564.

Suzuki, N., S. Suzuki, G.S. Duncan, D.G. Millar, T. Wada, C. Mirtsos, H. Takada, A. Wakeham, A. Itie, S. Li, J.M. Penninger, H. Wesche, P.S. Ohashi, T.W. Mak, and W.C. Yeh. 2002. Severe impairment of interleukin-1 and Toll-like receptor signalling in mice lacking IRAK-4. *Nature*. 416:750-756.

Takato, H., M. Yasui, Y. Ichikawa, Y. Waseda, K. Inuzuka, Y. Nishizawa, A. Tagami, M. Fujimura, and S. Nakao. 2011. The specific chymase inhibitor TY-51469 suppresses the accumulation of neutrophils in the lung and reduces silica-induced pulmonary fibrosis in mice. *Exp Lung Res*. 37:101-108.

Talabot-Ayer, D., N. Calo, S. Vigne, C. Lamacchia, C. Gabay, and G. Palmer. 2012. The mouse interleukin (Il)33 gene is expressed in a cell type- and stimulus-dependent manner from two alternative promoters. *Journal of leukocyte biology*. 91:119-125.

The Project on Emerging Nanotechnologies. 2012. http://www.nanotechproject.org/inventories/consumer/analysis_draft/

Tkaczyk, C., B.M. Jensen, S. Iwaki, and A.M. Gilfillan. 2006. Adaptive and innate immune reactions regulating mast cell activation: from receptor-mediated signaling to responses. *Immunol Allergy Clin North Am*. 26:427-450.

Tomimori, Y., T. Muto, K. Saito, T. Tanaka, H. Maruoka, M. Sumida, H. Fukami, and Y. Fukuda. 2003. Involvement of mast cell chymase in bleomycin-induced pulmonary fibrosis in mice. *Eur. J. Pharmacol.* 478:179-185.

Urankar, R.N., Lust R. M., Mann E., Katwa P., Wang X., Hilderbrand S. C., Harrison B. S., Chen P., Ke P. C., Rao A. M., Podila R., Brown J. M., & Wingard C. J. in submission 2012a. Expansion of Cardiac Ischemia/Reperfusion Injury in Respose to Instilled Multi-Walled Carbon Nanotubes.

Urankar, R.N.L.R.M.M.E., Katwa P.; Wang X.; Hilderbrand S. C.; Harrison B. S.; Chen P.; Ke P. C.; Rao A. M.; Podila R.; Brown J. M.; Wingard C. J. *In Submission*

2012b. Expansion of Cardiac Ischemia/Reperfusion Injury in Respose to Instilled Multi-Walled Carbon Nanotubes.

Vanhee, D., P. Gosset, A. Boitelle, B. Wallaert, and A.B. Tonnel. 1995. Cytokines and cytokine network in silicosis and coal workers' pneumoconiosis. *Eur Respir J*. 8:834-842.

Vanoirbeek, J.A., M. Rinaldi, V. De Vooght, S. Haenen, S. Bobic, G. Gayan-Ramirez, P.H. Hoet, E. Verbeken, M. Decramer, B. Nemery, and W. Janssens. 2010. Noninvasive and invasive pulmonary function in mouse models of obstructive and restrictive respiratory diseases. *American journal of respiratory cell and molecular biology*. 42:96-104.

Varadaradjalou, S., F. Feger, N. Thieblemont, N.B. Hamouda, J.M. Pleau, M. Dy, and M. Arock. 2003. Toll-like receptor 2 (TLR2) and TLR4 differentially activate human mast cells. *Eur. J. Immunol.* 33:899-906.

Veldhoen, M., C. Uyttenhove, J. van Snick, H. Helmby, A. Westendorf, J. Buer, B. Martin, C. Wilhelm, and B. Stockinger. 2008. Transforming growth factor-beta 'reprograms' the differentiation of T helper 2 cells and promotes an interleukin 9-producing subset. *Nat. Immunol.* 9:1341-1346.

Wagner, M.M., R.E. Edwards, C.B. Moncrieff, and J.C. Wagner. 1984. Mast cells and inhalation of asbestos in rats. *Thorax*. 39:539-544.

Walker, V.G., Z. Li, T. Hulderman, D. Schwegler-Berry, M.L. Kashon, and P.P. Simeonova. 2009. Potential in vitro effects of carbon nanotubes on human aortic endothelial cells. *Toxicology and applied pharmacology*. 236:319-328.

Wang, M., A. Saxon, and D. Diaz-Sanchez. 1999. Early IL-4 production driving Th2 differentiation in a human in vivo allergic model is mast cell derived. *Clin Immunol*. 90:47-54.

Wang, X., P. Katwa, R. Podila, P. Chen, P.C. Ke, A.M. Rao, D.M. Walters, C.J. Wingard, and J.M. Brown. 2011a. Multi-walled carbon nanotube instillation impairs pulmonary function in C57BL/6 mice. *Particle and fibre toxicology*. 8:24.

Wang, X., T. Xia, S.A. Ntim, Z. Ji, S. Lin, H. Meng, C.H. Chung, S. George, H. Zhang, M. Wang, N. Li, Y. Yang, V. Castranova, S. Mitra, J.C. Bonner, and A.E. Nel. 2011b. Dispersal state of multiwalled carbon nanotubes elicits profibrogenic cellular responses that correlate with fibrogenesis biomarkers and fibrosis in the murine lung. *ACS nano*. 5:9772-9787.

Weidner, N., and K.F. Austen. 1991. Ultrastructural and immunohistochemical characterization of normal mast cells at multiple body sites. *J. Invest. Dermatol.* 96:26S-30S; discussion 30S-31S.

Weir, R.A., A.M. Miller, G.E. Murphy, S. Clements, T. Steedman, J.M. Connell, I.B. McInnes, H.J. Dargie, and J.J. McMurray. 2010. Serum soluble ST2: a potential novel mediator in left ventricular and infarct remodeling after acute myocardial infarction. *Journal of the American College of Cardiology*. 55:243-250.

Wiener, Z., A. Falus, and S. Toth. 2004. IL-9 increases the expression of several cytokines in activated mast cells, while the IL-9-induced IL-9 production is inhibited in mast cells of histamine-free transgenic mice. *Cytokine*. 26:122-130.

Wilhelm, M., R. Silver, and A.J. Silverman. 2005. Central nervous system neurons acquire mast cell products via transgranulation. *Eur J Neurosci*. 22:2238-2248.

Wingard, C.J., D.M. Walters, B.L. Cathey, S.C. Hilderbrand, P. Katwa, S. Lin, P.C. Ke, R. Podila, A. Rao, R.M. Lust, and J.M. Brown. 2011. Mast cells contribute to altered vascular reactivity and ischemia-reperfusion injury following cerium oxide nanoparticle instillation. *Nanotoxicology*. 5:531-545.

Wolters, P.J., J. Mallen-St Clair, C.C. Lewis, S.A. Villalta, P. Baluk, D.J. Erle, and G.H. Caughey. 2005. Tissue-selective mast cell reconstitution and differential lung gene expression in mast cell-deficient Kit(W-sh)/Kit(W-sh) sash mice. *Clinical and experimental allergy : journal of the British Society for Allergy and Clinical Immunology*. 35:82-88.

Woolhiser, M.R., K. Brockow, and D.D. Metcalfe. 2004. Activation of human mast cells by aggregated IgG through FcgammaRI: additive effects of C3a. *Clin Immunol*. 110:172-180.

Wynn, T.A. 2011. Integrating mechanisms of pulmonary fibrosis. *J. Exp. Med.* 208:1339-1350.

Yagami, A., K. Orihara, H. Morita, K. Futamura, N. Hashimoto, K. Matsumoto, H. Saito, and A. Matsuda. 2010. IL-33 mediates inflammatory responses in human lung tissue cells. *J Immunol*. 185:5743-5750.

Yanaba, K., A. Yoshizaki, Y. Asano, T. Kadono, and S. Sato. 2011. Serum IL-33 levels are raised in patients with systemic sclerosis: association with extent of skin sclerosis and severity of pulmonary fibrosis. *Clinical rheumatology*. 30:825-830.

Yong, L.C. 1997. The mast cell: origin, morphology, distribution, and function. *Exp Toxicol Pathol*. 49:409-424.

Yoshikawa, T., T. Imada, H. Nakakubo, N. Nakamura, and K. Naito. 2001. Rat mast cell protease-I enhances immunoglobulin E production by mouse B cells stimulated with interleukin-4. *Immunology*. 104:333-340.

Yu, M., M. Tsai, S.Y. Tam, C. Jones, J. Zehnder, and S.J. Galli. 2006. Mast cells can promote the development of multiple features of chronic asthma in mice. *The Journal of clinical investigation*. 116:1633-1641.

Zhang, Y., B.F. Ramos, and B.A. Jakschik. 1992. Neutrophil recruitment by tumor necrosis factor from mast cells in immune complex peritonitis. *Science*. 258:1957-1959.

Zhao, J., and V. Castranova. 2011. Toxicology of nanomaterials used in nanomedicine. *J Toxicol Environ Health B Crit Rev*. 14:593-632.

Zhiguang, X., C. Wei, R. Steven, D. Wei, Z. Wei, M. Rong, L. Zhanguo, and Z. Lianfeng. 2010. Over-expression of IL-33 leads to spontaneous pulmonary inflammation in mIL-33 transgenic mice. *Immunology letters*. 131:159-165.

Zhuang, X., A.J. Silverman, and R. Silver. 1996. Brain mast cell degranulation regulates blood-brain barrier. *J Neurobiol*. 31:393-403.

Zhuang, X., A.J. Silverman, and R. Silver. 1997. Mast cell number and maturation in the central nervous system: influence of tissue type, location and exposure to steroid hormones. *Neuroscience*. 80:1237-1245.

APPENDIX: ANIMAL CARE AND USE COMMITTEE PROTOCOL APPROVAL

East Carolina University

Animal Care and
Use Commitee
212 Ed Warren Life
Sciences Building
East Carolina University
Greenville, NC 27834

252-744-2436 office
252-744-2355 fax

July 22, 2010

Jared Brown, Ph.D.
Department of Pharmacology
Brody 6S-10
ECU Brody School of Medicine

Dear Dr. Brown:

Your Animal Use Protocol entitled, "Mechanisms of Mast Cell Directed Carbon Nanotube Toxicity," (AUP #W219) was reviewed by this institution's Animal Care and Use Committee on 7/22/10. The following action was taken by the Committee:

"Approved as submitted"

Please contact Dale Aycock at 744-2997 prior to biohazard use

A copy is enclosed for your laboratory files. Please be reminded that all animal procedures must be conducted as described in the approved Animal Use Protocol. Modifications of these procedures cannot be performed without prior approval of the ACUC. The Animal Welfare Act and Public Health Service Guidelines require the ACUC to suspend activities not in accordance with approved procedures and report such activities to the responsible University Official (Vice Chancellor for Health Sciences or Vice Chancellor for Academic Affairs) and appropriate federal Agencies.

Sincerely yours,

Robert G. Carroll, Ph.D.
Chairman, Animal Care and Use Committee

RGC/jd

enclosure

East Carolina University

1907-2007
CENTENNIAL

Animal Care and
Use Committee
212 Ed Warren Life
Sciences Building
East Carolina University
Greenville, NC 27834

252-744-2436 office
252-744-2355 fax

January 21, 2010

Christopher Wingard, Ph.D.
Department Physiology
Brody 6N-98
ECU Brody School of Medicine

Dear Dr. Wingard:

Your Animal Use Protocol entitled, "Cardiovascular Impact of Inhaled Multiwalled Carbon Nanotubes," (AUP #Q240a) was reviewed by this institution's Animal Care and Use Committee on 1/21/10. The following action was taken by the Committee:

"Approved as submitted"

Please contact Dale Aycock at 744-2997 prior to biohazard use

A copy is enclosed for your laboratory files. Please be reminded that all animal procedures must be conducted as described in the approved Animal Use Protocol. Modifications of these procedures cannot be performed without prior approval of the ACUC. The Animal Welfare Act and Public Health Service Guidelines require the ACUC to suspend activities not in accordance with approved procedures and report such activities to the responsible University Official (Vice Chancellor for Health Sciences or Vice Chancellor for Academic Affairs) and appropriate federal Agencies.

Sincerely yours,

Robert G. Carroll, Ph.D.
Chairman, Animal Care and Use Committee

RGC/jd

enclosure